23 OCTOBER 1979 NO. 8, AUGUST 1979 AND 1 OF 2

FOR OFFICIAL USE ONLY

JPRS L/8727

23 October 1979

USSR Report

METEOROLOGY AND HYDROLOGY

No. 8, August 1979

FBIS FOREIGN BROADCAST INFORMATION SERVICE

FOR OFFICIAL USE ONLY

APPROVED FOR RELEASE: 2007/02/08: CIA-RDP82-00850R000100100036-0

NOTE

JPRS publications contain information primarily from foreign newspapers, periodicals and books, but also from news agency transmissions and broadcasts. Materials from foreign-language sources are translated; those from English-language sources are transcribed or reprinted, with the original phrasing and other characteristics retained.

Headlines, editorial reports, and material enclosed in brackets [] are supplied by JPRS. Processing indicators such as [Text] or [Excerpt] in the first line of each item, or following the last line of a brief, indicate how the original information was processed. Where no processing indicator is given, the information was summarized or extracted.

Unfamiliar names rendered phonetically or transliterated are enclosed in parentheses. Words or names preceded by a question mark and enclosed in parentheses were not clear in the original but have been supplied as appropriate in context. Other unattributed parenthetical notes within the body of an item originate with the source. Times within items are as given by source.

The contents of this publication in no way represent the policies, views or attitudes of the U.S. Government.

For further information on report content call (703) 351-2938 (economic); 3468 (political, sociological, military); 2726 (life sciences); 2725 (physical sciences).

APPROVED FOR RELEASE: 2007/02/08: CIA-RDP82-00850R000100100036-0

JPRS L/8727

23 October 1979

USSR REPORT

METEOROLOGY AND HYDROLOGY

No. 8, August 1979

Selected articles from the Russian-language journal METEOROLOGIYA I GIDROLOGIYA, Moscow.

CONTENTS PAGE

CONTENTS (Continued) Page

APPROVED FOR RELEASE: 2007/02/08: CIA-RDP82-00850R000100100036-0

CONTENTS (Continued) Page

PUBLICATION DATA

English title	:	METEOROLOGY AND HYDROLOGY No. 8, Aug 79
Russian title	:	METEOROLOGIYA I GIDROLOGIYA
Author (s)	:	
Editor (s)	:	Ye. I. Tolstikov
Publishing House	:	GIDROMETEOIZDAT
Place of Publication	:	Moscow
Date of Publication	:	1979
Signed to press	:	23 Jul 79
Copies	:	3870
COPYRIGHT	:	"Meteorologiya i gidrologiya," 1979

UDC 551.(509.313:584.5)

NUMERICAL MODELING OF URBAN MICROCLIMATE

Moscow METEOROLOGIYA I GIDROLOGIYA in Russian No 8, Aug 79 pp 5-15

[Article by Academician USSR Academy of Sciences G. I. Marchuk, Doctor of Physical and Mathematical Sciences V. V. Penenko and Candidate of Physical and Mathematical Sciences A. Ye. Aloyan, G. L. Lazriyev, Computation Center Siberian Department USSR Academy of Sciences and Transcaucasian Scientific Research Hydrometeorological Institute, submitted for publication 1 December 1978]

Abstract: The article gives a numerical model of the microclimate of large cities, based on a model of atmospheric processes. The authors give an example of the modeling of the microclimate of a city typical for the middle latitudes and situated in lowland terrain for the summer season. The contribution of different factors to the formation of a heat island over a city is analyzed.

[Text] It is well known that the climate of a city differs from the climate of the surrounding area [9, 10, 12]. Numerous measurements of air temperature in a city and in its neighborhood show that a city is almost always warmer. The temperature difference ΔT between a city and its neighborhood sometimes attains rather high values (more than 10°C). In the literature this phenomenon is called an urban heat island (HI). It was found that a HI is expressed particularly well at night, in windless and cloudless weather. The intensity of a HI is also dependent on the season of the year, on geographic latitude, on the population of the city, etc.

Urban built-up areas exert a strong influence on the external wind. According to [9], the wind velocity in the lower 500-m layer over Moscow is 1-3 m/sec less than in the outskirts of Moscow. On the average the wind velocity in the city is 20-35% less than in the outskirts [10]. The city also changes other meteorological characteristics, such as relative humidity, the frequency of recurrence of fogs, the number of cases of falling of precipitation and its intensity, the intensity of solar radiation, etc.

An important role in the formation of urban microclimate is played by artificial heat flows, forming due to the operation of industrial enterprises, heating systems, auto transportation, etc. With time their influence will be intensified, since according to the data of the WMO world energy consumption is increasing on the average by 6% yearly. In some large cities, especially those situated in the high latitudes, which are reached by little solar energy, the quantity of heat released during the year is comparable with the quantity of solar radiation absorbed by the earth. For middle-latitude cities this factor is especially important in winter. For example, in Moscow the winter temperature is higher than in the suburbs, despite the fact that the radiation balance in Moscow is less than in the area surrounding Moscow.

In the opinion of many researchers [9, 12, 17], the following fundamental factors exert an influence on the formation of urban climate:
-- the urban built-up area, whose influence on the external wind is manifested through an increase in the roughness of the underlying surface;
-- the difference in the thermophysical properties of the underlying surface in the city and in the neighborhood;
-- artificial heat flows;
-- mechanical withdrawal of precipitation and a decrease in the freely evaporating surface in the city;
-- air contamination.

In addition to these factors, we should also mention albedo, which for a city during the course of the entire year is less than for a rural area. This is evidently attributable to the presence in the city of dark construction materials, with the contamination of snow and with its removal from the streets in winter, etc.

During recent years, together with experimental investigations, much attention has been devoted to the mathematical modeling of the microclimate of large industrial centers [11-14, 16-19], and this is natural because the concentration of industrial plants and transportation facilities in cities and densely populated regions has the result that cities more and more are feeling the negative influence of industrialization. The authors of [13, 16, 18-19] describe the results of numerical modeling of the microclimate of cities such as Montreal [13], Saint Louis [18], Tokio [16] and others. In these studies for the most part there was an investigation of the influence of some definite factor on the climate of a city. For example, in [13], on the basis of a two-dimensional model, a study was made of the influence of a HI on variations of the roughness parameter and an artificial heat flow at nighttime under winter conditions. In [19], also using a two-dimensional model, a study was made of the dependence of a nighttime HI on atmospheric stability and velocity of the geostrophic wind. We should mention [14], in which a study was made of a one-dimensional model, but for the first time use was made there of the heat balance equation for determining the temperature of the underlying surface in a city and in a rural area. Three-dimensional models were described in [11, 16, 18]. In [18] a study was made of the dependence of the

microclimate of Saint Louis on the velocity and direction of the external wind with stipulated ΔT. Reference [16], also with stipulated ΔT, gives a study of the dependence of the wind field on the HI in Tokio, taking into account the real shoreline in this region.

In this paper we describe a numerical model for study of the microclimate of large cities. First of all, we will examine the hydrodynamic aspects of the microclimate problem -- the interaction of an air mass with the underlying surface, the formation of a heat island and local circulations against the background of an external flow. The splitting method [5] is the methodological basis for constructing a numerical model.

1. The system of model equations has the following form [8]:

$$\frac{\partial u'}{\partial t} + \operatorname{div} \vec{u}u = -\frac{\partial \pi'}{\partial x} + \lambda\vartheta' \frac{\partial \delta}{\partial x} + lv' + \frac{\partial}{\partial z} \nu_u \frac{\partial u}{\partial z} + \Delta u, \tag{1}$$

$$\frac{\partial v'}{\partial t} + \operatorname{div} \vec{u}v = -\frac{\partial \pi'}{\partial y} + \lambda\vartheta' \frac{\partial \delta}{\partial y} - lu' + \frac{\partial}{\partial z} \nu_u \frac{\partial v}{\partial z} + \Delta v, \tag{2}$$

$$\frac{\partial \vartheta'}{\partial t} + \operatorname{div} \vec{u}\vartheta' = -S\left(w' + u' \frac{\partial \delta}{\partial x} + v' \frac{\partial \delta}{\partial y}\right) + \frac{\partial}{\partial z} \nu_\vartheta \frac{\partial \vartheta'}{\partial z} + \Delta\vartheta' - u'\Theta_x - v'\Theta_y + \frac{L_w}{c_p} \Phi + Q_r, \tag{3}$$

$$\frac{\partial q'}{\partial t} + \operatorname{div} \vec{u}q' = -\frac{\partial Q}{\partial z}\left(w' + u' \frac{\partial \delta}{\partial x} + v' \frac{\partial \delta}{\partial y}\right) + \frac{\partial}{\partial z} \nu_\vartheta \frac{\partial q'}{\partial z} + \Delta q' - u'Q_x - v'Q_y - \Phi, \tag{4}$$

$$\frac{\partial \pi}{\partial z} = \lambda\vartheta', \tag{5}$$

$$\frac{\partial u'}{\partial x} + \frac{\partial v'}{\partial y} + \frac{\partial w'}{\partial z} = 0, \tag{6}$$

$$u = U + u', \; v = V + v', \; w = W + w', \; \vartheta = \Theta + \vartheta', \; q = Q + q',$$

$$\pi = \Pi + \pi'.$$

$$\left(\Delta = \frac{\partial}{\partial x} \tilde{\mu}_1 \frac{\partial}{\partial x} + \frac{\partial}{\partial y} \tilde{\mu}_2 \frac{\partial}{\partial y}\right).$$

Here t is time, x, y, z are curvilinear coordinates; x, y are mutually orthogonal and are directed along the relief, $z = z_1 - \delta(x, y)$, z_1 is elevation above sea level, the equation $z_1 = \delta(x, y)$ describes relief, $\vec{u}$ is the wind velocity vector, u, v, w are its components in the directions x, y, z respectively, λ, l, S are the convection, Coriolis and stratification parameters, $\tilde{\mu}_1$, $\tilde{\mu}_2$ are the horizontal turbulence coefficients, ν_u, ν_ϑ are the vertical turbulence coefficients for momentum and heat, π is

potential temperature, q is specific humidity, Π is a value proportional to pressure, U, V, W, Θ, Q, Π are the background values of the meteorological fields, u', v', w', ϑ', q', Π' are deviations from the background, Θ_x, Θ_y and Q_x, Q_y are the horizontal gradients of background potential temperature and background specific humidity, L_w is the latent heat of evaporation, c_p is the specific heat capacity of air at constant pressure, Φ is the rate of formation of the liquid phase, Q_r is the radiation component of the heat influx.

In order to describe the surface layer we use the following system of equations:

$$\varkappa z \frac{\partial |V|}{\partial z} = u_* \varphi_u(\zeta), \quad \varkappa \frac{\partial p}{\partial z} = p_* \varphi_\vartheta(\zeta) \quad (p = \vartheta, q), \tag{7}$$

$$\varkappa |v| = u_* f_u(\zeta, \zeta_u), \quad p - p_0 = p_* f_\vartheta(\zeta, \zeta_0), \quad \zeta = \frac{z}{L},$$

$$\zeta_u = \frac{z_u}{L}, \quad \zeta_0 = \frac{z_\vartheta}{L}, \tag{8}$$

$$\nu_i = \frac{u_* \varkappa z}{\varphi_i(\zeta)}, \quad (\nu_i)_h = \frac{u_* \varkappa h}{\varphi_i(\zeta_h)} \ (i = u, \vartheta), \quad \zeta_h = \frac{h}{L}, \quad L = \frac{u_*^2}{\varkappa^2 \vartheta_*}, \tag{9}$$

where $|V| = \sqrt{u^2 + v^2}$ is the wind velocity modulus, u_* is friction velocity, ϑ_*, q_* are the scales of potential temperature and specific humidity, $\varkappa$ is the Karman constant, z_u, z_ϑ are the roughness parameters for wind and temperature, h is the height of the surface layer, the subscripts 0 and h denote the meteorological fields when $z = z_\vartheta$ and $z = h$ respectively), L is scale length, ζ is dimensionless length, φ_i, f_i are continuous universal functions [4]. The initial conditions are stipulated in the following form [8]:

$$u' = v' = 0, \ q' = 0, \ \vartheta' = 0 \quad \text{when } t = 0. \tag{10}$$

The system is solved with the following boundary conditions [8]:

$$\frac{\partial u'}{\partial x} = 0, \ \frac{\partial v'}{\partial x} = 0, \ \frac{\partial \vartheta'}{\partial x} = 0, \ \frac{\partial q'}{\partial x} = 0 \quad \text{when } x = \pm X, \tag{11}$$

$$\frac{\partial u'}{\partial y} = 0, \ \frac{\partial v'}{\partial y} = 0, \ \frac{\partial \vartheta'}{\partial y} = 0, \ \frac{\partial q'}{\partial y} = 0 \quad \text{when } y = \pm Y, \tag{12}$$

$$u' = 0, \ v' = 0, \ \vartheta' = 0, \ q' = 0, \ w' = 0 \quad \text{when } z = H, \tag{13}$$

$$w = 0, \ h \frac{\partial}{\partial z} \begin{Bmatrix} u \\ v \end{Bmatrix} = \frac{\varphi_u(\zeta_h)}{f_u(\zeta_h, \zeta_u)} \begin{Bmatrix} u \\ v \end{Bmatrix}, \ h \frac{\partial p}{\partial z} =$$

$$= \frac{\varphi_\vartheta(\zeta_h)}{\varphi_\vartheta(\zeta_h, \zeta_0)} (p - p_0) \quad \text{when } z = h. \tag{14}$$

Here H is the height of the boundary layer of the atmosphere, X, Y are the lateral boundaries of the region.

Over the water ϑ_0 and q_0 are considered stipulated:

$$\vartheta_0=\Theta_0,\ q_0=q_H(\Theta_0). \tag{15}$$

Over the land the q_0 function is computed using the formula

$$q_0=\eta_0 q_H(\vartheta_0), \tag{16}$$

where η_0 is relative humidity, assumed to be a known function of x, y and t, q_H is saturating specific humidity, which is computed using the Magnus formula [6].

For determining temperature at the ground surface we write the heat balance equation

$$G_s-\rho c_p\left(\nu_\vartheta\frac{\partial\vartheta}{\partial z}\right)_0-a_r\rho L_w\left(\nu_\vartheta\frac{\partial q}{\partial z}\right)_0=I_0(1-A_s)+I_s-F_s, \tag{17}$$

where $G=\lambda_s(\partial T/\partial z)_s$ is heat transfer through the surface z = 0 (the subscript s denotes values when z = 0), λ_s is the heat conductivity coefficient, A_s is albedo, T is absolute soil temperature, ρ is air density, F_s is effective long-wave radiation [6], a_r is a dimensionless coefficient, making it possible to take into account the fact that at different points on the underlying surface an unlike quantity of heat is expended on evaporation (condensation) as a result of its inhomogeneity, I_0 is short-wave solar radiation, which is determined using the Albrecht formula [2], $I_s(x, y, t)$ is a function describing the flow of heat which is released in the process of production and consumption of energy in a city.

The problem of taking into account artificial heat flows in models of urban microclimate for the time being remains open [13-14, 17]. A release of thermal energy into the atmosphere is possible either in the form of real or in the form of latent heat, and depending on this, different methods for its parameterization are possible. In this model the artificial heat flow, by analogy with [14], is taken into account as an increment to the radiation heat influx.

Under calm conditions the temperature drop between the levels z = 0 and $z = z_\vartheta$ can attain rather large values. Accordingly, in solving equation (17) it is desirable to use a known semi-empirical parameterization formula for a viscous sublayer [3, 15]

$$\vartheta_s-\vartheta_0=0{,}0962\,\vartheta_*(u_* z_\vartheta/\nu)^{0.45}, \tag{18}$$

where ν is the kinematic viscosity coefficient for air.

Then the solution of equation (17) is written in the following form [4]:

$$\vartheta_0 = (\tilde{\vartheta}_0 + \tilde{D}\vartheta_h)/(1 + \tilde{D}), \quad \tilde{D} = \tilde{C}F, \tag{19}$$

where

$$\tilde{C} = Ac_p + [B + 4(F_s/T_s)^{l-1}]\frac{0{,}0962\, c_\vartheta}{\varkappa}\left(\frac{c_u |V|_h z_\vartheta}{\nu}\right)^{0{,}45},$$

$$\tilde{\vartheta}_0 = \vartheta_0^{l-1} + F\left[J_0(1 - A_s) - F_s^{l-1} - B\left(0{,}414\,\tau_s^{l-1} + \sum_{n=2}^{4} K_n \tau_s^{l-n}\right)\right] +$$

$$+ (q_h - q_0^{l-1})\,AFL_w + AFL_w\,\mu\,(\vartheta_0^{l-1} - \vartheta_s^{l-1}), \quad A = \rho c_u c_\vartheta |V|_h,$$

$$B = 2\lambda_s/(K_s \pi \Delta t)^{1/2}, \quad K_0 = 1, \quad K_n = (n+1)^{1/2} - 2n^{1/2} + (n-1)^{1/2}$$

when $n > 1$.

The expressions for μ and F were given in [4]. The remaining notations are: K_s is the soil thermal conductivity coefficient, c_u, c_ϑ are the friction and heat transfer coefficients, Δt is the time interval, $\tau_s^{i-n} = (T_s^{j-n} - \bar{T})$ is the temperature deviation of the underlying surface from its mean daily value $\bar{T}$ at the time $t = (j - n)\Delta t$.

On the basis of ϑ_0, from (17) it is possible to determine ϑ_s.

Now we will enumerate the principal input data necessary for modeling the microclimate of specific cities:
-- geographic coordinates and plan of the city;
-- local relief;
-- characteristics of the underlying surface: roughness parameter, relative humidity, albedo, mean daily temperature, heat and thermal conductivity coefficients for the soil; distribution and intensity of artificial heat sources; thermal stratification of the background atmosphere and the values of the background fields of meteorological elements: temperature, specific humidity and components of the velocity vector.

All the values stipulated at the input information level are functions of space coordinates. The background values of the meteorological elements for prognostic purposes are obtained from models of large-scale atmospheric processes and in solution of problems in a diagnostic regime are stipulated using the results of processing measurement data for the real atmosphere.

2. As an illustration we will consider the example of modeling of the microclimate of a city for summer. Figure 1 schematically illustrates the plan of a city whose boundaries are encompassed by a dashed line whereas the most densely built-up areas are surrounded by a thick line and shaded. We will assume that the city is situated in the middle latitudes in a lowland area. A river divides the city into two parts and the sea (lake, reservoir)

is situated alongside it. A considerable part of the territory is occupied by green plantings, for the most part pine forest typical for the middle latitudes (grid points of intersection with circles), whereas the remaining area can be regarded as rural, characterized by scattered one-story buildings, low shrubs, fields, etc.

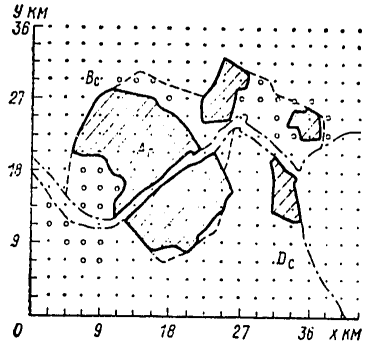

Fig. 1. Schematic plan of city.

Table 1

Parameters of Underlying Surface

	Местность 1	z_0, м	z_b, м	$10^2 K_s$, $м^2/сек$ 5	λ_s 6, $\frac{кал}{м \cdot сек \cdot °C}$	A_s	I_s 7, $\frac{кал}{м^2 \cdot сек}$	8 a_r
2	Город	1	0,01	12,5	0,62	0,2	$\tilde{I}(t)$	0,25
3	Село	0,1	0,01	5	0,26	0,3	0	1
4	Бор	0,5	0,01	5	0,26	0,4	0	1

KEY:

1. Area (land use)
2. City
3. Countryside
4. Forest
5. m^2/sec
6. $cal/m \cdot sec \cdot °C$
7. $cal/m^2 \cdot sec$
8. a_r

For the computations we used a numerical scheme, constructed by analogy with [7-8] with some modifications taking into account the specifics of the model. All the numerical experiments described below were carried out with the following values of the input parameters:
$X = Y = 21.375$ km; $h = 50$ m; $H = 1650$ m; $\Delta t = 1200$ sec; $\Delta x = \Delta y = 2250$ m; $\Delta z = \begin{cases} 100 \text{ m when } z \leqslant 300 \text{ m}, \\ 150 \text{ m with } 300 \text{ m} < z \leqslant 1650 \text{ m} \end{cases}$; $\lambda = 0.035$ m/(sec^2·K); $\zeta = 10^{-4}$ sec^{-1}; $\tilde{\mu}_1 = \tilde{\mu}_2 = 1000$ m^2/sec; $\varkappa = 0.35$; $S = 3 \cdot 10^{-3}$ K/m; $c_p = 0.24$ cal/(g·K); $L_w = 530$ cal/g; $\rho = 1300$ g/m^3; $\nu = 15 \cdot 10^{-6}$ m^2/sec; $\overline{T} = 300$ K; $\theta_0 = 295°$K.

The remaining values of the parameters are given in Table 1. The function I(t) in this table is determined in the following way:

$$\tilde{T}(t) = \begin{cases} 5 + 7 \sin[\pi(t-6)/18], & \text{if } 6 \leqslant t \leqslant 24 \text{ (t in hours)} \\ 5 & \text{for other times} \end{cases}$$

The z_u parameter for a city is assumed equal to 1 m, which corresponds to a built-up area with a height 20-30 m, whereas for a rural area and the forest we took values typical for such land use areas [3]. The A_s, λ_s, K_s values cited in the table are frequently used in similar computations [13, 14]; we note only that in the city these correspond to sandy-stony materials, whereas in a rural area and in a forest they correspond to moistened soil. For an approximate allowance for the additional reflection in the forest A_s was assumed to be 0.1 greater than in the rural area. The I_s and a_r values are characteristic for large middle-latitude cities [13-14, 19]. As z we used the micrometeorological values of the roughness parameter. In the computations it was assumed that $\Phi = 0$, $Q_r = 0$, $\delta(x,y) = 0$. The vertical turbulence coefficients, relative humidity and background temperature and specific humidity fields were stipulated the same as in [8].

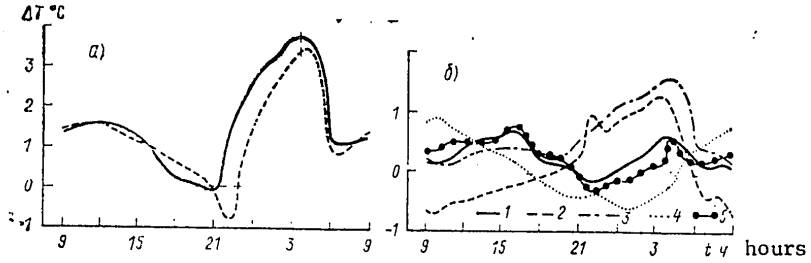

Fig. 2. Diurnal variation of the temperature difference between the points A_{city}-B_{rural} (solid curve) and A_{city}-D_{rural} (dashed curve) at a height of 2 m (a) and difference in intensities of HI in main and auxiliary experiments (b).

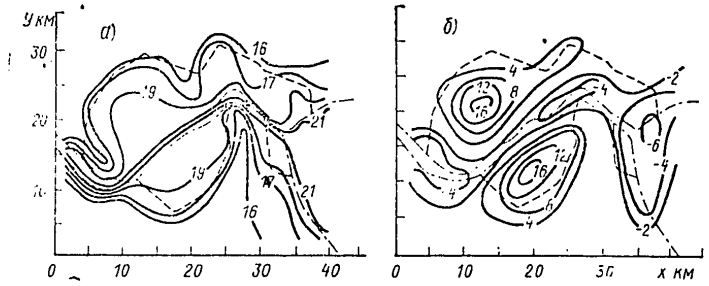

Fig. 3. Temperature distribution (°C) at a height of 2 m for t = 4 hours (a) and vertical velocities (cm/sec) at a height of 500 m for t = 14 hours (b).

Experiment 1. It is known that under calm conditions, especially at nighttime and in the early morning, when surface inversions are frequently observed, there is an increase in the danger of atmospheric contamination by

harmful substances [1]. Accordingly, it is of interest to examine the case of the absence of a background wind, that is, when $\bar{V} = 0$ and the microclimate of the city is formed only due to the influence of local inhomogeneities of the underlying surface.

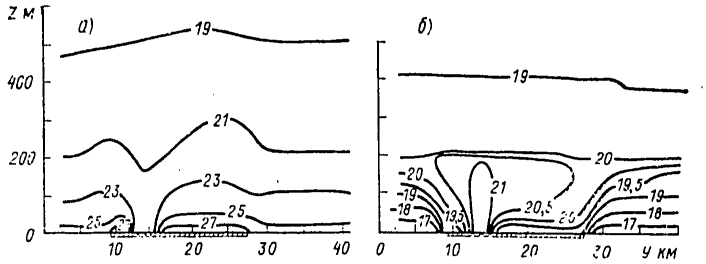

Fig. 4. Vertical structure of HI (°C) in section x = 13.5 km for t =14 hours (a) and for t = 4 hours (b).

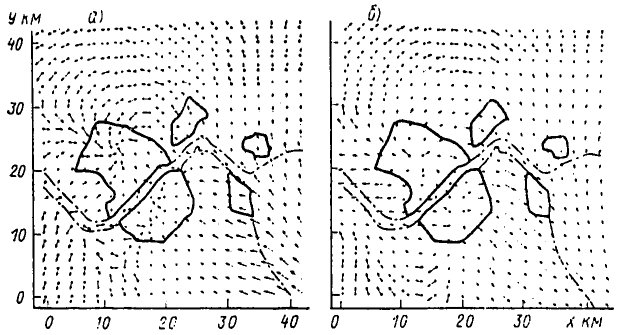

Fig. 5. Pattern of local circulation for t = 12 hours in sections z = 50 m (a) and z = 1400 m (b). The maximum vector corresponds to a value 6.2 m/sec (a) and 1.5 m/sec (b).

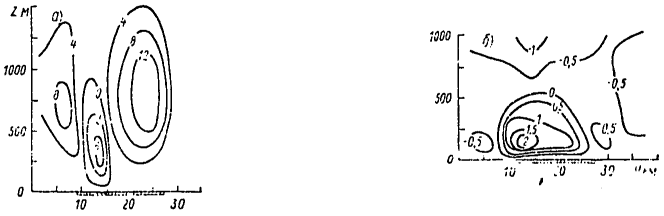

Fig. 6. Isolines w (cm/sec) in section x = 13.5 km for t = 14 hours (a) and for t = 2 hours (b).

It follows from the results of numerical experiments that in this case the temperature in the city is almost always higher than in the outskirts, except in a small time interval after sunset (2031 hours). As indicated in Fig. 2a, which shows the diurnal variation of the temperature difference at a height z = 2 m between a point of grid intersection A_{city} in the city and points B_{rural} (solid curve) and D_{rural} (dashed curve) in a rural area, ΔT is dependent on the relative positioning of these points. Under the influence of the sea at the point D_{rural} at nighttime there is a lesser cooling than at B_{rural}. Both curves have two peaks: one near midday and the other at nighttime, prior to sunrise. Beginning with sunrise (0441 hours) the rural area begins to be heated more intensively than the city and this leads to a decrease in ΔT. The transverse lines on the curves indicate the values for times corresponding to sunrise and sunset and the longitudinal lines correspond to the moments in time when the function changes sign.

Figure 3a shows the temperature field at a height of 2 m at the time 0400 hours when the HI intensity attains a maximum. It follows from this figure that the central parts of a city on the average are 3° warmer than the surrounding territory.

Now we will examine the vertical structure of the HI in the section x = 13.5 km for 1400 hours, when the "heat dome" over the city is particularly clearly expressed (Fig. 4a). The shaded region on the y-axis represents the city and the wavy line represents the water surface. It can be seen that its own "dome" is formed over each part of the city. These domes are destroyed with height and seemingly are joined into one common dome whose height attains 600 m. Despite the fact that ΔT at the 2-m level at nighttime is greater than during the daytime, the height of the "dome" at nighttime is less (Fig. 4b). This is evidently attributable to difficult turbulent mixing due to the inversion which is formed both over the city and over the rural area approximately 2-3 hours after sunset. After forming, the inversion gradually intensifies and directly prior to sunrise attains a maximum value over the city of about 1°C at a height of about 100 m, whereas over a rural area it attains approximately 3°C at a height of about 200 m. Beginning with sunrise the inversion weakens and is destroyed over the city somewhat earlier than over a rural area.

The heat island stimulates a local circulation which in the lower layers is directed toward the most heated sectors of the city. Over densely built-up regions two zones of convergence of air masses are formed in whose region vertical currents and temperature assume maximum values. Under the influence of a sea breeze, whose velocity attains 6 m/sec, such zones in other parts of the city are absent. Turning to the right with height, the wind above 1000 m changes its direction to the opposite in comparison with the surface direction. An antibreeze with a maximum velocity of 1.5 m/sec corresponds to the breeze.

At nighttime the flows, like during the daytime, are directed from the cold sectors of the terrain to warmer sectors, but convergence zones are no longer formed. Since the temperature contrast between the rural area and the sea

is greater than the intensity of the HI, there is a predominance of transfer in the direction of the sea. The maximum velocity of the well-expressed shore breeze is 2 m/sec at 0400 hours.

Figure 5 shows the vector fields of wind velocity at the levels z = 50 m (Fig. 5a) and z = 1400 m (Fig. 5b) at midday. The arrows with the square ends correspond to small velocity values.

The vertical currents over the city are always positive. They attain the greatest values during the daytime, at the time of maximum development of circulation at a height of about 500 m (Fig. 3b). At nighttime the vertical currents are an order of magnitude less than during the daytime. Over water surfaces descending movements are observed during the daytime, whereas ascending movements are observed at nighttime.

Figure 6 shows w isolines in the section x = 13.5 km for 1400 hours (Fig. 6a) and 0200 hours (Fig. 6b).

Thus, in the absence of an external wind a local circulation at the center of the city will favor the vertical transfer of air masses from the lower layers of the atmosphere into the upper layers, and from there their advection toward the margins of the city.

In addition to the main experiment 1, a series of auxiliary experiments was carried out in which each one of the physical characteristics corresponding to the city, such as albedo, the roughness parameter, etc. was assigned the same value as for the rural area. The difference in the intensity of the HI in the main and auxiliary experiments, the diurnal variation of which is given in Fig. 2b, was used in evaluating the contribution of different physical processes to the formation of urban microclimate.

Experiment 2. In order to study the influence of urban built-up areas on the HI, the z parameter was assigned a value corresponding to rural areas.

At nighttime the attenuation of turbulent mixing in comparison with experiment 1 leads to a decrease in the heat flow from the atmosphere to the underlying surface, as a result of which the temperature near the earth's surface at a height of 2 m decreases, that is, the HI attenuates. During the daytime, also due to attenuation of turbulent mixing in comparison with experiment 1, there is a decrease in the heat flow into the atmosphere and accordingly, the intensity of the HI decreases.

Figure 2b (curve 1) shows that the maximum contribution of the z_u parameter is 0.7 at nighttime and 0.6°C during the daytime.

Experiment 3. It is assumed that the underlying surface in the city has the same thermophysical properties as in a rural area.

During the daytime, when the heat flow is directed into the soil, due to a decrease in the heat conductivity coefficient λ_s and the flux value G_s associated with it, the underlying surface in the city, in comparison with experiment 1, is heated more, and as a result, there is an increase in the intensity of the HI. At nighttime the flow is already directed from the soil and therefore a decrease in λ_s in the city leads to a temperature decrease of the underlying surface and an attenuation of HI intensity.

Figure 2b (curve 2) shows that the maximum contribution of this factor at nighttime is 1.3 and during the daytime 1.1°C.

Experiment 4. A case is considered when there are no artificial heat sources. As indicated by Fig. 2b (curve 3), during the daytime the contribution of the artificial heat flow is small for the reason that I_s is a small value in comparison with short-wave solar radiation. At nighttime, despite the small value (5 cal/(m^2·sec)), the artificial flow is comparable to the heat flow from the soil and to the effective long-wave radiation, which are the basic components in the heat balance equation. Therefore, the contribution of I_s to the intensity of the HI at nighttime is substantial and attains 1.6°C. Beginning with the time corresponding to sunrise, curve 3 bends sharply downward.

Experiment 5. It is assumed that humidity processes in the city and in the rural area are identical. In the heat balance equation $a_r = 1$ is stipulated.

As indicated by Fig. 2b (curve 4), the mechanical removal of precipitation and the decrease in the free evaporating surface in the city give a maximum contribution to the HI during the daytime of about 1°C and at nighttime -- 0.6°C. During the daytime an increase in heat expenditures on evaporation (in comparison with experiment 1) leads to an attenuation of the HI. In the evening and at nighttime, when the moisture flux is directed toward the underlying surface, an intensification of the condensation process favors heating of the city and an intensification of the HI greater than in experiment 1 for this same time interval.

Experiment 6. The albedo of the underlying surface in the city assumes the same value as for a rural area. Then during the daytime, due to a decrease in absorbed short-wave solar radiation, the underlying surface is heated less and in comparison with experiment 1 the HI intensity weakens. During the daytime the maximum albedo contribution is 0.8°C.

As indicated by Fig. 2b (curve 5), a small difference from the results of experiment 1 is noticeable also at nighttime when albedo plays no role. This is evidently attributable to the fact that under the influence of a decrease in albedo during the daytime there is a restructuring of the wind and temperature fields and from the moment in time corresponding to sunset the problem is actually solved with other initial conditions.

3. The results of the numerical experiments qualitatively reflect the principal patterns of formation of the hydrometeorological regime over a city. A comparative analysis of the computations with different input data makes it possible to draw conclusions concerning the relative role of different factors of natural and anthropogenic origin. It is obvious that the problem of the microclimate of cities is of interest not only as a problem in meteorology. A heat island and a system of local circulations in interaction with the underlying surface and large-scale atmospheric processes constitute a background against which there occurs, in particular, a transformation of contaminating impurities. Taking into account the further application of the numerical modeling method for a study of industrial regions, the model described in the article is realized in the form of a complex of algorithms and programs of a universal character, without an algorithmic tie-in to a specific object. Adaptation of the model for solving specific problems is accomplished at the level of the input information. In its structure this model is part of a project to be carried out at the Computation Center Siberian Department USSR Academy of Sciences for studying hydrodynamic problems of the environment.

BIBLIOGRAPHY

1. Berlyand, M. Ye., SOVREMENNYYE PROBLEMY ATMOSFERNOY DIFFUZII I ZAGRYAZNENIYA ATMOSFERY (Modern Problems in Atmospheric Diffusion and Contamination of the Atmosphere), Leningrad, Gidrometeoizdat, 1975.

2. Budyko, M. I., TEPLOVOY BALANS ZEMNOY POVERKHNOSTI (Heat Balance of the Earth's Surface), Leningrad, Gidrometeoizdat, 1956.

3. Zilitinkevich, S. S., DINAMIKA POGRANICHNOGO SLOYA ATMOSFERY (Dynamics of the Atmospheric Boundary Layer), Leningrad, Gidrometeoizdat, 1970.

4. Kazakov, A. L., Lazriyev, G. L., "Parameterization of the Surface Layer of the Atmosphere and the Active Soil Layer," IZVESTIYA AN SSSR, FIZIKA ATMOSFERY I OKEANA (News of the USSR Academy of Sciences, Physics of the Atmosphere and Ocean), Vol 14, No 3, 1978.

5. Marchuk, G. I., CHISLENNOYE RESHENIYE ZADACH DINAMIKI ATMOSFERY I OKEANA (Numerical Solution of Problems in Dynamics of the Atmosphere and Ocean), Leningrad, Gidrometeoizdat, 1974.

6. Matveyev, L. T., OSNOVY OBSHCHEY METEOROLOGII (Principles of General Meteorology), Leningrad, Gidrometeoizdat, 1965.

7. Penenko, V. V., Aloyan, A. Ye., "Numerical Method for Computing the Fields of Meteorological Elements in the Atmospheric Boundary Layer," METEOROLOGIYA I GIDROLOGIYA (Meteorology and Hydrology), No 6, 1976.

8. Penenko, V. V., Aloyan, A. Ye., Lazriyev, G. L., "Numerical Model of Local Atmospheric Processes," METEOROLOGIYA I GIDROLOGIYA, No 4, 1979.

9. Pogosyan, Kh. P., Bachurina, A. A., METEOROLOGICHESKIY REZHIM GORODA I GRADOSTROITEL'STVO (Meteorological Regime of a City and City Construction), Leningrad, Gidrometeoizdat, 1977.

10. Rastorguyeva, G. P., "Peculiarities of the Thermal Regime of Cities," TRUDY GGO (Transactions of the Main Geophysical Observatory), No 238, 1969.

11. Atwater, M. A., "Thermal Changes Induced by Urbanization and Pollutants," J. APPL. METEOROL., Vol 14, No 6, 1975.

12. Garstand, M., Tyson, P. D., Emmitt, G. D., "The Structure of Heat Islands," J. REV. GEOPHYS. AND SPACE PH., Vol 13, No 2, 1975.

13. Gutman, D. P., Torance, K. E., "Response of the Urban Boundary Layer to Heat Addition and Surface Roughness," BOUNDARY LAYER METEOROL., Vol 9, No 2, 1975.

14. Myrup, L., "A Numerical Model of the Urban Heat Island," J. APPL. METEOROL., Vol 8, No 6, 1969.

15. Pielke, R. A., Mahrer, J., "Representation of the Heated Planetary Boundary Layer in Mesoscale Models With Coarse Vertical Resolution," J. ATMOS. SCI., Vol 32, No 3, 1975.

16. Saito, T., "A Numerical Experiment of the Land and Sea Breeze Circulation," METEOROL. AND GEOPHYS., No 4, 1976.

17. Sawai, T., "Formation of the Urban Air Mass and the Associated Local Circulation," J. METEOROL. SOC. JAPAN, Ser. II, Vol 56, No 3, 1978.

18. Vukovich, F. M., Dunn, T. W., Crissman, B. W., "A Theoretical Study of the St. Louis Heat Island. The Wind and Temperature Distribution," J. APPL. METEOROL., Vol 15, No 5, 1976.

19. Yu, T. W., Wagner, N. K., "Numerical Study of the Nocturnal Urban Boundary Layer," BOUNDARY LAYER METEOROL., Vol 9, No 2, 1975.

UDC 551.(509.313+510.522)(215-17)

NUMERICAL PREDICTION OF THE PRESSURE AND GEOPOTENTIAL FIELDS FOR THE NORTHERN HEMISPHERE WITH ALLOWANCE FOR THE BAROTROPIC BOUNDARY LAYER

Moscow METEOROLOGIYA I GIDROLOGIYA in Russian No 8, Aug 79 pp 16-23

[Article by Candidates of Physical and Mathematical Sciences L. V. Berkovich and V. A. Shnaydman, USSR Hydrometeorological Scientific Research Center and Odessa Hydrometeorological Institute, submitted for publication 24 October 1978]

Abstract: The article describes the results of numerical experiments with a hemispherical prognostic model with allowance for the effects of the planetary boundary layer in prediction of meteorological elements for 1-3 days in advance. For this purpose the authors compute the frictional vertical velocities by the use of two methods for parameterization of the boundary layer: a priori stipulation of the friction coefficient and determination of the parameters of the barotropic boundary layer. Statistical evaluations of the success of forecasts are cited, with and without the boundary layer being taken into account.

[Text] The purpose of this study is a quantitative evaluation of the dynamic effect of the planetary boundary layer (PBL) on processes of a synoptic scale and its influence on the accuracy of numerical forecasts of meteorological elements. The method used here for parameterization of the barotropic PBL in the prognostic models was described in [3, 4]. Allowance for the PBL effects was accomplished in a hemispherical prognostic model constituting a variant of the USSR Hydrometeorological Center operational model [2] in which for purposes of economy the computation region was reduced from 1625 to 1201 points of intersection of a checkerboard grid [1]. The indicated model is based on solution of a system of full equations in hydrothermodynamics. Computation of vertical velocities is accomplished by means of integration of the continuity equation

$$\frac{\partial \omega}{\partial \zeta} = -\left(\frac{\partial u}{\partial x} + \frac{\partial v}{\partial y}\right) = -D$$

from the upper boundary of the atmosphere to the 1000 mb surface using the formula

$$\omega_1 = \int_1^0 D\,(\zeta)\,d\zeta = \int_{\zeta_H}^0 D\,(\zeta)\,d\zeta + \int_1^{\zeta_H} D\,(\zeta)\,d\zeta, \tag{1}$$

where ζ = p/1000 is reduced pressure, ζ_H is its value at the upper boundary of the PBL, D is divergence of horizontal velocity.

The first integral on the right-hand side of formula (1) gives a quantitative evaluation of processes in the free atmosphere and is computed by the trapezia method using the divergence values at the computation levels of the model above the PBL: 850, 700, 500, 300, 100 mb.

The second integral in formula (1) is a quantitative evaluation of the PBL effect and is determined using the theory of the barotropic boundary layer and employing a formula for frictional vertical currents at the upper boundary of the PBL.

$$\omega_f = -\frac{g}{f}\,\mathrm{rot}\,\vec{\tau}_0, \tag{2}$$

where $\vec{\tau}_0$ is the vector of near-surface frictional shearing stress, g is the acceleration of free falling, f is the Coriolis parameter.

Two methods are employed for computing the vector $\vec{\tau}_0(\tau_{0x}\,\tau_{0y})$:

$$1)\ \tau_{0x} = \rho C_D |\vec{V}|\,u,$$

$$\tau_{0y} = \rho C_D |\vec{V}|\,v; \tag{3}$$

$$2)\ \tau_{0x} = \rho v_*^2 \cos(\alpha + \xi),$$

$$\tau_{0y} = \rho v_*^2 \sin(\alpha + \xi), \tag{4}$$

or taking into account

$$v_* = \varkappa\chi |\vec{V}_g|;\quad \sin\xi = v_g/|\vec{V}_g|;$$

$$\cos\xi = u_g/|\vec{V}_g|;$$

$$\tau_{0x} = \rho\varkappa^2\chi^2 |\vec{V}_g| (u_g\cos\alpha - v_g\sin\alpha); \tag{5}$$

$$\tau_{0y} = \rho\varkappa^2\chi^2 |\vec{V}_g| (u_g\sin\alpha + v_g\cos\alpha).$$

where $\vec{V}(u, v)$ and $\vec{V}_g(u_g, u_g)$ are the vectors of the surface and geostrophic winds respectively, C_D is the friction coefficient, $\chi = v_*/\varkappa \mid \vec{V}_g \mid$ is the geostrophic friction coefficient, α is the angle between $\vec{V}$ and $\vec{V}_g$, reckoned from the vector $\vec{V}_g$ counterclockwise, ρ is air density, $\varkappa = 0.38$ is the Karman constant.

In computations the C_D value was assumed equal to $1.5 \cdot 10^{-3}$ for the land and $0.5 \cdot 10^{-3}$ for the oceans. For determining χ and α we used a method developed in [4], according to which these values are computed using the Rossby number:

$$\mathrm{Ro} = |\vec{V}_g|/(l \cdot z_0)$$

and the two stratification parameters:

$$M = \frac{g}{l\,|\vec{V}_g|}\frac{\delta\vartheta}{\vartheta_0}; \qquad \nu = \frac{\varkappa^2(\gamma_a - \gamma_H)}{l^2\vartheta_0}.$$

Here z_0 is the roughness of the underlying surface, determined at the points of intersection of a regular grid using the maps cited in [5], $\delta\vartheta = \vartheta_H - \vartheta_0$ is the difference in potential temperatures at the upper and lower boundaries of the PBL, scalable from the difference in potential temperatures at the two lower computation levels for the model (ϑ_{850}, ϑ_{1000}) in accordance with [3], γ_a is the dry adiabatic temperature gradient, γ_H is the vertical temperature gradient in the layer between the isobaric surfaces 700-850 mb.

For computation of potential temperatures at the computation levels on the basis of the geopotential field by means of the equation of statics, the vertical profile of geopotential is approximated by a third-degree interpolation polynomial for the variable ln p with interpolation intervals 1000, 850, 700 and 500 mb.

The computation of vertical currents ω_1 with the use of the two described methods for parameterization of the vector $\vec{\tau}_0$ was accomplished in each time interval. The resulting prognostic fields for surface pressure and geopotential were compared with an adiabatic variant of forecasting and with actual fields. Numerical experiments were carried out using archives of routine data for 3-12 June 1976 and 22-31 January 1977 for 0000 and 1200 GMT.

As follows from formula (2), with use of (5) the dynamic effect of the PBL is determined by the spatial distribution of surface pressure, dynamic velocity v_* and the angle of deviation α. We will examine the v_* and α fields, computed using the initial fields of meteorological elements (diagnostic) and on the basis of the results of daily forecasts (prognostic). An analysis of the resulting fields shows that they are characterized by a quite great spatial variability. Large v_* values (80-100 cm/sec) are observed at the rear of well-developed cyclonic formations; in the central parts of pressure formations there are values $v_* = 5$-15 cm/sec. The v_* differences at two adjacent points of intersection in a regular grid on the average are about 20 cm/sec, whereas the maximum values are 60 cm/sec. The

diagnostic and prognostic fields of dynamic velocity are in qualitative agreement with one another, but the discrepancy between them can attain 30 cm/sec. Table 1 gives the mean v_* values for different latitude zones of the northern hemisphere for diagnostic and prognostic fields. The greatest mean values are observed in the temperate latitudes; the differences between the latitude zones and the v_* values themselves during winter are greater; the discrepancies between the prognostic and diagnostic v_* do not exceed 8 cm/sec and are maximum in summer.

Table 1

Mean v_* cm/sec and α ° Values According to Diagnostic and Prognostic Data

Широтная зона, град 1	2 Диагностические		3 Прогностические		2 Диагностические		3 Прогностические	
	v_*	α	v_*	α	v_*	α	v_*	α
	4 Июнь 1976 г.				5 Январь 1977 г.			
65—90	21	15,7	13	18,7	23	17,2	25	19,0
40—65	24	16,2	18	20,9	30	22,3	31	22,2
20—40	17	17,0	16	20,0	20	20,2	21	20,6
20—90	20	16,4	16	20,2	24	20,4	25	21,1

KEY:
1. Latitude zone
2. Diagnostic
3. Prognostic
4. June
5. July

Table 2

Distribution of Frictional Currents by Gradations, %

	+40	+(39—20)	+(19—0)	—(0—19)	—(20—39)	—40
	1 Фактические					
2 Июнь	—	1	53	45	1	—
3 Январь	0,5	2	56	39	2	0,5
4 Обе выборки	0,25	1,5	54,5	42	1,5	0,25
	5 Прогностические					
2 Июнь	—	—	51	49	—	—
3 Январь	—	1	54	43	2	—
4 Обе выборки	—	0,5	52,5	46	1	—

KEY:
1. Actual
2. June
3. January
4. Both samples
5. Prognostic

The fields of angles between the vectors of the surface and geostrophic winds are characterized by a considerably lesser spatial variability than v_*. Their spatial change is associated to a lesser degree with the synoptic situation and to a great extent is determined by the nature of the underlying surface. For the continents these angles are 20-35°, whereas for the ocean areas they are 10-25°. In the α fields it is easy to trace the continent-ocean discontinuity. Table 1 shows that during the winter the mean α values are

4-6° greater than in summer, which evidently is caused by the different degree of atmospheric thermal stability.

In a specific synoptic situation the v_* and α fields are associated with the corresponding fields of frictional vertical currents, which to a considerable degree match with the distribution of surface pressure. It should be noted that the spatial fields ω_f, determined by the PBL method, are characterized by a considerable asymmetry relative to the centers of pressure formations, in contrast to the frictional currents, computed from the geostrophic vortex with a constant a priori stipulated turbulence coefficient. The maximum ascending currents, in absolute value attaining 80-100 mb/12 hours, are observed in the rear of well-developed cyclones, and the maximum descending currents -- 40-50 mb/12 hours are displaced 300-500 km from the centers of the anticyclones toward the periphery, into the region of increased horizontal pressure gradients.

Table 3

Statistical Evaluations of Success of Forecasts for 24, 48 and 72 Hours

Вариант прогноза 1	Земля 2		500 мб		Земля 2		500 мб		Земля 2		500 мб	
	E	R	E	R	E	R	E	R	E	R	E	R
I	24 ч 3				48 ч				72 ч			
4 Адиабатический	0,86	0,59	0,81	0,65	0,89	0,55	0,87	0,54	0,97	0,51	0,92	0,58
II												
5 С использованием коэфф. C_D	0,82	0,60	0,78	0,66	0,86	0,54	0,84	0,57	0,94	0,58	0,91	0,60
III												
6 С учетом методики ППС	0,80	0,64	0,79	0,66	0,83	0,58	0,85	0,61	0,90	0,60	0,88	0,63
II—I	—0,04	0,01	—0,03	0,01	—0,03	—0,01	—0,30	0,03	—0,03	0,07	—0,01	0,02
III—I	—0,06	0,05	—0,02	0,01	—0,06	0,03	—0,02	0,07	—0,07	0,09	—0,04	0,05

KEY:

1. Variant of forecast
2. Surface
3. Hours
4. Adiabatic
5. Using coefficient C_D
6. With PBL method taken into account

The fields of frictional vertical currents are characterized by a greater spatial variability; the absolute differences of the ω_f values at adjacent points of grid intersection can attain 80 mb/12 hours. The distributions of diagnostic and prognostic ω_f are close to one another, but the maximum absolute values of prognostic ω_f are 10-15 mb/12 hours less than the diagnostic values. According to archival samples, the mean absolute ω_f values are: diagnostic 20.4 and 21.2 mb/12 hours, prognostic 20.0 and 20.6 mb/12 hours for June and January periods respectively.

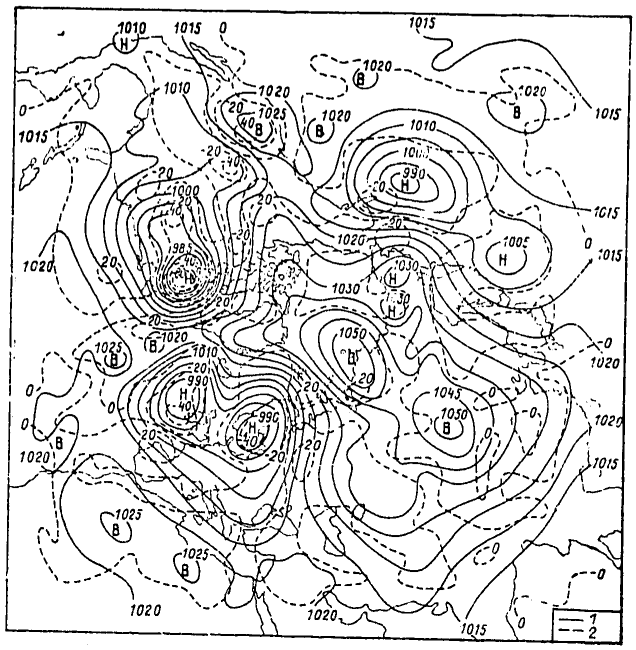

Field of surface pressure (1) and field of frictional vertical velocities (2) at 1200 GMT on 27 January 1977.

Table 2 gives the distribution of frictional currents (mb/12 hours) by gradations. As might be expected, the values of diagnostic wf are observed in a broader range of gradations; for the January period this range is broader than for June. The distribution curves are virtually identical for the diagnostic and prognostic currents. As an example of the ω_f computations, in Figures 1-3 we show the fields of diagnostic and prognostic ω_f for 1200 hours GMT on 27 and 28 January 1977.

Now we will examine the effectiveness of taking into account the dynamic effect of the PBL on large-scale atmospheric processes on the basis of statistical evaluations of the success of forecasts. For this purpose for the inner part of the region of computation of forecasts, including 525 points of intersection of a regular grid, covering the territory of the Atlantic, Europe and Western Siberia, we computed the relative errors E and the correlation coefficients R between the actual and predicted changes in surface pressure and geopotential of the 500-mb isobaric surface. An analysis of evaluations of the success of the initial data obtained from the archives shows that among the 20 considered cases of a forecast of surface pressure at 2400 hours, with the PBL taken into account, in 13 there was a decrease in E (increase in R) on the average by 0.09 (by 0.08) with E = 0.91 (R = 0.61) for adiabatic forecasts (maximum $\Delta E = 0.17$, $\Delta R = 0.15$), in four

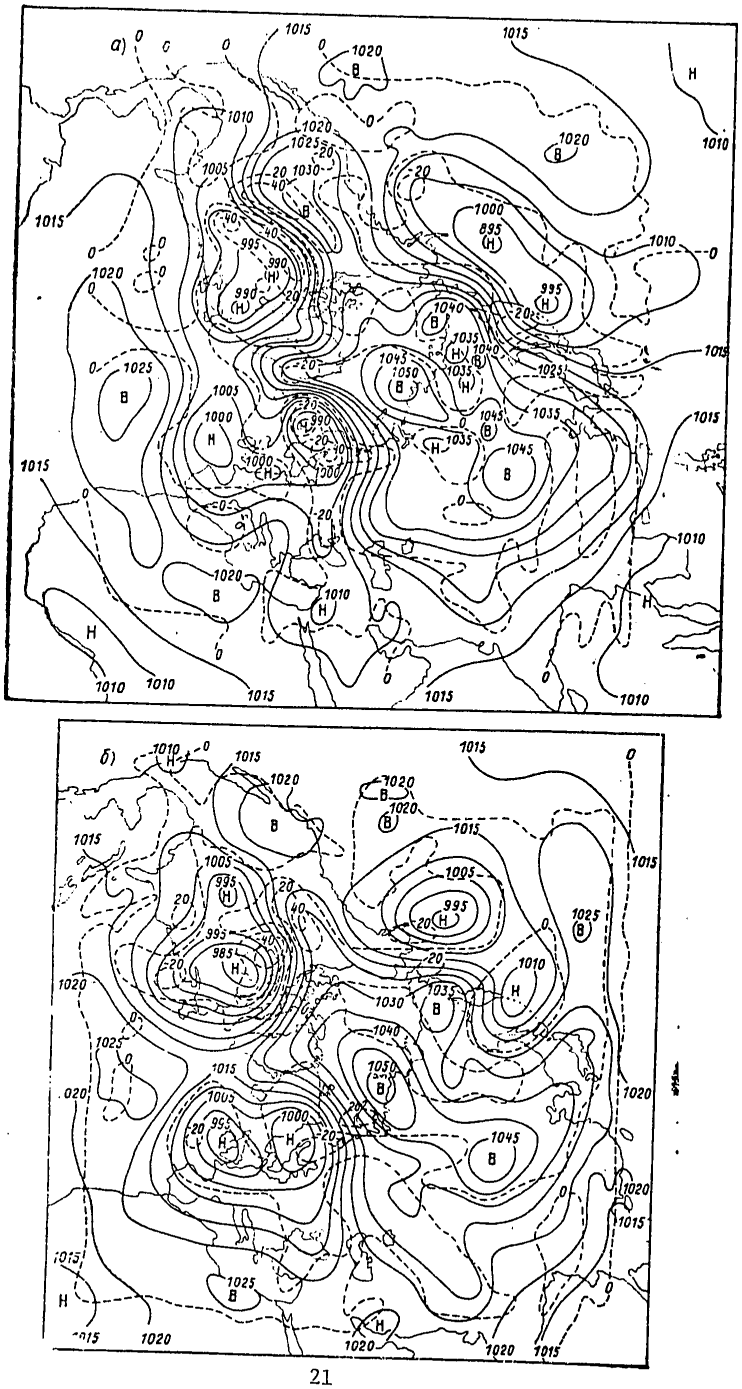

Fig. 2. Actual (a) and prognostic (b) fields of surface pressure (1) and frictional vertical velocities (2) for 1200 GMT on 28 January 1977.

---

cases the relative errors and correlation coefficients virtually did not change, and only in three cases was there a deterioration in the quality of the forecasts with respect to the relative error on the average by 0.06 and with respect to the correlation coefficient by 0.07. Similar differences between the evaluations of success were obtained for forecasts for 48 and 72 hours in advance. Table 3 gives the mean evaluations of success of three variants of forecasts for 24, 48 and 72 hours. It follows from the table that allowance for the PBL in the considered method reduces the relative errors and increases the correlation coefficients for all forecasting times. The success of forecasts with the use of the friction coefficient C_D is higher than in the adiabatic variant, but is lower than the success of forecasts with the PBL taken into account.

Now we will examine a specific example of a 24-hour forecast on the basis of initial data for 1200 GMT on 27 January 1977. The initial synoptic situation in Fig. 1, which shows the surface pressure field, is characterized by the presence of three extensive regions of low pressure: over North America, over Europe and over the Pacific Ocean, and also a well-developed anticyclone over the northern part of Asia with ridges over the polar basin, central and eastern parts of the Asian continent. In the course of the considered days there were the following changes in the position and intensity of the pressure formations: a cyclone over America was intensively filled, pressure at the center increased by 15 mb and the center of the cyclone shifted to the northwest a distance of about 1000 km. A cyclone with two centers over Europe was filled by 10 mb in the region of the westerly wind and by 4 mb in the region of the easterly center. The westerly center was displaced toward the southeast, and the easterly center -- toward the northwest, in both cases by approximately 1000 km. In the Pacific Ocean cyclone the centers came closer together; the filling of the westerly center was by 6 mb and the deepening of the easterly center was by 9 mb. In the anticyclone region the position of the centers virtually did not change, but the pressure decreased somewhat -- by 3-4 mb. The ridge over the polar regions intensified and joined with a high-pressure nucleus; the pressure here increased by 7 mb.

The described processes were differently reflected in forecasts with and without allowance for the PBL. In an adiabatic forecast it was possible to predict correctly the movement of cyclones over America and Europe and an intensification of a ridge over the polar basin, but the predicted intensity of pressure formations differs considerably from the actual intensity: in an intensively filling cyclone over America the pressure was reduced by 17 mb, in cyclones over Europe -- by 7 and 3 mb, in the centers of anticyclones over Asia the pressure increased by 2-3 mb. In forecasts with the PBL effects taken into account these errors in forecasting the intensity of pressure centers are substantially less.

Figure 2 gives the actual and predicted (with the PBL taken into account) surface pressure charts for 1200 GMT on 28 January 1978. As indicated in Fig. 2b, the predicted pressure in the cyclone over America was below the actual pressure by 7 mb, in cyclones over Europe -- by 3 mb; in anticyclones the difference is 1-2 mb. A less successful forecast of evolution of the Pacific Ocean cyclone was in the forecasting variant with allowance for the PBL and in the adiabatic variant. In the variant of the forecast with use of the C_D coefficient the predicted intensity of the pressure centers differs by several millibars from the corresponding values in a forecast which involves use of the barotropic PBL method.

The relative errors E in forecasts of surface pressure in the considered case for variants with use of the C_D coefficient and the PBL method were 0.05 and 0.08 less than in the adiabatic variant, and the correlation coefficients R are 0.03 and 0.07 higher respectively, with E_a and R_a values for adiabatic forecasts -- 0.83 and 0.67 respectively. Surface pressure forecasts for 48 and 72 hours were more successful than adiabatic forecasts by 0.09 and 0.13 with respect to E and by 0.06 and 0.11 with respect to R respectively.

Thus, computation of the velocities of vertical movements at the lower boundary of the atmosphere, with frictional currents taken into account, reflecting the integral effect of the PBL, leads to a more correct description of evolution of large-scale synoptic processes in the prognostic model.

BIBLIOGRAPHY

1. Berkovich, L. V., "Six-Level Model for Predicting Meteorological Elements for a Large Territory," TRUDY GIDROMETTSENTRA SSSR (Transactions of the USSR Hydrometeorological Center), No 100, 1972.

2. Belousov, S. L., et al., "Operational Model of Numerical Forecasting of Meteorological Elements for the Northern Hemisphere," TRUDY GIDROMETTSENTRA SSSR, No 212, 1978.

3. Tarnopol'skiy, A. G., Shnaydman, V. A., "Parameterization of the Planetary Boundary Layer in Prognostic Models," TRUDY GIDROMETTSENTRA SSSR, No 145, 1974.

4. Tarnopol'skiy, A. G., Shnaydman, V. A., "Parameterization of the Baroclinic Planetary Boundary Layer of the Atmosphere," TRUDY GIDROMETTSENTRA SSSR, No 180, 1976.

5. Baumgartner, A., Mayer, H., Metz, W., "Weltweite des Rauhigkeits parameters Zo mit Anwending auf die Energiedissipation an der Erdoflache," METEOR. RDSCH., Bd 30, No 2, 1977.

MODELING OF A CLOUD ENSEMBLE

Moscow METEOROLOGIYA I GIDROLOGIYA in Russian No 8, Aug 79 pp 24-33

[Article by Candidate of Physical and Mathematical Sciences A. I. Fal'kovich, USSR Hydrometeorological Scientific Research Center, submitted for publication 29 January 1979]

Abstract: The author investigates the problems involved in constructing a model of a cloud ensemble for the purposes of parameterization of moist convection processes in problems of general circulation of the atmosphere and long-range weather forecasting. The investigation is based on observational data obtained in GATE polygon AB. A variant of a model of a cloud ensemble is obtained in which use is made of the ideas of Yanai, Arakawa and Shubert. The paper gives the results of computations of model parameters using GATE data. The equations for the cloud ensemble are investigated. The problem is generalized for the case of allowance for the solid phase of water in clouds.

[Text] Recent decades have been characterized by vigorous progress in the development of meteorology. This has been brought about for the most part by the introduction of numerical methods. But even today many gaps remain in our knowledge of atmospheric processes. In order to eliminate these it is necessary to carry out the attack from two directions: both theoretically, by means of numerical modeling, and experimentally, by the planning and carrying out of different expeditions for the collection of empirical data, expeditions such as TROPEKS-72 and GATE [2, 3]. In the numerical models there is a cutoff of a part of the spectrum of movements (subgrid processes) and its influence on the remaining part must be parameterized, that is, there must be a quantitative expression of the energy redistribution and momentum redistribution between these parts of the spectrum. Parameterization problems are now the most important problems in meteorology. Poor parameterization of "subgrid" processes is one of the main reasons for the failures in long-range numerical forecasting. The second reason is the absence of an approximation of both initial data and the prognostic equations themselves. True, now-existing parameterization methods for subgrid processes make possible entirely successful solution of problems

relating to general circulation of the atmosphere. In the solution of such problems the influence of parameterization and approximation errors is considerably smoothed due to averaging in time. But they exert a substantial influence on the forecast.

The processing of parameterization schemes in numerical models is frequently made difficult because the defects of parameterization of any subgrid process can be compensated by errors in taking into account another factor and the great computation viscosity of the model.

In experimental polygons we obtain characteristics of the atmosphere which are a result of interaction of atmospheric processes of all scales, and not the product of artificial computation viscosity and parameterization errors, as sometimes is the case in modeling.

This paper is devoted to an investigation of one of the methods for parameterization of moist convection on the basis of GATE data.

Many different methods have now been proposed for the parameterization of moist convection. In the first approximation they can be divided into three groups. The first group includes convective adjustment (adaptation) methods. Their idea is very simple. As soon as the vertical temperature gradient or the relative humidity in the calculations at any point of grid intersection become greater than their critical values, they are replaced by critical values. In different realizations the critical value of the temperature gradient varies between the dry and the moist adiabatic values and the relative humidity between 80 and 100%. It is assumed that the kinetic energy of small-scale eddies, which arise due to cumulus convection, instantaneously dissipates, the total energy of a column of the atmosphere does not change, and all the moisture condensed as a result of convection processes instantaneously falls in the form of precipitation. This procedure replaces the natural decrease in the temperature and humidity gradient in the real atmosphere as a result of cumulus convection. We note that the realization of convective adjustment schemes is not so simple as their idea and as a rule requires the use of iteration methods and additional hypotheses.

The second group of schemes includes methods based on the CISK (conditional instability of the second kind [6]) hypothesis. These are so-called penetrating convection schemes. In contrast to the schemes in the first group, for which it is assumed that instability is manifested locally only in saturated regions or where the temperature gradient is greater than critical, this group of schemes assumes that convection affects the entire thickness of the troposphere, transporting heat and moisture upward. The appearance of convection is associated not only with stratification, but also with dynamic factors. The heat released in cumulus convection cells in these schemes is assumed to be proportional to vertical velocity at the upper boundary of the boundary layer of the atmosphere. These schemes differ from one another in different stipulation of the dependence of the proportionality factor on altitude.

The third group includes methods based on construction of a model of a cloud ensemble. Third-group schemes appeared quite recently and their formulation is far from complete. They are rather unwieldy and difficult in application; they require considerably more computer time. But since they describe the physics of moist convection more thoroughly than other schemes, they can be considered the most promising. We will also concern ourselves with them. The formulation of the cloud ensemble model proceeded in the following way. Yanai, et al. [9] generalized the experience accumulated up to 1973 in the modeling of an individual cloud and a group of clouds. They diagnostically investigated the properties of cloud clusters in a polygon in the Marshall Islands. Using the values of the influx of heat and moisture computed on the basis of observational data, these influxes being the result of large-scale movements, together with a simple model of cumulus clouds, including entrainment and expulsion processes, they obtained the vertical distribution of the vertical flux of mass, the entrainment and expulsion parameters, temperature, humidity and quantity of liquid water as an average for the cloud ensemble. Arakawa and Shubert [7] in 1974 proposed a new theory of parameterization of moist convection based on a spectral representation of a cloud ensemble. This theory makes it possible to determine not only the general properties of the cloud ensemble, but also the properties of individual types of clouds.

Now we will briefly discuss the derivation of the principal equations of the model. We will examine the continuity equation, equation for the conservation of energy and water vapor equation

$$\overline{\nabla \cdot \vec{v}} + \frac{\partial \overline{\omega}}{\partial p} = 0, \tag{1}$$

$$\frac{\partial \overline{S}}{\partial t} + \overline{\nabla \cdot \vec{S}\vec{v}} + \frac{\overline{\partial S \omega}}{\partial p} = Q_R + L\,(c - e), \tag{2}$$

$$\frac{\partial \overline{q}}{\partial t} + \overline{\nabla \cdot q\vec{v}} + \frac{\partial \overline{q\omega}}{\partial p} = e - c. \tag{3}$$

Here the notations are those generally employed:

$S = c_pT + gz$, $h = c_pT + gz + Lq$ is the static energy of dry and moist air, Q_R is the rate of radiation heating, c is the rate of condensation of a unit mass of air, e is the rate of evaporation of cloud particles.

The line at the top denotes averaging along a horizontal region, which must be sufficiently large to contain a cloud ensemble but sufficiently small in order to be only a part of a large-scale disturbance.

For convenience in investigating the cloud ensemble we will rewrite equations (2) and (3) in the form

$$Q_1 \equiv \frac{\partial \overline{S}}{\partial t} + \overline{\nabla \cdot \vec{S}\vec{v}} + \frac{\partial \overline{S\omega}}{\partial p} = Q_R + L\,(c - e) - \frac{\partial}{\partial p}\,\overline{S'\omega'}, \tag{4}$$

$$Q_2 = -L\left(\frac{\partial \overline{q}}{\partial t} + \overline{\nabla \cdot q\vec{v}} + \frac{\partial \overline{q}\,\overline{\omega}}{\partial p}\right) = L(c-e) + L\frac{\partial}{\partial p}\overline{q'\omega'}. \tag{5}$$

Here the primes denote deviations from mean values.

It follows from (4) that Q_1 (it is called apparent heating due to large-scale movements) is governed by radiation heating, the release of the latent heat of condensation and vertical convergence of vertical turbulent transfer of sensible heat. Equation (5) shows that Q_2 (it is called the apparent loss of moisture due to large-scale movements) is governed by condensation and vertical divergence of the vertical transfer of moisture.

From equations (4)-(5) it is easy to derive the equation

$$Q_1 - Q_2 - Q_R = -\frac{\partial}{\partial p}\overline{(S' + Lq')\,\omega'} = -\frac{\partial}{\partial p}\overline{h'\omega'}, \tag{6}$$

where $\overline{h'\omega'}$ is the measure of the vertical turbulent transfer of energy. This value can serve as a measure of activity of cumulus convection.

Using the conservation of mass, heat and water vapor equations in each cloud, averaging them for the cloud ensemble, equations (4)-(5) can be reduced to the form (see [9])

$$Q_1 - Q_R = M_c\frac{\partial \overline{S}}{\partial p} - LD\hat{l}, \tag{7}$$

$$Q_2 = LM_c\frac{\partial \overline{q}}{\partial p} - LD(\overline{q}^* - \overline{q} + \hat{l}), \tag{8}$$

where M_c is the total vertical flux of mass in clouds, multiplied by g (its dimensionality coincides with the dimensionality of ω), D is the rate of expulsion (detrainment) of mass from the clouds for a unit pressure interval, $\hat{l}$ is the ratio of the mixture of liquid water in the clouds at the expulsion level.

In the derivation of these equations we made the following assumptions:

1. Active clouds occupy only an insignificant part of the cloud ensemble. These are columns occupied by an ascending flow of a section constant in height. Their bases lie at the level z_B.

2. All the liquid water which is expelled from the cloud is also evaporated here and the rate of evaporation is determined from the expression $e = D\hat{l}$.

3. Each cloud produces an outsurge in a very thin layer where the cloud loses its buoyancy, that is, where $h_c = \overline{h}^*$.

Excluding $\hat{l}$ from (7) and (8), it is possible to obtain a fundamental equation for the cloud ensemble

$$Q_1 - Q_2 - Q_R = D\,(\bar{h}^* - \bar{h}) - M_c \frac{\partial \bar{h}}{\partial p}. \tag{9}$$

In a study by Yanai, et al. [9] equations (7)-(8) are used jointly with the mass budget equation, equation for the static energy of dry air, water vapor and liquid water equations for the entire cloud ensemble. In order to close the system of equations it is necessary to use a sufficiently artificial dependence of the rate of falling of precipitation on the quantity of liquid water. The derived nonlinear system of equations is solved by the iterations method. When $Q_1 - Q_R < 0$, as is frequently observed in the Trades zone, the scheme is not suitable. At the same time, the Yanai method does not give explicit information on the spectrum of distribution of different types of clouds.

Arakawa and Shubert [7] postulated that the single positive parameter λ can completely characterize the type of cloud. Here λ is selected in such a way that the level of the outsurge $z_D(\lambda)$ decreases when λ increases.

Then the total flux of mass in the clouds M_c can be expressed (7) as

$$M_c(z) = \int_0^{\lambda_D(z)} m(z, \lambda)\, d\lambda, \tag{10}$$

where

$$m(z, \lambda)\, d\lambda = \sum_{\lambda_i \in (\lambda,\ \lambda + d\lambda)} M_i(z)$$

is the mass flux into subensemble clouds for which λ_i falls in the interval $(\lambda, \lambda + d\lambda)$. The total outsurge at the z level will be

$$D(z) = -\,m(z, \lambda_D(z)) \frac{d\lambda_D(z)}{dz}. \tag{11}$$

It is convenient to normalize $m(z, \lambda)$:

$$m(z, \lambda) = m_B(\lambda)\, \eta(z, \lambda).$$

Here $m_B(\lambda) = m(z_B, \lambda)$ is the density of the mass flux at the z-level for a cloud subensemble λ.

It is easy to find, that

$$\sum_{\lambda_i \in (\lambda,\ \lambda - d\lambda)} E_i(z) = m(z, \lambda)\, \mu(z, \lambda)\, d\lambda,$$

where $E_i(z)$ is entrainment in clouds of the type λ_i at the z-level,

$$\mu(z, \lambda) = \frac{1}{\eta} \frac{\partial \eta(z, \lambda)}{\partial z}$$

is the fractional rate of entrainment of the subensemble λ.

Substituting (10)-(11) into (9) and transforming to a p-coordinate system, we arrive at the following form of the fundamental equation for a cloud ensemble

$$Q_1 - Q_2 - Q_R = (\bar{h}^* - \bar{h})\, m_B\ (\lambda_D(p))\ \eta_i(p, \lambda_D(p))\ \frac{d\lambda_D(p)}{dp} - \\ - \frac{\partial \bar{h}}{\partial p} \int_0^{\lambda_D(p)} m_B(\lambda)\, \eta_i(p, \lambda)\, d\lambda. \qquad (12)$$

Thus, for formulating a model of a cloud ensemble it is necessary to select the λ parameter and obtain $m_B(\lambda)$ and $\eta(p,\lambda)$. In order to simplify solution of the problem substantially, Arakawa and Shubert [7] postulated that the fractional velocity of entrainment of the flux of mass in a cloud, averaged for the lifetime of the cloud, is constant with altitude. It is also selected as the parameter λ, assuming that $\mu(z,\lambda) \equiv \lambda$. Hence we immediately derive an equation for $\eta(z, \lambda)$

$$\frac{\partial \eta_i(p,\lambda)}{\partial p} = -\frac{\lambda}{g\rho}\, \eta_i(p, \lambda). \qquad (13)$$

In this paper the physics of cloud clusters is investigated diagnostically on the basis of observational data. Therefore, the Q_1 and Q_2 values can be considered stipulated (they are determined on the basis of experimental data). Thus, expression (12) can be considered as an equation for obtaining $m_B(\lambda)$ if the λ_D distribution is known. (In forecasting problems, in order to describe the parameterization scheme completely and derive an equation for determining $m_B(\lambda)$, one other additional condition is required. For this purpose Arakawa and Shubert propose use of the hypothesis that a cloud ensemble is in a state of quasi-equilibrium with a large-scale effect.)

In determining $\lambda_D(p)$ we use the expression

$$h_c(p, \lambda) = \frac{1}{\eta_i(p, \lambda)} \left[h_B(\lambda) + \lambda \int_{p_B}^{p} \eta_i(p', \lambda)\, \bar{h}(p')\, dz(p') \right], \qquad (14)$$

which is derived by integration of the equation for conservation of the static energy of moist air in the cloud subensemble. Here $h_c(p, \lambda)$ and $h_B(\lambda)$ is the static energy of moist air of the subensemble λ at the levels p and p_B. We note that the choice $h_B(\lambda)$ and p_B for the time being is arbitrary. We will find $\lambda_D(p)$ from the condition that $h_c(p, \lambda)$ at the level of the outburst, where the cloud loses its buoyancy, coincides with $\bar{h}^*(p_D)$.

A similar problem in investigation of the properties of the cloud ensemble was solved in a study by Nitta [8]. That author used data from aerological sounding in the Trades zone, obtained during the BOMEX expedition. The sounding was carried out to an altitude of 500 mb. Integration was carried out with a 20-mb interval. In our case, since we will use observational data in GATE polygon AB at the principal isobaric surfaces, integration will be carried out with an interval 50 mb up to the 100-mb surface. As h_B we will take $h_B = \bar{h}^*(p_B)$, and p_B = 950 mb. This assumption means that all the clouds have an identical energy at their bases. The same condition is also used in [7, 8].

For numerical solution of the problem the entire troposphere from 950 to 100 mb is broken down into layers with a 50-mb interval. We will examine all the clouds having an outsurge between p_i and p_{i+1} and will assign them the mean value λ_i. Then the mass flux at the base of these clouds will be

$$M_B(\lambda_i) = \int_{\lambda_D(p_{i+1})}^{\lambda_D(p_i)} m_B(\lambda)\, d\lambda.$$

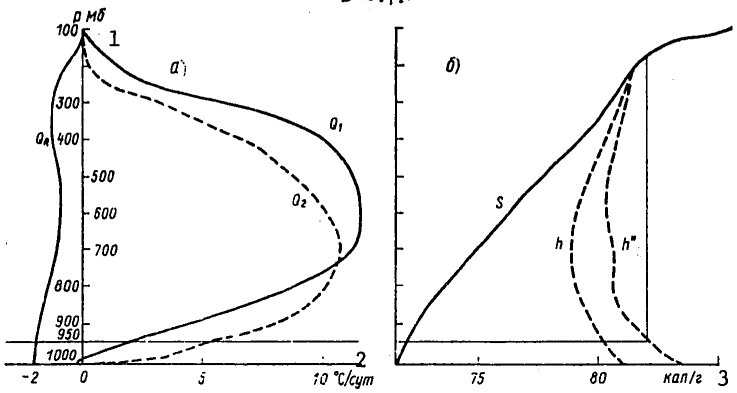

Fig. 1. Vertical profiles of the apparent heat source Q_1, apparent loss of moisture Q_2 and radiation cooling Q_R (a) and also profiles of static energy of dry (S), moist (h) and saturated air (h^*) (b)

KEY:
1. mb
2. °C/day
3. cal/g

It is also convenient to introduce the mean outsurge and entrainment (p_i, p_{i+1}). From the transcendental equation (14), by the iterations method, we find λ_i for each interval. Equation (12) is the Volterra integral equation of the second kind (in it the upper integration limit is dependent on p). Averaging this equation in the interval (p_i, p_{i+1}), it can be reduced to an algebraic system of equations for the unknowns $M_B(\lambda_i)$.

After finding M_B, having the corresponding parameterization of precipitation, it is already easy to compute all the parameters of the cloud ensemble. Now we will cite the results of computations on the basis of observational data for polygon AB in the GATE program. The computations were made for mean values in class "B" [4] (class "B" included situations when well-developed cumulonimbus cloud cover was observed over polygon AB).

Figure 1a shows the vertical profiles of the apparent heat source Q_1 and the apparent moisture loss Q_2 in units of heating rate. These values are means for class "B" (24 observation times in the first phase of observations in

polygon AB). The profiles shown here are very similar to the Q_1 and Q_2 profiles obtained by Yanai, et al. [9] for the Marshall Islands. True, since for us the averaging was carried out using cases of a strongly developed ICZ (class "B"), the maximum Q_1 and Q_2 values in our case are almost twice greater. The same as in [9], the Q_1 maximum is situated appreciably higher than the Q_2 maximum. In order to compute the vertical turbulent energy flux it is also necessary to know the profile of radiation cooling Q_R. Since direct measurements of Q_R were made in GATE only at nighttime, here we were forced to use the climatic profile Q_R obtained by Doplik and already used in a study by Yanai, et al. This profile is also shown in Fig. 1a.

Now we will proceed (Fig. 1b) to an investigation of the static energy of dry (S), moist (h) and saturated (h^*) air. In the upper troposphere (above 300 mb) these profiles were very close to the profiles obtained by Yanai, et al. [9]; on the other hand, in the lower troposphere the values of all three characteristics in our case were appreciably less.

In our opinion, this is attributable to the fact that the mean stratification, obtained using data registered on island stations, characterizes regions with the strongest convection, since clouds, as indicated in [5], are most frequently formed over the islands. The mean stratification for polygon AB, even when there is considerable cloud cover over the polygon, is far from the stratification within the cloud cluster. Polygon AB (a hexagon with a 3.5° side) is sufficiently large that together with regions of thick cloud cover there are regions with a Trades regime, where there is a predominance of descending compensation movements. Thus, the mean stratification in polygon AB does not give any idea about the maximum altitude of the clouds over them, as can be seen easily in Fig. 1b. Even under the condition $h_B = \overline{h}^*(p_B)$ the clouds cannot be above 175 mb, although $Q_1 - Q_2 - Q_R$ is still small there. Therefore, the latter two λ values were stipulated from the condition $\lambda_{n-1} = 1/2\lambda_{n-2}$ and $\lambda_n = 1/2\lambda_{n-1}$. We note that in the upper troposphere the difference $(\overline{h}^* - h)$ tends to zero and already at the level 100 mb becomes 2 orders of magnitude less than its values in the middle troposphere.

Figure 2a shows the distribution of the mass flux in clouds in dependence on the level of the outburst (on the mean altitude of the cloud). The same as in the study by Yanai, et al. [9], here there is a predominance of low and very high clouds. The mass flux in the clouds, responsible for the outsurge in the middle troposphere, is very small. This spectrum differs substantially from the spectrum obtained in a study by Nitta [8], where the Trades zone is investigated.

Figure 2b shows the vertical distribution of entrainment and outsurge of mass, computed by the described spectral method. Since different types of clouds are simultaneously operative at each level, the mean entrainment and expulsion of mass is observed at all altitudes. The entrainment has a maximum at the bottom, gradually decreasing with altitude. The outburst has two maxima. Figure 2 shows a bimodal distribution in the spectrum of the ensemble, that is, the coexistence of very powerful and very small clouds.

Clouds having an outburst in the middle troposphere from 700 to 400 mb are virtually absent. Similar results were obtained in the study by Yanai [9], where evidently special attention was turned for the first time to the bimodal nature of the distribution in the cloud ensemble spectrum.

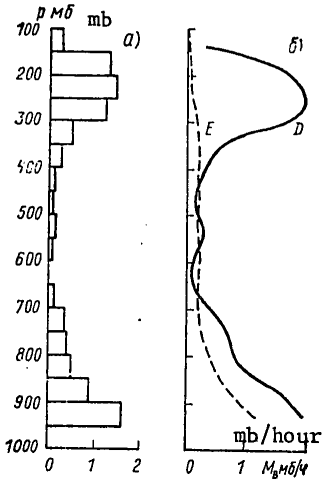

Fig. 2. Vertical mass flux at base of clouds in dependence on level of outsurge (a) and vertical profiles of entrainment (E) and outsurge of mass (D) in cloud ensemble (b).

Is this fact observed in nature? We do not know of its experimental confirmation. Physically it also for the time being is not validated and can be governed by the roughness of the model. In actuality, the numerical solution of integral equation (12) leads to a poorly stipulated system of algebraic equations (its eigenvalues differ by two orders of magnitude). The reason for this is that the coefficient $(\overline{h^*} - \overline{h})$ in equation (9) in the upper troposphere decreases rapidly and at the 100-mb level becomes very small. One of the reasons for the poor causality of the system can be failure to take the solid phase into account. The fact is that high clouds expel water not only in the liquid phase, but also in the solid phase. The latent heat of fusion brought into consideration also increases the maximum altitude of clouds in the calculations.

Now we will consider how the cloud ensemble equations change when the solid phase of water is taken into account. From the equation for the balance of static energy of dry air and water vapor it can be found that

$$Q_1 - Q_R = -M_c \frac{\partial \overline{s}}{\partial p} - LD\hat{l} - (L + L_1)\,\hat{Di}, \qquad (15)$$

$$-\frac{Q_2}{L} = -M_c\frac{\partial\overline{q}}{\partial p} + D\hat{l} + D\hat{i} + D(\overline{q}^* - \overline{q}). \tag{16}$$

Here L_1 is the latent heat of fusion, $\hat{l}(p)$ and $\hat{i}(p)$ are the quantity of the liquid and solid phases of water in the clouds having an outsurge at the level p.

Excluding $\hat{i}(p)$ from these equations, we arrive at the following form of the fundamental equation for a cloud ensemble:

$$Q_1 - Q_2' - Q_R = -M_c\frac{\partial(\overline{h} + L_1\overline{q})}{\partial p} + D[(L + L_1)(\overline{h}^* - \overline{h}) + L_1\hat{l}], \tag{17}$$

where

$$Q_2' = Q_2\frac{L + L_1}{L}.$$

For convenience it is proposed that the following concepts be introduced:

$$H = c_pT + gz + Lq + L_1q = h + L_1q,$$
$$H_c = c_pT + gz + Lq^* + L_1q^* + L_1l = h^* + L_1(q^* + l).$$

Here H and H_c are the total static energy of moist air and the total static energy of saturated air in the presence of the liquid phase, Lq is the energy reserve of 1 g of moist air which can be realized in the condensation of all the vapor present in it.

With allowance for the formation of the solid phase the potential energy reserve increases by the value L_1q, and in the presence of the liquid phase -- by $L_1(q^* + \hat{l})$. We note that in contrast to S, h, h^*, H and H_c will not be conserved when there is an adiabatic rising of a particle. Now the fundamental equation of the model assumes the form

$$Q_1 - Q_2' - Q_R = -M_c\frac{\partial\overline{H}}{\partial p} + D(\hat{H}_c - \overline{H}). \tag{18}$$

Whereas earlier the fundamental equation of model (9) included only two unknown parameters of the cloud ensemble M_c and D, the relationship between which was determined from expressions (10) and (11), now equation (18) also includes $\hat{l}$. Equation (18) was derived by a linear combination of the equations for the conservation of the static energy of dry air and water vapor. Here we have not used the equations for conservation of the liquid and solid phases, which obviously include precipitation.

But $\hat{l}$ is dependent on the rate of falling of precipitation and the formation of the solid phase. Therefore, for closing the problem it is necessary either to parameterize $\hat{l}$ or bring into consideration the balance equations for the liquid and solid phases in clouds.

Now we will proceed to the derivation of the remaining equations of the model. We will write the equations for the conservation of mass, S, q, $\hat{l}$, i for the k-th cloud at the entrainment level, considering the cloud to be steady or averaged for its lifetime:

$$E_k + \frac{\partial M_k}{\partial p} = 0, \tag{19}$$

$$E_k \overline{S} + \frac{\partial}{\partial p}(M_k S_k) + Lc_k + L_1 I_k + Q_{R_k} = 0, \tag{20}$$

$$E_k \overline{q} + \frac{\partial}{\partial p}(M_k q_k) - c_k = 0, \tag{21}$$

$$\frac{\partial}{\partial p}(M_k l_k) + c_k - I_k - R_k^l = 0, \tag{22}$$

$$\frac{\partial}{\partial p}(M_k i_k) + I_k - R_k^i = 0. \tag{23}$$

Here E_k is entrainment into the cloud, M_k is the vertical mass flux in the cloud, c_k is the condensation rate, I_k is the rate of water transformation into the solid phase, R_k^l and R_k^i are the rates of falling of precipitation in the liquid and solid phases, Q_{Rk} is radiation cooling.

Summing these equations for the cloud ensemble λ and assuming that all the clouds of the subensemble have identical characteristics, we can derive the expressions

$$\frac{\partial S_c(p,\lambda)}{\partial p} + \nu(p,\lambda)[S_c(p,\lambda) - \overline{S}(p)] = -Lc(p,\lambda) - L_1 I(p,\lambda) - Q_R, \tag{24}$$

$$\frac{\partial q_c(p,\lambda)}{\partial p} + \nu(p,\lambda)[q_c(p,\lambda) - \overline{q}(p)] = c(p,\lambda), \tag{25}$$

$$\frac{\partial l(p,\lambda)}{\partial p} + \nu(p,\lambda)\, l(p,\lambda) = -c(p,\lambda) + I(p,\lambda) + R^l(p,\lambda), \tag{26}$$

$$\frac{\partial i(p,\lambda)}{\partial p} + \nu(p,\lambda)\, i(p,\lambda) = -I(p,\lambda) + R^i(p,\lambda), \tag{27}$$

where

$$p,\lambda) = \frac{1}{\tau_i}\frac{\partial \eta(p,\lambda)}{\partial p}, \quad c(p,\lambda)$$

is determined from the expression

$$\sum_{\lambda_k \in (\lambda,\, \lambda + d\lambda)} c_k = c(p,\lambda)\, m_B(\lambda)\, d\lambda.$$

The remaining characteristics of the cloud subensemble are introduced similarly.

Multiplying (25) by $(L + L_1)$, (26) by L_1 and adding them with (24), we obtain the expression

$$\frac{\partial H_c(p,\lambda)}{\partial p} + \nu(p,\lambda)[H_c(p,\lambda) - \overline{H}(p)] = -Q_R(p,\lambda) + L_1 \overline{R}^l(p,\lambda). \tag{28}$$

Adhering to Arakawa and Shubert, radiation cooling in the entrainment layer will be neglected. Integrating equation (28), it is possible to derive an expression similar to (14). True, here for a determination of $\lambda_D(p)$ it is necessary to know the vertical distribution of the liquid phase in the clouds of the subensemble $l(p,\lambda)$ and the rate of precipitation formation $R^l(p,\lambda)$.

Unfortunately, data on the distribution of liquid water and ice are virtually lacking for great altitudes. Flights of sounding aircraft are limited to altitudes 7 km. Over the territory of the USSR the liquid phase at an altitude 7 km was observed at a temperature -43°C [1]. In very well-developed towers of cumulonimbus clouds in the tropics the presence of the liquid phase can be expected up to the tropopause. If without allowance for the solid phase such parameters of the cloud ensemble as M_B and D can be found without data on the distribution of the liquid phase with altitude and the rate of falling of precipitation, now their parameterization becomes necessary. Thus, allowance for the solid phase, although it improves the physical formulation of the problem, considerably complicates it.

BIBLIOGRAPHY

1. AVIATSIONNO-KLIMATICHESKIY ATLAS-SPRAVOCHNIK SSSR. Vyp. 3, T I. STATISTICHESKIYE KHARAKTERISTIKI PROSTRANSTVENNOY I MIKROFIZICHESKOY STRUKTURY OBLAKOV (Aviation-Climatic Atlas-Handbook of the USSR. No 3, Vol I. Statistical Characteristics of the Spatial and Microphysical Structure of Clouds), edited by L. S. Dubrovina, Moscow, Gidrometeoizdat, 1975.

2. Petrosyants, M. A., "Basic Problems and Preliminary Results of the Interdepartmental Expedition Under the Program of the National Tropical Experiment TROPEKS-72," TROPEKS-72, Leningrad, Gidrometeoizdat, 1974.

3. Petrosyants, M. A., "Work of the Interdepartmental Expedition TROPEKS-74 in GATE," TROPEKS-74, Vol I, Leningrad, Gidrometeoizdat, 1976.

4. Fal'kovich, A. I., "On the Problem of the Energy Balance in the ICZ," TROPEKS-74, T I, Leningrad, Gidrometeoizdat, 1976.

5. Fal'kovich, A. I., "Thermodynamic Parameters and Convective Instability in the Tropical Atmosphere," METEOROLOGIYA I GIDROLOGIYA (Meteorology and Hydrology), No 9, 1977.

6. Fal'kovich, A. I., "Convection, Conditional Instability and Interaction of Movements of Different Scales in the Tropics," METEOROLOGIYA I GIDROLOGIYA, No 2, 1978.

7. Arakawa, A., Shubert, W., "Interaction of a Cumulus Cloud Ensemble With the Large-Scale Environment. Part I," J. ATMOS. SCI., Vol 31, No 3, 1974.

8. Nitta, T., "Observational Determination of Cloud Mass Flux Distributions," J. ATMOS. SCI., Vol 32, No 1, 1975.

9. Yanai, M., Esbensen, S., Chu, J., "Determination of Bulk Properties of Tropical Cloud Clusters from Large-Scale Heat and Moisture Budgets," J. ATMOS. SCI., Vol 30, 1973.

UDC 551.509.313

ABOUT ONE METHOD FOR INCREASING THE ACCURACY OF DIFFERENCE SOLUTIONS IN FORECASTING WITH THE USE OF NESTED GRIDS

Moscow METEOROLOGIYA I GIDROLOGIYA in Russian No 8, Aug 79 pp 34-39

[Article by Candidate of Physical and Mathematical Sciences Ye. Ye. Kalenkovich, West Siberian Regional Scientific Research Hydrometeorological Institute, submitted for publication 20 November 1978]

Abstract: The author proposes a method for increasing the accuracy of difference solutions using solutions on a sequence of nested grids. The method is based on a minimization of the mean square error. It is demonstrated that the results are no worse than in the case of use of extrapolation to the limit according to Richardson. Ways are outlined to use the method for solution of the prognostic equations and experimental determination of the order of convergence of the schemes. Examples are given of computations of hemispherical and regional forecasts and their combination by the method described in the paper.

[Text] In application of the "telescoping" method, for example, in a combination of the hemispherical and regional models for part of an area, there are two or more solutions obtained using schemes with different intervals of the difference grid. In addition to the advantages given by the "telescoping" method as a result of the variable values at the boundary of the inner region, it is desirable to make use of the presence of several solutions within the region for increasing accuracy.

Recently the idea of extrapolation to the limit according to Richardson has been developed in a number of studies [2]. We will briefly discuss the essence of this method.

Assume that some difference scheme is convergent. Then for some equations it is possible to represent the solution of the difference problem u_i^h when $h \to 0$ in the form

$$u_i^h = (u)_i + \sum_{l=n}^{l-1} h^l (v)_i^{(l)} + \eta_i^h, \tag{1}$$

where u is a precise solution of the differential problem, h is the grid interval, i is the generalized number of the grid point of intersection, n is the order of convergence, $v^{(j)}$ are adequately smooth functions, not dependent on h, η^h is a grid function having the order $O(h^l)$.

Then, using the set $(l - n + 1)$ of solutions with successively decreasing steps, we find a linear combination of these solutions in which the second term in the representation (1) is equal to zero. Accordingly, the total solution will have the order of convergence h^l in the initial grid. Thus, this method will make it possible, using simple schemes of the first or second order of accuracy, to obtain higher-order solutions.

We will note some shortcomings of the extrapolation method. The equality (1) in essence is another method for formulating convergence of the scheme. Naturally, proof of the correctness of expansion (1) can be accomplished only for a limited class of problems. Another shortcoming is related to the asymptotic nature of expression (1). For example, in applying short-range weather forecasting models the restrictions on the capabilities of electronic computers do not make it possible to use very small intervals. It therefore follows that an increase in the order of the approximation with specific finite h values does not give a guarantee of an actual decrease in the error of the corrected solution for any norm in comparison with the initial solutions.

In this paper we propose a new method for the correction of difference solutions in which the norm of the error in the result in L_2 is not greater than the errors in the initial solutions in a sequence of grids. If expansion (1) is correct, then at least in the case of a combination of two solutions it is possible to demonstrate an increase in accuracy by the order h for the norm C.

Assume that we have two difference solutions u_1 and u_2 for some problem with the intervals h and mh, for which expansions of the type (1) are correct:

$$\vec{u}_1 = (\vec{u}) + h^n (\vec{v}) + h^{n+1} \vec{\eta}_{1},$$

$$\vec{u}_2 = (\vec{u}) + (mh)^n (\vec{v}) + (mh)^{n+1} \vec{\eta}_{2}. \tag{2}$$

Here m was selected in such a way as to avoid reinterpolation from one grid to another (that is, m is either a whole number or a fraction with a numerator equal to unity). The grid functions u_i, η_i are taken in a set of points of the coarser grid. The precise solution u and the function v are projected onto this same set. Thus, the dimensionality of the vectors in (2) is determined by the number of points in the coarse grid. It is easy to show that the linear combination

$$a'\vec{u}_1+b'\vec{u}_2,$$

where $$a'=\frac{m^n}{m^n-1},\quad b'=\frac{-1}{m^n-1} \tag{3}$$

approaches a precise solution with the order h^{n+1}.

We will demonstrate the following statement.

Theorem. The linear combination of solutions (2) $\vec{au}_1 + \vec{bu}_2$ with the coefficients a, b, minimizing the square of the error $[\vec{au}_1 + \vec{bu}_2 - (\vec{u})]^2$, converges to a precise solution with the order h^{n+1}.

Proof. We will assume that the vectors $\vec{u}_1$, $\vec{u}_2$ are linearly independent. We will introduce notations for the scalar products:

$$c=((\vec{u}),\ (\vec{u})),\ d=((\vec{u}),\ (\vec{v})),\ e=((\vec{v}),\ (\vec{v})),$$
$$f=((\vec{u}),\ \vec{\eta}_{11}),\quad g=((\vec{u}),\ \vec{\eta}_{12}),\ S=((\vec{v}),\ \vec{\eta}_{11}),\ t=((\vec{v}),\ \vec{\eta}_{12}), \tag{4}$$

$$k=(\vec{\eta}_{11},\ \vec{\eta}_{12}),\quad q=(\vec{\eta}_{11},\ \vec{\eta}_{11}),\quad r=(\vec{\eta}_{12},\ \vec{\eta}_{12}),$$

$$r_{11}=(\vec{u}_1,\ \vec{u}_1),\ r_{22}=(\vec{u}_2,\ \vec{u}_2),\ r_{12}=(\vec{u}_1,\ \vec{u}_2),$$
$$r_{01}=((\vec{u}),\ \vec{u}_1),\ r_{02}=((\vec{u}),\ \vec{u}_2).$$

Then, in accordance with the least squares method,

$$a=\frac{r_{01}r_{22}-r_{02}r_{12}}{\Delta},$$

$$b=\frac{r_{02}r_{11}-r_{01}r_{12}}{\Delta}, \tag{5}$$

$$\Delta=r_{11}r_{22}-r_{12}^2.$$

We will write expressions for the scalar products, denoted by the letter r with the subscripts, through the preceding values in (4):

$$r_{11}=c+2\,dh^n+2\,fh^{n+1}+eh^{2n}+2\,sh^{2n+1}+qh^{2n+2},$$
$$r_{22}=c+2\,d\,(mh)^n+2g\,(mh)^{n+1}+e\,(mh)^{2n}+2\,t\,(mh)^{2n+1}+$$
$$+r\,(mh)^{2n+2},$$
$$r_{12}=c+d\,(1+m^n)\,h^n+(f+gm^{n+1})\,h^{n+1}+em^nh^{2n}+ \tag{6}$$
$$+(s+tm)\,m^nh^{2n+1}+km^{n+1}\,h^{2n+2},$$
$$r_{01}=c+dh^n+fh^{n+1},$$
$$r_{02}=c+d\,(mh)^n+g\,(mh)^{n+1}.$$

We will denote the numerators in the expressions for a, b by r_a, r_b. Substituting (6) into (5), we obtain

$$\Delta = (m^n - 1)^2 (ce - d^2)\, h^{2n} + 2(1 - m^n)(cs - ctm^{n+1} + dg - df)\, h^{2n+1} +$$
$$+ [cq + crm^{2n+2} - 2\, ckm^{n+1} - (f - gm^{n+1})^2]\, h^{2n+2} + O(h^{3n+1}),$$
$$r_a = (m^n - 1)\, m^n (ce - d^2)\, h^{2n} + m^n [ctm\,(2m^n - 1) - cs + df +$$
$$+ dgm\,(1 - 2m^n)]\, h^{2n+1} + m^{n+1} [crm^{n+1} - ck + g(f - gm^{n+1})]\, h^{2n+2} +$$
$$+ O(h^{3n+1});$$
$$r_b = -(m^n - 1)(ce - d^2)\, h^{2n} + [cs(2 - m^n) - ctm^{n+1} +$$
$$+ df(m^n - 2) + dgm^{n+1}]\, h^{2n+1} + (cq - ckm^{n+1} + gfm^{n+1} -$$
$$- f^2)\, h^{2n+2} + O(h^{3n+1}).$$

Hence it can be seen that $a = a' + 0(h)$, $b = b' + 0(h)$ and $r_a + r_b = \Delta + 0(h^{3n+1})$, that is, $a + b = 1 + 0(h^{n+1})$. The theorem is proved.

Remark. If the last terms in (2) have the order $0(h^{n+2})$, then the accuracy of the total solution will have the order h^{n+2}.

Assume now that there are $(l - n + 1)$ solutions in successively more "bunched" grids. The proof of such a theorem for the general case of the combination $(l - n + 1)$ of solutions is difficult since it is necessary to investigate expansions in powers of h of determinants of the order $(l - n + 1)$. But if we limit ourselves to the requirement of an increase in the accuracy of the solutions at the norm of the space L_2, then as follows from the least squares method, the error in the total solution in a general case also will not be greater than the error in the corresponding solution obtained by extrapolation.

A shortcoming of the method described in the paper is the necessity for a precise solution. In prognostic models, even if there is convergence and it is assumed that there is a possibility of reckoning with grid intervals as small as desired, with a sufficient accuracy we can obtain a solution of the initial system of differential equations which is only some model of the atmosphere. Therefore, in the specific use of the described algorithm for a forecast it is necessary to check the stability of the coefficients of linear combinations of solutions or investigate the nature of their behavior with time. This will make it possible to carry out time extrapolation of the coefficients.

The described method can also be used for an experimental determination of convergence of the scheme and the order of the convergence. In actuality, if, for example, we compute the coefficients a, b in two solutions and

decrease the intervals, then with $h \to 0$ a, b should tend to a', b'. Then from expressions (3) it is possible to compute the order of accuracy n of the initial solutions.

Table 1

Comparison of Evaluations of Hemispherical and Regional Forecasts and Their Combination

Уровень, мб Level, mb	ε %			r %			σ м		
	1	2	3	1	2	3	1	2	3
1000	22	16	13	27	13	10	17	10	8
850	15	13	6	16	7	4	7	8	4
700	15	8	3	17	3	3	6	7	5
500	11	3	0	8	2	2	9	4	1
300	15	0	0	6	1	1	13	1	1
200	17	1	0	12	0	1	14	1	0

Note. First columns -- comparison of hemispherical and regional forecasts; second columns -- comparison of regional forecast and combined forecast with coefficients from (5); third column -- same for combination of fields with "prediction" of coefficients.

Now we will cite some preliminary results of computations using the proposed method. We used one of the variants of a "telescoped" system for prediction with full equations in an isobaric coordinate system [1]. The computations were made for two regions: outer, covering the greater part of the northern hemisphere (hemispherical model), and inner, adapted for short-range forecasting in the West Siberian region (regional model). The problems for both models were formulated uniformly and differ only in the substitution of the lateral boundary conditions: the condition of absence of flows through the lateral boundaries is set in the hemispherical model, whereas the regional model uses the results of the hemispherical forecast for correcting the values of the meteorological elements at the boundaries of the region. The turbulent terms in the equations of motion and the heat influx equation, and also in the equation for predicting the geopotential of the 1000-mb surface, being the lower boundary condition, were written in the form of the Laplacian of the corresponding function with the constant coefficient $5 \cdot 10^5$ m^2/sec. Only horizontal turbulence was taken into account. The horizontal interval in the hemispherical model was 600 km, in the regional model -- 300 km; the time intervals were 1 hour and 30 minutes respectively.

The coefficients a and b from (5) for the combination of the hemispherical and regional predicted geopotential fields, and also the standard evaluations: ε -- the relative error, r -- the correlation coefficient for the geopotential trends and the mean square error σ for each of the six levels (1000, 850, 700, 500, 300, 200 mb) were computed for a limited territory.

Table 2

Comparison of Evaluations of Two Hemispherical Forecasts With a Different Resolution and Their Combinations

Уровень, мб / Level, mb	ε %					r %					σ м				
	1	2	3	4	5	1	2	3	4	5	1	2	3	4	5
1000	11	22	18	—27	—4	13	21	14	—12	—3	4	14	10	—16	—4
850	12	8	8	—35	—8	8	7	4	—15	—6	3	7	5	—18	—4
700	18	5	4	—37	—6	8	2	1	—10	—3	4	5	4	—16	—4
500	9	3	2	—31	—7	5	1	0	—14	—4	4	3	2	—19	—4
300	7	2	0	—25	—6	5	1	0	—11	—2	6	1	0	—20	—4
200	14	0	—4	—21	—3	8	1	—2	—8	—2	8	1	—2	—17	—3

Note. first-third columns -- same as in Table 1, but instead of a regional forecast, a hemispherical forecast in a fine grid; fourth columns -- extrapolation of first-order schemes; fifth columns -- extrapolation of second-order schemes.

Table 1 gives the characteristics of improvement (for ε and σ -- decreases, for r -- increases) in the probable success of the forecasts. In the first columns, for each type of evaluation we give a comparison of the hemispherical and regional models, in the second columns -- a comparison of the regional model and a combination of models by the described method. These values were averaged for two 24-hour forecasts with real initial data for 4, 5 April 1965. The table shows that the regional model gives much better evaluations than the hemispherical model. We will assume that this is primarily a result of better horizontal resolution. A total forecast, even with the use of a relatively poor hemispherical forecast, at the lower levels has a considerable advantage over a regional forecast. At the upper levels the improvement is insignificant, but it must be taken into account that in the cited example very good evaluations were obtained above for the initial forecast using the regional model: for example, at the level 300 mb ε = 48%, r = 88%.

Although in a small number of examples it was impossible to ascertain the nature of behavior of the coefficients a, b with time, we nevertheless attempted to use the simplest method for their "prediction": employ for the combination of forecasts the coefficients obtained using computations for the preceding day. In the third columns in Table 1 we give the results of a comparison of these, already in a literal sense, forecasts with a regional model, showing that even with the simplest method of extrapolation of the coefficients a considerable increase in probable success is obtained at the lower levels.

We note that although optimization was carried out on the basis of σ, the ε and r evaluations are also improved.

In the next group of experiments we carried out a comparison of two hemispherical models with horizontal intervals 600 and 300 km. In contrast to the preceding computations, the time intervals were 2 hours and 1 hour and convective terms were not taken into account. There was also a difference in the method for comparing the forecasts. In the preceding experiments the hemispherical forecast was interpolated using bicubic splines, which does not impair the accuracy of solution for the dense network for which the comparison was also made. Here the initial data for a model with good resolution were interpreted bilinearly in a dense network and the forecasting results -- inversely in a fine second-order grid.

Table 2 gives the experimental results. The notations are the same as in Table 1, but in place of a regional model we took a hemispherical model in a fine grid. Here a similar effect was obtained: at the lower levels there is a considerable improvement in the quality of the combined forecast (even greater than in the preceding computations); deterioration at the 200-mb level is extremely insignificant.

We also checked the combination of forecasts by the extrapolation method. Taking into account that the model does not use two-cycle splitting [2], and accordingly the schemes have a first order with respect to time, we computed a linear combination with the coefficients a = 2, b = -1(m = 2, n = 1). The results of the comparison with the hemispherical model in a fine grid are represented in the four columns in Table 2. It can be seen that these forecasts with respect to many indices are even worse than forecasts using a coarse grid (mesh). Since with respect to space variables the schemes have a second order of approximation, we made a combination with the coefficients a = 4/3, b = -1/3 (fifth columns). The results show that the evaluations deteriorate at all levels, but nevertheless the order of the schemes was closer to the second, although it is not attained due to the coarse resolution. We note that the coefficients, with respect to formulas (5), in all the computations were different for different levels, positive and less than unity.

Thus, the results of the described experiments show the great promise of using the method described in the paper for a combination of forecasts. Further investigations must be carried out using longer series of initial data for the purpose of finding methods for predicting the coefficients.

BIBLIOGRAPHY

1. Kalenkovich, Ye. Ye., Novikova, N. V., Cholakh, I. V., "The Forecasting Problem for the Northern Hemisphere and a Region," TRUDY ZAP.-SIB. RNIGMI (Transactions of the West Siberian Regional Scientific Research Hydrometeorological Institute), No 41, 1978 (in press).

2. Marchuk, G. I., METODY VYCHISLITEL'NOY MATEMATIKI (Methods in Computational Mathematics), Moscow, Nauka, 1977.

UDC 551.509.313(-062.5)

DYNAMIC ASSIMILATION OF POTENTIAL AND WIND FIELDS IN THE LOW LATITUDES

Moscow METEOROLOGIYA I GIDROLOGIYA in Russian No 8, Aug 79 pp 40-48

[Article by Candidate of Physical and Mathematical Sciences A. F. Kivganov and U. Ch. Mokhanti, Odessa Hydrometeorological Institute, submitted for publication 24 October 1978]

Abstract: The article describes the formulation of experiments for the dynamic assimilation of the geopotential and wind fields within the framework of a regional barotropic model employing full equations with the use of some variants of boundary conditions and different initial data. The results of assimilation in the low latitudes are given.

[Text] Prognostic models with the full equations of hydrothermodynamics impose increased demands on the representativeness and assimilation of initial fields. For the filtering of high-frequency noise in the initial fields, and also their assimilation within the framework of a specific prognostic model the dynamic assimilation method has come into extensive use [7, 14, 25]. In the temperate latitudes, in addition to the geopotential field, the geostrophic wind is used [3, 7, 8]. In the low latitudes the quasigeostrophic approximation loses sense and the use of a solenoidal approximation involves serious difficulties in solving the wind balance equation. Therefore, it is unquestionably of interest to investigate the possibility of the use of information on the real wind for the purposes of a hydrodynamic forecast using full equations. The desirability of such an approach was mentioned in the studies of Krishnamurti, Washington, Gordon and others [11-13].

In this paper we discuss the results of experiments for the dynamic assimilation of the wind and geopotential fields within the framework of a regional (3-40°N; 60-120°E) barotropic model employing full equations with the use of different initial information. In addition, a study is made of the influence of different boundary conditions on the assimilation process.

The latter matter is acquiring special importance in the realization of regional forecasting schemes and contains a number of fundamental difficulties.

The dynamic assimilation of the initial fields is accomplished within the framework of a barotropic model using the full equations

$$\frac{\partial X}{\partial t} = F. \tag{1}$$

Here

$$X = \left\| \begin{matrix} u \\ v \\ \Phi \end{matrix} \right\|,$$

$$F = \left\| \begin{matrix} -u\frac{\partial u}{\partial x} - v\frac{\partial u}{\partial y} - \frac{\partial \Phi}{\partial x} + lv \\ -u\frac{\partial v}{\partial x} - v\frac{\partial v}{\partial y} - \frac{\partial \Phi}{\partial y} - lu \\ -u\frac{\partial \Phi}{\partial x} - v\frac{\partial \Phi}{\partial y} - \Phi\left(\frac{\partial u}{\partial x} + \frac{\partial v}{\partial y}\right) \end{matrix} \right\|,$$

where u, v are the horizontal components of the wind velocity vector, $\bar{\Phi}$ is geopotential, l is the Coriolis parameter, X and F are the matrix columns of the dependent variables and the right-hand side respectively.

The system of equations (1) is integrated in time in the form of a four-element Matsuno scheme, that is, the dynamic assimilation of the initial wind and geototential fields is accomplished using the pseudoforecasting method [7]. As is well known [6, 15], the Matsuno scheme leads to the appearance of computation viscosity, favoring a considerable decrease in the amplitude of high-frequency noise caused by errors in the measurement and analysis of the initial fields and also generated in the process of a finite-difference solution of system (1).

Thus, the Matsuno scheme is reduced to the four following elements:
forward forecast

$$X^*_{n+1} = X^\nu_n + \tau F(X^\nu_n),$$
$$X^\nu_{n+1} = X^\nu_n + \tau F(X^*_{n+1});$$

backward forecast

$$X^*_n = X^\nu_{n+1} - \tau F(X^\nu_{n+1}),$$
$$X^{\nu+1}_n = X^\nu_{n+1} - \tau F(X^*_n). \tag{2}$$

Here X^*_{n+1} and X^*_n is the preliminary X value at the times n + 1 and n respectively, τ is the time interval, ν is the number of the iteration.

Table 1

Dependence of $|\delta \overline{X}|$ and $|\delta X|_m$ on Different Formulation of Boundary Conditions

1	2 Подобласти															
	I				II				III				IV			
Вариант	$\|\delta\overline{\Phi}\|$	$\|\delta\Phi\|_m$	$\frac{\|\delta\overline{u}\|}{\|\delta\overline{v}\|}$	$\frac{\|\delta u\|_m}{\|\delta v\|_m}$	$\|\delta\overline{\Phi}\|$	$\|\delta\Phi\|_m$	$\frac{\|\delta\overline{u}\|}{\|\delta\overline{v}\|}$	$\frac{\|\delta u\|_m}{\|\delta v\|_m}$	$\|\delta\overline{\Phi}\|$	$\|\delta\Phi\|_m$	$\frac{\|\delta\overline{u}\|}{\|\delta\overline{v}\|}$	$\frac{\|\delta u\|_m}{\|\delta v\|_m}$	$\|\delta\overline{\Phi}\|$	$\|\delta\Phi\|_m$	$\frac{\|\delta\overline{u}\|}{\|\delta\overline{v}\|}$	$\frac{\|\delta u\|_m}{\|\delta v\|_m}$
1	0,4	0,9	$\frac{0,7}{1,3}$	$\frac{2,9}{3,3}$	1,1	1,6	$\frac{2,3}{1,8}$	$\frac{7,8}{3,0}$	0,3	0,8	$\frac{1,1}{1,6}$	$\frac{1,8}{3,2}$	0,3	0,9	$\frac{1,1}{0,6}$	$\frac{2,2}{2,6}$
2	0,7	3,4	$\frac{5,7}{3,8}$	$\frac{7,9}{9,9}$	1,2	1,8	$\frac{3,1}{2,3}$	$\frac{9,4}{5,9}$	0,4	0,8	$\frac{1,3}{1,7}$	$\frac{3,9}{3,3}$	0,4	0,9	$\frac{1,2}{1,1}$	$\frac{2,3}{4,4}$
3	0,5	1,7	$\frac{1,0}{0,9}$	$\frac{3,1}{1,7}$	1,1	1,6	$\frac{2,2}{1,1}$	$\frac{6,5}{2,5}$	0,3	0,8	$\frac{1,1}{1,4}$	$\frac{1,8}{3,2}$	0,3	0,7	$\frac{0,9}{0,6}$	$\frac{1,7}{2,5}$
	(0,7)	(2,1)	$\left(\frac{1,1}{1,0}\right)$	$\left(\frac{4,4}{3,1}\right)$	(1,5)	(2,2)	$\left(\frac{2,5}{1,5}\right)$	$\left(\frac{7,5}{3,2}\right)$	(0,5)	(1,1)	$\left(\frac{1,2}{1,6}\right)$	$\left(\frac{2,1}{3,6}\right)$	(0,4)	(0,9)	$\left(\frac{1,0}{0,7}\right)$	$\left(\frac{2,0}{2,9}\right)$
4	0,6	2,5	$\frac{1,8}{2,1}$	$\frac{3,5}{5,9}$	1,1	1,6	$\frac{2,3}{1,3}$	$\frac{8,5}{3,4}$	0,3	0,8	$\frac{1,1}{1,4}$	$\frac{2,0}{3,1}$	0,4	0,9	$\frac{1,0}{0,6}$	$\frac{2,0}{2,8}$

KEY:
1. Variant
2. Subregions

FOR OFFICIAL USE ONLY

The finite-difference approximation of the right-hand sides of system (1) is carried out using the F. Shuman scheme (advective form with a filtering factor [9]). The horizontal grid interval is 210 km (21 x 31), the time interval is 10 minutes. The l parameter is assumed to be variable.

In variant 1 on the boundary of the grid region the values of the X functions were kept constant on the boundary of the grid region. Such a boundary condition in combination with the filtering procedure was used in a regional prognostic scheme for the low latitudes [1].

In variant 2 there was stipulation of a boundary condition of the solid wall type

$$V_n|_\Gamma = 0, \tag{3}$$

where V_n is the normal component of the wind velocity vector on the contour Γ. The u and Φ values at the boundary are found directly from the equations of motion of the system (1).

The following boundary condition was set in variant 3:

$$D_\Gamma = \left(\frac{\partial V_s}{\partial s} + \frac{\partial V_n}{\partial n}\right)_\Gamma = 0, \tag{4}$$

where D is horizontal divergence, V_s is the tangential component of the wind velocity vector, $\partial/\partial n$ is the derivative along the normal to the boundary, $\partial/\partial s$ is the derivative along the contour.

In variant 4 for the westerly and easterly boundaries of the grid region there was stipulation of the splicing conditions for periodicity [13, 15], for the northerly and southerly boundaries -- the solid wall conditions (3).

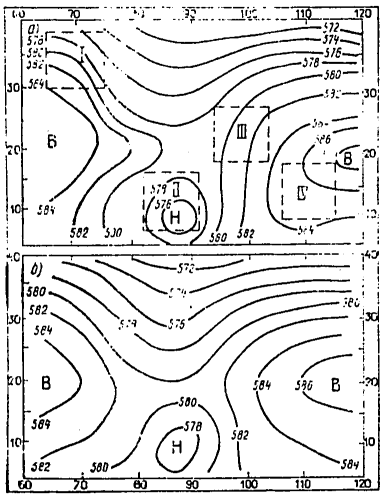

Fig. 1. Initial (a) and assimilated (b) AT_{500} fields at 0300 hours on 6 November 1973.

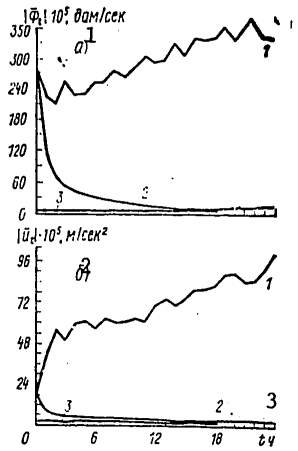

KEY:
1. dam/sec
2. m/sec^2
3. years

Fig. 2. Changes in $|\bar{\bar{\Phi}}_t|$ (a) and $|\bar{u}_t|$ (b) in process of dynamic assimilation and forecasting: 1) in forecast without assimilation; 2) in forecasting with assimilation; 3) in the assimilation process.

A comparison of the results of experiments with different formulation of the boundary conditions is given for four subregions I, II, III, IV (Fig. 1a), which were selected with circulation conditions taken into account. For each subregion (25 grid points of intersection) we computed the mean absolute differences of the assimilated and initial fields $|\delta\bar{X}|$ and the maximum values $|\delta X|_m$.

The results of the experiments, presented in Table 1, were obtained for a free assimilation regime when not one of the three fields u, v, $\Phi(\Psi)$ is regenerated either within or after completion of the Matsuno cycle. As the initial data we use the real wind, from which the stream function Ψ field [2] is computed with subsequent inversion of the wind balance equation. As the boundary conditions on the contour we stipulated the actual geopotential values and a solution of the equation was obtained by the iteration method for the internal region 5-38°N and 62-118°E. Thus, before the initialization process proper there is preliminary assimilation of the wind and geopotential fields within the framework of solenoidal equilibrium.

Figure 2 shows the dependence on the number of cycles (n), averaged for the entire region of assimilation of the absolute values of the trends $|\bar{u}_t|$ and $|\bar{\bar{\Phi}}_t|$ for variant 4. It can be seen that the greatest variability in the trends is observed during the first 4-5 hours of the pseudoforecast, and their variation is quite smooth. Therefore, for detecting the effect of influence of the boundary conditions on the process of assimilation the results of the experiments in Table 1 were obtained for 25 cycles corresponding to the characteristic adaptation time. The numerator gives the $|\delta\bar{u}|$ and $|\delta u|_m$ values; the denominator gives the $|\delta\bar{v}|$ and $|\delta\bar{v}|_m$ values; the figures in parentheses are the corresponding characteristics for 72 assimilation cycles.

An analysis of Table 1 shows that for the internal subregion III, and also the boundary subregion IV, characterized by a low-gradient pressure field, the results of all experiments differ little from one another, that is, the assimilation is virtually not dependent on the type of boundary conditions. For subregion I -- a region with high pressure gradients -- the solid wall condition gives the poorest results in comparison with the other boundary conditions. The changes in $|\delta \overline{X}|$ in subregion II for all variants are much greater than for the remaining subregions. This can be attributed to the presence of a tropical cyclone, inadequate initial information and closeness to the boundary. A comparison of experiments 2 and 4 shows that the splicing condition for periodicity for the eastern and western boundaries leads to an appreciable decrease in the $|\delta X|$ values.

Thus, an analysis of the results shows that for regional prognostic schemes in the low latitudes it is possible to use boundary conditions in the form of variants 3 and 4 as being the most preferable. However, further experiments for developing a regional prognostic scheme indicated that the best forecasting results are obtained from the use of a boundary condition in the form of variant 4 in comparison with variant 3. Therefore, all the subsequent results from this study were obtained using a boundary condition in the form of variant 4.

We also note that in the wind and geopotential fields, obtained 18 hours after the pseudoforecast, high-frequency noise is virtually absent, and therefore no need arises for additional use of space filters.

Now we will discuss the content of experiments in the field of dynamic assimilation with different initial data.

Scheme 1. As the initial field we will use the real wind field. The geopotential field is reconstructed on the basis of the wind field by means of computing the stream function Ψ with subsequent inversion of the balance equation. In the assimilation process the fields are not regenerated, that is, we solve the reciprocal adaptation problem (so-called free assimilation regime). This scheme was used above in obtaining the results represented in Table 1.

Scheme 2. The initial fields are the actual wind and geopotential fields, that is, independent fields. A free assimilation regime is carried out.

Scheme 3. The geopotential and wind fields are stipulated the same as in scheme 1, but in the assimilation process the wind field is regenerated before the onset of this cycle, that is there is solution of the problem with reconstruction of the geopotential field on the basis of the wind field.

Scheme 4. In contrast to scheme 3, in this experiment there is introduction of artificial "mismatching of the fields," when the values of the wind velocity components are assumed equal to half the values of the real wind.

Scheme 5. The initial fields are stipulated completely in accordance with scheme 1, but instead of the Matsuno procedure, in the free assimilation process use is made of the Okamura scheme

$$X^*_{n+1} = X^\nu_n + \tau F(X^\nu_n); \quad X^{**}_n = X^*_{n+1} - \tau F(X^*_{n+1}); \qquad (5)$$

$$X^{\nu+1}_n = 3X^\nu_n - 2X^{**}_n,$$

having, in comparison with the Matsuno cycle, a doubled damping characteristic curve [4].

Table 2

$|\delta\overline{X}|$ and $|\delta X|_m$ Values for Different Assimilation Schemes

Схема Scheme	$\lvert\delta\overline{\Phi}\rvert$	$\lvert\delta\Phi\rvert_m$	$\lvert\delta\overline{u}\rvert$	$\lvert\delta u\rvert_m$	$\lvert\delta\overline{v}\rvert$	$\lvert\delta v\rvert_m$
1	0,4 (0,7)	2,5 (3,0)	1,1 (1,3)	8,7 (9,6)	1,1 (1,3)	3,6 (4,1)
2	0,7 (1,1)	3,3 (4,2)	1,1 (1,4)	8,8 (9,6)	1,1 (1,4)	3,6 (4,1)
3	0,6	2,8	—	—	—	—
4	1,2	4,1	—	—	—	—
5	0,8	3,0	1,3	9,2	1,3	(4,1)

The results of the experiments are given in Table 2, where the $|\delta\overline{X}|$ and $|\delta X|_m$ values relate to the entire assimilation region (the corresponding values for 72 cycles are given in parentheses).

The results obtained using scheme 1 show that geopotential changes in the assimilation process are small. This is possible due to two principal factors: as a result of the procedure of preliminary assimilation of the geopotential and wind fields within the framework of a solenoidal approximation and as a result of the specifics of the adaptation process itself, caused by the smallness of the Coriolis parameter and pressure gradients in the low latitudes.

As an example, Fig. 1 shows the initial and assimilated geopotential fields 18 hours after the pseudoforecast. The comparison shows that the nature of the field did not change in the assimilation process; the pressure gradients in this case somewhat decreased, especially in the region of pressure formations.

A comparison of the results obtained using schemes 1 and 2 shows that the $|\delta\overline{u}|$ and $|\delta\overline{v}|$ values, and also $|\delta u|_m$ and $|\delta v|_m$ differ insignificantly (0.1-0.2 m/sec), whereas the mean and maximum absolute differences of the geopotential fields in scheme 2 are greater than in scheme 1 by a factor of 1.5-2, although as before, they remain small, not exceeding 0.7 dam, and

their maximum values are 4 dam.

This comparison gives basis for concluding that in the low latitudes, the same as in the temperate latitudes, the geopotential field adjusts to the wind field. This is also confirmed by a comparison of the results obtained using schemes 1 and 3. With an increase in the "mismatching" of the initial fields (schemes 3 and 4) the change in the geopotential field occurs more intensively in the adaptation process. This is also correct for the free assimilation regime (schemes 1 and 2).

The difference in the results obtained using schemes 1 and 5 can be attributed to the fact that when using the Okamura method the assimilated fields are obtained more averaged than in the Matsuno method as a result of an increase in computation viscosity and in this case the assimilation process transpires far more intensively.

Comparison of assimilation processes in the low and temperate latitudes for similar experiments [7] indicated that the reaching of a steady regime in the low latitudes is attained somewhat earlier than in the temperate latitudes.

The effectiveness of the process of assimilation of initial fields was checked in a series of experiments for developing a regional prognostic scheme. It can be seen from an analysis of Fig. 2 that the prognostic trends $|\overline{X}_t|$ increase rapidly in experiments using nonassimilated initial fields in the forecasting process, reflecting clear indications of computation instability. In contrast, in a forecast using assimilated fields no significant fluctuations are noted in the course of the averaged trends during the course of the entire time of the forecast.

However, in the predicted fields themselves, obtained using assimilated data, especially near the boundaries, there is a localization of high-frequency oscillations with a wavelength of about two grid intervals. This noise is generated in a prognostic model, in particular, due to the boundary conditions, and can be suppressed using spatial-temporal filters. Thus, in contrast to the problem of assimilation in a prognostic regional model it is necessary to have additional filtering of high-frequency noise. In this study the spatial filter, based on the procedure of "smoothing-desmoothing" of prognostic fields [5], was applied after each four time intervals (the time interval in the forecasting scheme was assumed equal to 5 minutes). This made possible a complete filtering of noise in the entire forecasting region.

The effectiveness of the assimilation process and filtering can also be judged using the data in Table 3, which gives the results of a spectral breakdown of the kinetic energy K of the initial and predicted fields for 6-7 November 1973. Here use was made of the fast Fourier transform method [10] and a filter with the parameter $\beta = 0.07$.

Table 3

Results of Spectral Analysis of Kinetic Energy

Характеристика спектра 1	Исходное поле 2		Прогностическое поле 3			Фактическое поле 4
	без соглас. 5	с согласов. 6	без соглас. 5	с соглас. 6	с соглас. и фильтр. 7	
8 Фон (K_0); $m=0$	1034	1019	1867	920	889	924
9 Длинные волны $L>3400$ км; $m=1, 2$	207	162	406	158	149	218
10 Синоптические волны 1100 км $\leqslant L<3400$ км; $m=3\div6$	16	10	1413	16	10	41
11 Короткие волны 420 км $\leqslant L<1100$ км; $m=7\div15$	7	5	212	9	2	19
$\sum_{m=0}^{15} K_m$	1264	1196	3898	1103	1050	1202
$\sum_{m=0}^{15} K_m/K_0$	1,2	1,2	2,1	1,2	1,2	1,3

12 Примечание. m — волновое число, L — длина волны.

KEY: 1) Spectral characteristics; 2) Initial field; 3) Predicted field; 4) Actual field; 5) Without assimilation; 6) With assimilation; 7) With assimilation and filtering; 8) Background; 9) Long waves; 10) Synoptic waves; 11) Short waves; 12) Note. m -- wave number, L -- wavelength

It can be seen from an analysis of Table 3 that the assimilation and filtering regimes are expressed first and foremost in the short-wave range, to a lesser degree -- in the synoptic and long-wave ranges, and there is virtually no change in the kinetic energy of zonal flow.

A comparison with the results of a forecast made using unassimilated fields indicated that the assimilation and filtering regimes are indispensable parts of a regional forecasting model using full equations in the low latitudes.

In conclusion, the authors consider it their pleasant duty to express appreciation to M. S. Fuks-Rabinovich and L. V. Berkovich for useful comments and advice expressed in the course of discussion of the results of this study.

BIBLIOGRAPHY

1. Bedi, Kh. S., Datta, R. K., Krichak, S. O., "Numerical Forecast of Meteorological Elements Under Summer Monsoon Conditions," METEOROLOGIYA I GIDROLOGIYA (Meteorology and Hydrology), No 5, 1976.

2. Kivganov, A. F., Mokhanti, U. Ch., "Computation of the Stream Function With Different Formulation of Boundary Conditions," METEOROLOGIYA, KLIMATOLOGIYA I GIDROLOGIYA (Meteorology, Climatology and Hydrology), Kiev, No 14, 1978.

3. Kluge, I., Esberg, E., "Effectiveness of Some Methods for Assimilation of the Geopotential and Wind Fields," METEOROLOGIYA I GIDROLOGIYA, No 1, 1976.

4. Nitta, T., "Preparation of Initial Data and Objective Analysis for a Model of Primitive Equations," TRUDY VTOROGO TOKIYSKOGO SIMPOZIUMA PO CHISLENNYM METODAM PROGNOZA POGODY (Transactions of the Second Tokio Symposium on Numerical Weather Forecasting Models), Leningrad, 1971.

5. Spektorman, A. D., Fuks-Rabinovich, M. S., "Baroclinic Prognostic Model Using the Full Equations of Atmospheric Dynamics With Detailed Horizontal Resolution," TRUDY GIDROMETTSENTRA SSSR (Transactions of the USSR Hydrometeorological Center), No 180, 1976.

6. Fal'kovich, A. I., Yurko, T. A., "Wind Reconstruction in the Low Latitudes by the Dynamic Assimilation of Fields Method," TRUDY GIDROMETTSENTRA SSSR (Transactions of the USSR Hydrometeorological Center), No 103, 1972.

7. Fedorova, N. G., Fuks-Rabinovich, M. S., "On Dynamic Assimilation of Initial Fields for Models Using Full Equations in Hydrothermodynamics," METEOROLOGIYA I GIDROLOGIYA, No 5, 1972.

8. Fedorova, N. G., "Application of the Method of Dynamic Assimilation of Fields in Computing Wind for a Prognostic Model in the Full Equations of Hydrodynamics," TRUDY GIDROMETTSENTRA SSSR, No 103, 1972.

9. Shuman, F. G., Stekaul, Dzh. D., "On the Problem of Writing Finite-Difference Equations With Allowance for Map Scale," LEKTSII PO CHISLENNYM METODAM KRATKOSROCHNOGO PROGNOZA POGODY (Lectures on Numerical Methods for Short-Range Weather Forecasting), Leningrad, Gidrometeoizdat, 1969.

10. Cooley, J. W., Tukey, J. W., "An Algorithm for the Machine Calculation of Complex Fourier Series," MATH. COMPUT., Vol 19, 1965.

11. Gordon, C. G., Umscheid, L., Miyakoda, K., "Simulation Experiments for Determining Wind Data Requirements in the Tropics," J. ATMOS. SCI., Vol 29, No 6, 1972.

12. Houghton, D. D., Washington, W. M., "On Global Initialization of the Primitive Equations," Part I, J. APPL. METEOROL., Vol 8, No 5, 1969.

13. Krishnamurti, T. N., "An Experiment in Numerical Weather Prediction in Equatorial Latitudes," QUART. J. ROY. METEOROL. SOC., Vol 95, No 405, 1969.

14. Miyakoda, K., Moyer, R. W., "A Method of Initialization of Dynamical Weather Forecasting," TELLUS, Vol 20, No 1, 1968.

15. Nitta, T., Hovermale, B. J., "A Technique of Objective Analysis and Initialization for the Primitive Forecast Equations," MON. WEATHER REV., Vol 97, No 9, 1969.

UDC 551.509.313(-062.4)

TWO NONLINEAR PROBLEMS IN DYNAMICS OF THE EQUATORIAL ATMOSPHERE

Moscow METEOROLOGIYA I GIDROLOGIYA in Russian No 8, Aug 79 pp 49-54

[Article by S. Evtimov, Professor S. Panchev and R. Chakalov, Sofia University, Bulgaria, submitted for publication 6 December 1978]

Abstract: The authors have derived precise solutions for two stationary systems of equations (1)-(3) and (17)-(20) modeling movements in the equatorial atmosphere. The peculiarities of these solutions are discussed.

[Text] First Problem. Dobryshman [2] proposed the following dimensionless system of equations of motion for the equatorial atmosphere:

$$v\frac{\partial u}{\partial y}+w\frac{\partial u}{\partial z}=yv-w, \tag{1}$$

$$v\frac{\partial v}{\partial y}+w\frac{\partial v}{\partial z}=-yu-\frac{\partial \Phi}{\partial y}, \tag{2}$$

$$\frac{\partial v}{\partial y}+\frac{\partial w}{\partial z}=0, \tag{3}$$

where x, y, z are the axes of coordinates directed to the east, north and zenith respectively; u, v, w are the velocity components and $\partial\Phi/\partial y$ is the meridional pressure gradient. The latter is usually considered stipulated, that is, system (1)-(3) is closed. It has been solved by many authors and by different methods [2, 3, 5, 6, 9]. Here we propose still another class of elementary precise solutions which can have importance in the interpretation of observed atmospheric circulation in the equatorial region. In addition to (u, v, w), a solution is obtained for Φ. This is achieved by the introduction of requirements on the separation of variables, which is equivalent to the addition of a new equation to (1)-(3).

In actuality, in accordance with (3) we write that

$$\begin{aligned} v(y, z)&=f(y)h'(z),\\ w(y, z)&=-f'(y)h(z), \end{aligned} \tag{4}$$

where the prime denotes differentiation for the argument. Then equations (1) and (2) assume the form

$$\frac{h'}{h}\left(\frac{\partial u}{\partial y} - y\right) - \frac{f'}{f}\left(\frac{\partial u}{\partial z} + 1\right) = 0, \tag{5}$$

$$ff'(h'^2 - hh'') = -yu - \frac{\partial \Phi}{\partial y}. \tag{6}$$

In order for the variables to be separated in equation (5) it must be assumed that

$$\frac{\partial u}{\partial y} - y = A(z), \quad \frac{\partial u}{\partial z} + 1 = B(y), \tag{7}$$

where A(y) and B(z) for the time being are arbitrary functions. However, $\partial^2 u/\partial y \partial z = \partial^2 u/\partial z \partial y$, hence we obtain $A'(z) = B'(y) = \beta = \text{const}$, which gives $A(z) = \beta(z - z_0)$ and $B(y) = \beta y$. Substituting this into (7) and integrating, we obtain an expression for zonal velocity

$$u(y, z) = u_0 + \frac{1}{2}y^2 + (\beta y - 1)(z - z_0), \tag{8}$$

where $z_0 > 0$ is some fixed altitude. This is a new equation which closes the system (1)-(3).

Now equation (5) assumes the form

$$\frac{h'}{h}\beta(z - z_0) = \frac{f'}{f}\beta y = \alpha_1 = \text{const}. \tag{9}$$

After integration we find

$$\begin{aligned} f(y) &= f_0 y^\alpha, \\ h(z) &= h_0 (z - z_0)^\alpha, \end{aligned} \tag{10}$$

where $\alpha = \alpha_1/\beta$, and f_0, h_0 are the integration constants. Finally, from equation (6) we also obtain the pressure field

$$\frac{\partial \Phi}{\partial y} = -yu - v_0^2 \alpha^2 y^{2\alpha-1}(z - z_0)^{2\alpha-2}, \tag{11}$$

where $v_0^2 = f_0 h_0$, and u(y, z) is given by expression (8). Finally, for solving the initial system we obtain

$$\begin{aligned} u(y, z) &= u_0 + \frac{1}{2}y^2 + (\beta y - 1)(z - z_0), \\ v(y, z) &= \alpha v_0 y^\alpha (z - z_0)^{\alpha-1}, \\ w(y, z) &= -\alpha v_0 y^{\alpha-1}(z - z_0)^\alpha, \\ \Phi(y, z) &= \Phi_0 - \frac{1}{2}u_0 y^2 - \frac{1}{8}y^4 - \left(\frac{5}{3}y^3 - \frac{1}{2}y^2\right)(z - z_0) - \\ &\quad - \frac{\alpha}{2}v_0^2 y^{2\alpha}(z - z_0)^{2(\alpha-1)}. \end{aligned} \tag{12}$$

This solution has the free parameter α. Varying this, it is possible to derive formulas approximating the real wind and pressure fields in the equatorial atmosphere. In order that there be no singularities in (12), it is necessary to adhere to the conditions

$$\alpha \geqslant 1 \quad \text{or} \quad \alpha = 0. \tag{13}$$

We will examine some special cases. Assume that $\alpha = 0$. Then, in accordance with (12),

$$v = w = 0,$$
$$u = u_0 + \frac{1}{2} y^2 + (\beta y - 1)(z - z_0), \tag{14}$$
$$\partial \Phi / \partial y = -yu,$$

that is, we have obtained purely zonal geostrophic motion.

Such a conclusion also follows directly from the initial system with v = w = 0, with the exclusion of an explicit dependence of u and Φ on y and z in accordance with (14). As can be seen from (14), at the altitude $z = z_0$ the F field is symmetric, and the equation $\partial \Phi / \partial y = 0$ has the roots $y_1 = 0$ and $y_{2,3} = \pm \sqrt{-2u_0}$. With $u_0 < 0$ (easterly wind at the equator itself) Φ has a minimum at the equator and a maximum at latitudes $y_{2,3} = \pm \sqrt{-2u_0}$. With $u_0 > 0$ Φ has one extremum (maximum) at the equator. At other altitudes ($z \neq z_0$) the number and form of the extrema will be determined by the relationship of the parameters u_0, β and $z - z_0$. We also note that a geostrophic solution in the case of a symmetric pressure field was also obtained by Bulakh [1].

We will assume that $\alpha = 1$. We obtain

$$v = v_0 y,$$
$$w = -v_0 (z - z_0), \tag{15}$$
$$\partial \Phi / \partial y = -yu - v_0^2 y.$$

In this example v_0 has the sense of meridional (dimensionless) velocity at the boundary y = 1 of the equatorial atmosphere. If $v_0 = 0$ there, then, as can be seen from (15), in the entire region $|y| \leqslant 1$ we will have v = w = 0 and a geostrophic balance between u and $\partial \Phi / \partial y$.

Finally, if $\alpha = 2$, then

$$v = 2v_0 y^2 (z - z_0),$$
$$w = -2v_0 y (z - z_0)^2, \tag{16}$$
$$\partial \Phi / \partial y = -yu - 4v_0^2 y^3 (z - z_0)^2.$$

It can be seen that $v_0 = \frac{1}{2} \frac{\partial v}{\partial z}\Big|_{y=1}$,

that is, v_0 is proportional to the vertical gradient of meridional velocity at the discontinuity y = 1 of the equatorial atmosphere. If $v_0 = 0$, we again arrive at the preceding derivation.

The selection of a specific solution from all the possible solutions must be made on the basis of their comparison with observational data.

Second Problem

For seeking wave solutions the authors of [4] proposed a more complete system of equations of motion, which in dimensional form reads

$$\frac{du}{dt} = 2\omega\left(\frac{y}{r_0}v - w\right), \tag{17}$$

$$\frac{dv}{dt} = -\frac{1}{\rho}\frac{\partial p}{\partial y} - 2\omega\frac{y}{r_0}u, \tag{18}$$

$$\frac{dw}{dt} = -\frac{1}{\rho}\frac{\partial p}{\partial z} + 2\omega u - g, \tag{19}$$

$$\frac{\partial v}{\partial y} + \frac{\partial w}{\partial z} = 0, \tag{20}$$

where $\frac{d}{dt} = \frac{\partial}{\partial t} + v\frac{\partial}{\partial y} + w\frac{\partial}{\partial z}$,

r_0 is the earth's radius, ω is the angular velocity of its rotation. On the basis of this system we will investigate the influence of Coriolis force on stationary movements of the equatorial atmosphere within the framework of its zonal model.

Introducing, as usual, the stream function Ψ, $v = -\partial\Psi/\partial z$, $w = d\Psi/dy$, we obtain from (17) and (18)-(19) respectively

$$\frac{\partial}{\partial t}U + \{\Psi, U\} = 0, \tag{21}$$

$$\frac{\partial}{\partial t}\Delta\Psi + \{\Psi, \Delta\Psi\} = \{U, \Omega\}, \tag{22}$$

where $\Delta\Psi$ and $\{A, B\}$ are the Laplacian and the Jacobian for the variables y, z,

$$\Omega = -\frac{\omega}{r_0}y^2 + 2\omega z, \quad U = u + \Omega. \tag{23}$$

With $\partial/\partial t = 0$ equations (21) and (22) give

$$U = F(\Psi), \tag{24}$$

$$\{\Psi, \Delta\Psi - F'(\Psi)\Omega\} = 0, \tag{25}$$

where $F' = dF/d\Psi$, and $F(\Psi)$ is an arbitrary function.

Integrating (25), with (23) taken into account, we obtain the equation

$$\Delta\Psi - \left(2\omega z - \frac{\omega}{r_0}y^2\right)F'(\Psi) = H(\Psi), \tag{26}$$

where $H(\Psi)$ is also an arbitrary function. The further solution of (26) is possible only after the specific choice of $F(\Psi)$ and $H(\Psi)$. For this we use physical considerations.

Since the initial system (17)-(20) does not contain derivatives of x (zonality), it will apply only near the equator, where this condition is approximately satisfied. Outside this region, due to the well-expressed zonal transfer, meridional and vertical movements must be absent. Accordingly, solutions of equation (26) must be localized near the equator, that is, with increasing distance from the latter Ψ and its derivatives must tend rather rapidly to zero. Then it follows from (26) that

$$F'(0)=H(0)=0 \quad \text{when} \quad y\to\pm\infty. \tag{27}$$

Limiting ourselves to the first nontrivial terms in the expansion of the $F(\Psi)$ and $H(\Psi)$ functions, we obtain

$$F(\Psi)=\delta+\frac{\alpha}{2}\Psi^2, \quad H(\Psi)=\beta\Psi, \tag{28}$$

where α, β, δ are constants.

These expressions for F and H correspond to a regime of "weak nonlinearity" and a "weak influence" of Coriolis force. It is a circumstance of not a little importance that only in this case is it possible to obtain a precise analytical solution of equation (26).

In actuality, substituting (28) into (26), we find the linear equation

$$\Delta\Psi-\left(2\,\omega\alpha z-\frac{\omega\alpha}{r_0}\,y^2\right)\Psi=\beta\Psi, \tag{29}$$

which formally coincides with the stationary Shrödinger equation.

We will solve (29) by the method of separation of variables:

$$\Psi(y, z)=Y(y)Z(z).$$

Substituting into (29), we obtain two boundary problems:

$$Y''+\left(\frac{\omega z}{r_0}\,y^2-\mu\right)Y=0, \quad Y(\pm\infty)=0; \tag{30}$$

$$Z''-(2\,\omega\alpha z+\nu)\,Z=0, \quad Z(0)=Z(h)=0, \tag{31}$$

where $\mu+\nu=\beta$, and h is the altitude of the atmospheric layer where movement occurs. In other words, we will assume that w(0) = w(h) = 0 ("solid top" condition).

The solution of equation (30) has the form

$$Y=e^{-\xi^2/2}\sum_n A_n H_n(\xi), \quad \xi=\left(\frac{\omega|\alpha|}{r_0}\right)^{1/4} y, \tag{32}$$

where $H_n(\xi)$ are Hermite polynomials [7] and α and μ are related by the expression

$$\left(\frac{\omega|\alpha|}{r_0}\right)^{-\frac{1}{2}}\mu = -2n-1, \quad \alpha<0, \tag{33}$$

n is a whole number, A_n are constants.

Introducing into (31) the new variable

$$\eta(z) = (2\omega\alpha)^{1/3} z + \nu (2\omega\alpha)^{-2/3},$$

we write equation (31) in the form

$$Z'' - \eta Z = 0. \tag{34}$$

A general solution of this equation is given by the Airy functions [8]

$$Z(\eta) = C_1 A_i(\eta) + C_2 B_i(\eta). \tag{35}$$

Assume that $\eta_0 = \eta(0)$ and $\eta_h = \eta(h)$. Since $\alpha < 0$, then $\eta_k < \eta_0$. The functions $Ai(\eta)$ and $Bi(\eta)$ are monotonic when $\eta > -1.02$ and, oscillating, tend to zero when $\eta \to -\infty$. Accordingly, the boundary conditions (31) will be satisfied if $\eta_h < -1.02$, and, as it is easy to see, if

$$Ai(\eta_0)\, Bi(\eta_h) - Ai(\eta_h)\, Bi(\eta_0) = 0. \tag{36}$$

With fixed h this transcendental equation relates α and ν. In addition, $C_2 = -C_1 Ai(\eta_0) / Bi(\eta_0)$.

Thus, for the stream function we finally obtain

$$\Psi(y, z) = e^{-\xi^2/2}\left[Ai(\eta) - \frac{Ai(\eta_0)}{Bi(\eta_0)} Bi(\eta)\right] \Sigma A_n H_n(\xi). \tag{37}$$

and the constant C_1 is included in A_n. It can be seen that the solution (37) contains the free constants A_n, δ, α and h. They determine different possible regimes of cellular circulation.

In conclusion it can be stated that within the framework of a stationary zonal model of the equatorial atmosphere the fundamental effect of Coriolis force is a strong localization of vertical and meridional movements near the equator and the setting in of a cellular circulation regime.

The authors express appreciation to Ye. M. Dobryshman for discussion of the problems touched upon in this work.

BIBLIOGRAPHY

1. Bulakh, B. M., "Correlation Between Wind Velocity and Pressure at the Equator," IZV. AN SSSR, FIZIKA ATMOSFERY I OKEANA (News of the USSR Academy of Sciences, Physics of the Atmosphere and Ocean), Vol VII, No 3, 1971.

2. Dobryshman, Ye. M., "Some Peculiarities of Circulation in the Troposphere in the Equatorial Region," METEOROLOGIYA I GIDROLOGIYA (Meteorology and Hydrology), No 5, 1964.

3. Dobryshman, Ye. M., Fal'kovich, A. N., "Some Models of Stationary Movement of Air in the Equatorial Zone," METEOROLOGIYA I GIDROLOGIYA, No 7, 1967.

4. Dobryshman, Ye. M., "Wave Movements in the Equatorial Zone (Zonal Model)," METEOROLOGIYA I GIDROLOGIYA, No 1, 1977.

5. Ingel', L. Kh., "A Model of Circulation in the Troposphere in the Low Latitudes," METEOROLOGIYA I GIDROLOGIYA, No 9, 1975.

6. Panchev, S., Chakalov, R., "One Class of Precise Solutions of Nonlinear Equations of Dynamics of the Equatorial Atmosphere," KHIDROLOGIYA I METEOROLOGIYA (Hydrology and Meteorology), Sofia, No 5, 1974.

7. Smirnov, V. I., KURS VYSSHEY MATEMATIKI (Course in Higher Mathematics), Part 2, Vol III, Moscow, Nauka, 1974.

8. Fok, V. A., PROBLEMY DIFRAKTSII I RASPROSTRANENIYA ELEKTROMAGNITNYKH VOLN (Problems in Diffraction and Propagation of Electromagnetic Waves), Moscow, Sovetskoye Radio, 1970.

9. Chakalov, R., "Some Special Solutions of Hydrodynamic Equations for the Equatorial Atmosphere," KHIDROLOGIYA I METEOROLOGIYA, Sofia, No 5, 1975.

UDC 551.571

VERTICAL DISTRIBUTION OF ABSOLUTE HUMIDITY OF AIR AND MOISTURE CONTENT IN THE ATMOSPHERE OVER THE OCEANS

Moscow METEOROLOGIYA I GIDROLOGIYA in Russian No 8, Aug 79 pp 55-62

[Article by Candidate of Physical and Mathematical Sciences N. A. Timofeyev, Marine Hydrophysical Institute, submitted for publication 27 December 1978]

Abstract: On the basis of an analysis of radiosonde data from Soviet scientific research ships the author has derived formulas describing in the annual variation the mean latitudinal vertical profiles of the volume concentration of water vapor a_H and the moisture content of the atmosphere ω_H (H -- altitude) as a function of cloud cover and air humidity at the ice-free ocean surface. An evaluation is given for the errors in computations of a_H and ω_H using these formulas under conditions extremely different from those in the middle latitudes. Data are given on the total atmospheric moisture content ω_0 over the oceans, in arctic regions, over the land and as a whole for the earth.

[Text] Water is present in the atmosphere in the form of vapor, droplets and ice crystals. The ratio of the droplet and crystalline moisture present in the clouds to the mass of water vapor as a whole for the earth is less than 1% [3]. Therefore, the total atmospheric moisture content ω_0 with great accuracy can be identified with its vapor content in an equivalent layer of precipitable water which could be formed as a result of water vapor condensation. The ω_0 value is determined most accurately using radiosonde data or data obtained by the optical [4], IR [3] or laser [11] methods. However, for the time being these data are still available in inadequate volume for climatic generalizations directly for oceanic conditions. Climatic maps of the ω_0 value for the oceans (for example, in [2, 6]) were compiled for the most part using radiosonde data from island and coastal stations. However, information on atmospheric water vapor, especially on its vertical distribution, is necessary for solving a broad range of problems relating to the radiation regime, moisture cycle, climate and conditions for the propagation of radio waves. This circumstance motivates a search for empirical

dependences between the moisture content ω_H in the layer from the height H to the upper limit of the atmosphere and different characteristics of air humidity (absolute humidity a_0, water vapor elasticity e_0, etc.), measured at the level of standard shipboard observations.

In the author's paper [20], on the basis of an analysis of data from 1,187 shipboard radiosonde observations it was demonstrated that

$$\omega_0 = (1{,}55 + 0{,}046\ n)\ e_0^{1{,}075}, \qquad (1)$$

where ω_0 and e_0 are expressed in millimeters and the total cloud coverage n -- in tenths.

With fixed gradations of cloud cover the correlation coefficient between lg ω_0 and lg e_0 in the entire range of their values characteristic for the ice-free surface of the world ocean changes in the range 0.90-0.94. The computation errors $(\omega_0)_{comp}$ using formula (1) had a normal distribution. The probability of the falling of $(\omega_0)_{act}$ values determined from one radiosonde observation into the interval $(\omega_0)_{comp} \pm \sigma_{\omega_0}$ is approximately 70%. The mean square error σ_{ω_0} is 14%. The σ_{ω_0} value, in addition to the real variability of the moisture content with fixed e_0 and n, also includes the computation error $(\omega_0)_{act}$ based on radiosonde data. The latter is equal to 5-6% [7, 10].

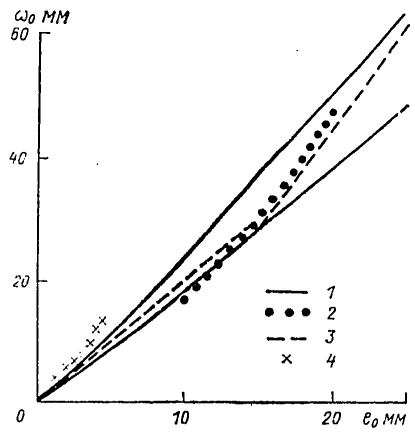

Fig. 1. Dependence of total atmospheric moisture content ω_0 on water vapor elasticity e_0 at ocean surface. 1) computations made using formula (1) with n = 0 (lower curve) and n = 10/10; 2 and 3) on the basis of [22] and [19] respectively; 4) observations of drifting stations "SP-4, -5 and -6" during the period from April through September [15, 17].

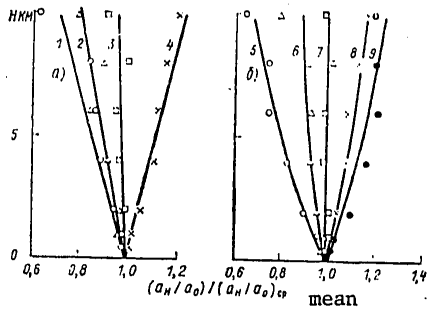

Fig. 2. Normalized relative vertical profiles of absolute air humidity a_H with its different gradations at the ocean surface (a) and with different gradations of total cloud cover (b). 1) $a_0 \leqslant 10$; 2) a_0 = 10.1-15; 3) a_0 = 15.1-20 and 4) $a_0 \geqslant 20.1$ g/m^3; 5) n = 0-2; 6) n = 3-4, 7) n = 5-6, 8) n = 7-8 and 9) n = 9-10/10.

Table 1

Absolute Air Humidity a_H(g/m^3) at Different Altitudes and Total Atmospheric Moisture Content ω_0 (mm) Over the Oceans for Different Gradations a_0 and Cloud Cover n

H км	a_0 г/м³ 1				n баллы 2					
	<10	10,1÷15	15,1÷20	>20,1	0÷2	3÷4	5÷6	7÷8	9÷10	0÷10
	7,2	5,3	4,6	6,0	1,1	3,4	5,4	7,6	9,8	5,7*
0	7,24	13,23	18,68	22,00	17,46	18,87	17,77	18,16	16,52	17,60
0,5	5,83	10,62	15,01	17,78	14,00	15,00	14,25	14,86	13,60	14,21
1	4,63	8,32	12,01	14,48	10,98	11,93	11,60	11,95	11,00	11,41
2	2,86	5,22	7,63	9,64	6,50	7,46	7,41	7,77	7,53	7,36
4	1,06	1,94	2,97	3,99	2,36	2,83	2,82	3,18	3.15	2,92
6	0,40	0,71	1,13	1,56	0,82	1,10	1,10	1,23	1,27	1,12
8	0,13	0,26	0,40	0,55	0,28	0,37	0,39	0,44	0,44	0,39
10	0.03	0,08	0,13	0,19	0,09	0,11	0,13	0,16	0.15	0,13
N (число РЗ) 3	179	165	344	499	256	263	152	151	365	1187
% радиозондирования 4	15.1	27,6	40,2	50,4	35,0	39,2	38,7	41,1	39,1	38,6
% (1)	15.5	29,7	42,9	53,1	36,0	42,7	41.4	44,8	42,3	41,2
% (4)	15,2	27,9	40,4	50,2	34,7	39,8	38,7	41,5	39,0	38,6

5 * Средние значения общей облачности.

KEY:

1. g/m^3
2. n tenths
3. Number of radiosonde observations
4. Radiosonde observations
5. Mean total cloud cover values

Table 2

Atmospheric Moisture Content ω_H(mm) Over Oceans

H км	1 a_0 г/м³											
	1		5		10		15		20		25	
	2 n баллы											
	0	10	0	10	0	10	0	10	0	10	0	10
0	1,72	2,07	8,84	10,67	18,30	22,24	28,47	34,80	39,40	48,52	51,21	63,55
0,5	1,29	1,63	6,69	8,45	14,00	17,77	21,95	28,08	30,67	39,51	40,25	52,23
1	0,97	1,27	5,05	6,66	10,66	14,14	16,90	22,56	23,84	32,03	31,58	42,76
2	0,53	0,76	2,83	4,06	6,09	8,80	9,86	14,31	14,20	20,73	19,20	28,22
3	0,29	0,45	1,57	2,43	3,45	5,38	5,70	8,92	8,36	13,19	11,54	18,32
4	0,16	0,26	0,86	1,43	1,93	3,23	3,25	5,47	4,88	8,26	6,87	11,72
5	0,083	0,15	0,46	0,83	1,07	1,91	1,83	3,31	2,81	5,10	4,05	7,38
6	0,041	0,083	0,25	0,47	0,58	1,11	1,02	1,97	1,61	3,10	2,37	4,59
7	0,023	0,046	0,13	0,27	0,31	0,64	0,57	1,16	0,91	1,86	1,37	2,77
8	0,012	0,025	0,069	0,15	0,17	0,36	0,31	0,67	0,51	1,10	0,79	1,70
9	0,006	0,014	0,036	0,081	0,088	0,20	0,17	0,38	0,28	0,64	0,45	1,02
10	0,003	0,007	0,018	0,043	0,046	0,11	0,090	0,22	0,15	0,37	0,25	0,60

KEY:
1. g/m^3
2. n tenths

Table 3

Atmospheric Moisture Content (mm) Over Pacific Ocean in Layer 0-5 km on the Basis of Radiosonde Data (1) and Computations (2)

Широта, град 1	2 Февраль		3 Май	
	(1)	(2)	(1)	(2)
50—60 с. 4	6,3	7,7	10,6	11,0
40—50	11,0	12,5	14,8	15,5
30—40	16,0	18,0	21,6	23,0
20—30	23,0	25,4	30,4	31,9
10—20	32,5	34,3	38,8	41,2
0—10	38,3	40,6	42,2	44,5
0—10 ю. 5	42,1	43,0	40,3	42,4
10—20	40,3	40,8	34,1	36,6
20—30	34,1	34,2	26,6	28,0
30—40	24,8	26,3	18,3	21,2
40—50	17,8	19,3	12,9	16,2
50—60	12,6	13,1	8,6	11,1

KEY:
1. Latitude, degrees
2. February
3. May
4. N
5. S

Expression (1) was checked in definite regions of the Pacific and Indian Oceans with the most diverse weather types on the basis of independent radiosonde data. It was found that the maximum computation error $(\omega_0)_{comp}$

with the averaging of observations over a period of 1-3 weeks does not exceed 10% [20]. The same conclusion was drawn by B. N. Yegorov [8] on the basis of an analysis of radiosonde data from scientific research ships sailing in the North Atlantic. For other regions of the oceans the results of computations of the total moisture content of the atmosphere on the basis of expression (1) in the case of average cloud cover conditions are in satisfactory agreement with the values $(\omega_0)_{comp}$, computed on the basis of the empirical formulas published by I. A. Shatunov [22] and V. G. Snopkov [19] (Fig. 1). However, these dependences cannot be recommended for use in the high latitudes of oceans covered with ice. For example, in the Central Arctic Basin the $(\omega_0)_{act}$ values, obtained from radiosonde observations, in the warm half of the year exceed the computed values $(\omega_0)_{comp}$ by approximately a factor of 1.5-2.

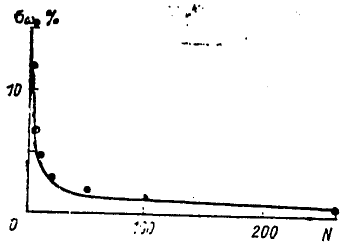

Fig. 3. Dependence of mean square error in computation of $(\omega_0)_{comp}$ value using formula (4) on number N of radiosonde observations. The solid curve corresponds to the case $\sigma_{\omega_0} = 12/\sqrt{N}$, the dots correspond to the experimental data.

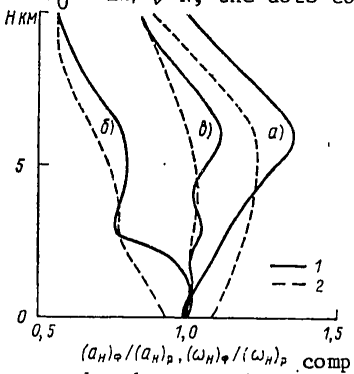

Fig. 4. Comparison of measured and computed vertical profiles of absolute air humidity (1) and atmospheric moisture content (2) in ICZ (a), outside it (b) and for entire GATE-74 (c) [Φ = act; p = comp]

It follows from expression (1) that the ω_0 value with fixed e_0 increases with an increase in cloud cover. An increase in the number of clouds is usually associated with an increase in the intensity of vertical movements in the atmosphere and with an increase in the level of transfer of water

vapor upward from the underlying surface. A singular valve effect is the result [6]: air currents, rich in water vapor, rise upward, leave a part of their moisture there and impoverished of moisture, descend toward the underlying surface, where they again become saturated. Then the process is repeated again and again. The presence of a positive correlation between cloud cover and humidity, summed vertically, was confirmed by satellite observations [14]. In the case of a fixed cloud cover an increase in ω_0 with an increase in e_0 occurs more rapidly than in accordance with the linear law. The physical nature of this effect is also associated with an intensification of vertical air movements as a result of an increase in fluctuations of its density with an increase in moisture content [12].

The noted regularities must also be reflected in the vertical distribution of absolute air humidity a_H. For this purpose the entire mass of data from shipboard radiosonde observations was broken down into a number of submasses with different gradations of a_0 and n (Table 1). For each submass we constructed the vertical profiles of the dimensionless ratios a_H/a_0, which then were normalized by dividing by the values $(a_H/a_0)_{mean}$, found from the mean (for the entire mass of data) a_H profile. In Table 1 this profile corresponds to values $a_0 = 17.60$ g/m^3 and n = 5.7 tenths. The experimental profiles $(a_H/a_0)/(a_H/a_0)_{mean}$ are shown by different notations in Fig. 2. The solid curves represent the results of computations (with corresponding a_0 and n values) using the expression

$$a_H = \frac{a_0 (1 + 0{,}012\, nH)}{10^{(0{,}214\, H + 0{,}0024 H^2)(1{,}14 - 0{,}005\, a_0)}}, \qquad (2)$$

which describes the vertical distribution of the volume concentration of water vapor a_H in the atmosphere in dependence on absolute air humidity at the ice-free surface of the oceans and cloud cover. A reconstruction of the vertical profiles a_H using the ordinarily employed formula $a_H = a_0 \cdot 10^{-bH}$, where $b = 0.434\, a_0/\omega_0$, is carried out with an error especially appreciable at great altitudes [19]. A decrease in the a_H value with altitude H, in accordance with (2), occurs the more slowly the greater the cloud cover and a_0. By knowing the law of change in a_H as a function of H it is possible to find the quantity of precipitable water ω_H as the integral

$$\omega_H = \int_H^\infty a_H\, dH = a_0 \int_H^\infty \frac{(1 + 0{,}012\, nH)\, dH}{10^{(0{,}214\, H + 0{,}0024\, H^2)(1{,}14 - 0{,}008\, a_0)}}. \qquad (3)$$

The ω_H values, obtained by numerical integration with a vertical interval $\Delta H = 100$ m, are shown in Table 2. In turn, these data with a very small error are approximated using the following formulas:

$$\omega_0 = (1{,}72 + 0{,}04\, n)\, a_0^{1{,}01} + 0{,}0018\, a_0, \qquad (4)$$

$$\omega_H = \omega_0 \cdot 10^{-[(0{,}243 - 0{,}0034\, n - 0{,}0017\, a_0)\, H + 0{,}0038\, H^2]}. \qquad (5)$$

Here a_H and a_0 have the dimensionality g/m^3, ω_H and ω_0 are in mm, H is in km, n is in tenths.

Employing the expressions (4) and (5) with arbitrary a_0 and n it is easy to find the quantity of water vapor present in a column of the atmosphere between the levels H_1 and H_2 ($H_2 > H_1$), as $\omega_{H_1,2} = \omega_{H_1} - \omega_{H_2}$.

Expressions (1) and (4) are virtually identical for the case n = 0. In the case of a continuous cloud cover and its mean conditions the $(\omega_0)_{comp}$ values, computed using formula (1), are exaggerated by 6-7% (Table 1). The mean square error σ_{ω_0} for formula (4) with N = 1 (N is the number of radiosonde observations) is 12% and decreases inversely proportionally to $\sqrt{N}$ (Fig. 3). Thus, with N = 151-499 (Table 1) the value $\sigma_{\omega_0} = 0.8\%$.

In the new edition of the MARINE ATLAS OF THE PACIFIC OCEAN [2] there are maps of moisture content of the atmosphere in the layer 0-5 km for February, May, July and November, constructed using data from measurements of air humidity at 160 radiosonde stations during a period from one to eighteen years. The layer 0-5 km contains approximately 90% of all atmospheric moisture. Source [2] also gives the initial information necessary for computing atmospheric moisture content using formulas (4) and (5). In order to exclude the random errors related to a different period for the averaging of radiosonde data we examined the mean latitudinal characteristics of moisture content (Table 3). The computed values were exaggerated by an average of 6.6%. This can be a result of systematic discrepancies in humidity measurements when using radiosondes of different designs. Formulas (4) and (5) were obtained from an analysis of Soviet data and moisture content maps in [2], compiled for the most part on the basis of data from foreign radiosonde observations. The latter, as indicated by comparisons made during the GATE period [10], usually give lower air humidity values. With the exclusion of the systematic discrepancy, formulas (4) and (5) describe the spatial-temporal distributions of the mean-latitudinal values of atmospheric moisture content in the layer 0-5 km over the oceans with a mean square error ±4%.

It is natural to raise the question of the accuracy in obtaining mean a_H and ω_H estimates in fixed regions. For this purpose we used radiosonde data obtained aboard a number of Soviet scientific research ships during the period when an expedition was carried out in the Atlantic Ocean under the international GATE-74 program [1, 9, 21]. One of the peculiarities of the considered region is the presence of a Trades inversion consisting vertically of three blocking layers, whose characteristics have a clearly expressed latitudinal dependence [16]. With approach to the axis of the intratropical convergence zone (ICZ) the frequency of recurrence, intensity and thickness of the blocking layers decrease and the altitudes of their greatest frequencies of recurrence increase. This property is expressed most clearly in the lower troposphere and least clearly in the upper troposphere, where the mentioned characteristics can have even an opposite tendency with approach to the ICZ axis.

Two subregions were defined in connection with the noted peculiarities of the blocking layers and the conditions for the development of cloud cover. The first of these is a polygon of the scale AB, situated in the ICZ zone. Here there was a predominance of gloomy weather with a well-developed cloud cover with vertical development, yielding abundant precipitation. The mean measured moisture content values $(\omega_0)_{act}$ were variable -- from 46 mm in the northern to 54 mm in the central parts of the ICZ [18]. The computed values $(a_H)_{comp}$, and $(\omega_H)_{comp}$ were understated relative to the actual values $(a_H)_{act}$ and $(\omega_H)_{act}$ in polygon AB on the average by 20% to an altitude 5-6 km, where there was a second blocking layer. Above this level the errors decrease with an increase in H (Fig. 4).

The second subregion was situated near the equator, with increasing distance from the ICZ axis -- to the south 600-1200 miles. According to observations on the scientific research ships "Mikhail Lomonosov" and "Akademik Kurchatov," here for the most part there were thin good-weather cumulus clouds with an upper boundary with altitudes not greater than 1-1.5 km. There was little precipitation. The measured $(\omega_0)_{act}$ values varied in the range from 22 to 49 mm [7, 21] with a modal value of 33 mm. Under these conditions, with a clearly expressed (especially with respect to the nature of the vertical distribution of relative humidity) lower blocking layer, which prevented the upward penetration of moisture, the computed $(a_H)_{comp}$ and $(\omega_H)_{comp}$ values were exaggerated on the average by 15% in the layer up to 5 km and by 30% above this level.

The errors in computing $(\omega_0)_{comp}$ using expression (4) for both subregions both as a whole for the entire period of the expedition and for each of its three phases were in the range ±10%. The measured and computed vertical profiles of absolute humidity and moisture content for the entire GATE-74 region virtually coincided (Fig. 4).

The cited data characterize the maximum possible errors in computations of the mean vertical profiles a_H and ω_H using formulas (2), (4) and (5) for regions with development of vertical movements and cloud cover in the atmosphere extremely different from mean latitudinal conditions. In particular, it can be surmised that the $(a_H)_{comp}$ and $(\omega_H)_{comp}$ values will be understated in cyclonic and vice versa, exaggerated in anticyclonic atmospheric formations. In general, the mentioned errors do not exceed the errors in reconstructing the a_H and ω_H profiles at fixed points using AES by the numerical experiments method [13] and errors in the extrapolation of radiosonde data at the points of intersection of a regular geographic grid in the oceans arising as a result of the inadequacy of the spatial density of the network of aerological stations to modern requirements on study of general circulation of the atmosphere [23].

Thus, formulas (4) and (5) are correct in the annual variation for the mean latitudinal conditions in the oceans. At fixed points the computed vertical profiles $(\omega_H)_{comp}$ can be corrected when one has maps of the total moisture content in the atmosphere $(\omega_0)_{act}$, compiled using radiosonde data.

According to the computations made, in the atmosphere over the ice-free surface of the world ocean (latitude zone 70°N-60°S) the annual average content of precipitable water is 28 mm. On the whole, for the earth ω_0 = 25 mm [6]. If the latter value is compared with the total quantity of precipitation, which according to modern estimates [5] is close to 1130 mm, we find that the moisture in the atmosphere is renewed 45 times annually. The moisture content in the atmosphere over the arctic and antarctic regions as an average for the year does not exceed 5 mm (for example, see Fig. 1). On the basis of the data cited above we find, with allowance for areal "weights," that the moisture content of the atmosphere over the land is characterized by a value ω_0 = 23 mm. Accordingly, the moisture content over the oceans in general remains greater than over the land, and only over the continents of the northern hemisphere in summer, when there are powerful ascending air movements in the atmosphere, is there a somewhat greater [6] moisture content than over the surrounding seas.

BIBLIOGRAPHY

1. Antsypovich, V. A., Snitkovskiy, A. I., Fal'kovich, A. I., "Orders of Magnitude of Meteorological Elements in Polygon AB During the GATE Period," TROPEKS-74. T I. ATMOSFERA (Tropex-74. Vol I. Atmosphere), Leningrad, Gidrometeoizdat, 1976.

2. ATLAS OKEANOV. TIKHIY OKEAN (Atlas of the Oceans. Pacific Ocean), Moscow, MO VMF SSSR, Section "Climate," Maps Nos 52, 55, 78, 80, 83 and 84, 1974.

3. Basharinov, A. Ye., Gurvich, A. S., Yegorov, S. T., RADIOIZLUCHENIYE ZEMLI KAK PLANETY (The Earth's Radioemission as a Planet), Moscow, Nauka, 1974.

4. Brounshteyn, A. M., Kozakova, K. V., "On Optical Determination of the Total Content of Water Vapor in the Atmosphere," TRUDY GGO (Transactions of the Main Geophysical Observatory), No 237, 1969.

5. Budyko, M. I., Sokolov, A. A., "The Earth's Water Balance," MIROVOY VODNYY BALANS I VODNYYE RESURSY ZEMLI (World Water Balance and the Earth's Water Resources), Leningrad, Gidrometeoizdat, 1974.

6. Drozdov, O. A., Grigor'yeva, A. S., VLAGOOBOROT V ATMOSFERE (Moisture Cycle in the Atmosphere), Leningrad, Gidrometeoizdat, 1963.

7. Yevseyeva, L. S., Yershov, A. T., Samoylenko, V. S., "Patterns of Vertical Distribution of Water Vapor in the Atmosphere of the Equatorial Latitudes of the Atlantic Ocean," TROPEKS-74. T 1. ATMOSFERA (Leningrad, Gidrometeoizdat, 1976.

8. Yegorov, B. N., "Atmospheric Transparency Over the North Atlantic," TRUDY GGO, No 282, 1972.

9. Zaychikov, B. P., Romanov, Yu. A., "Peculiarities of the Wind, Temperature and Air Humidity Regime in the Equatorial Region of the Central Atlantic," TROPEKS-74. T 1. ATMOSFERA, Leningrad, Gidrometeoizdat, 1976.

10. Zaytseva, N. A., "Comparisons of Radiosonde Data in GATE," TROPEKS-74. T 1. ATMOSFERA, Leningrad, Gidrometeoizdat, 1976.

11. Zuyev, V. Ye., "Laser Sounding of the Atmosphere," VESTNIK AN SSSR (Herald of the USSR Academy of Sciences), No 11, 1973.

12. Kraus, Ye., VZAIMODEYSTVIYE ATMOSFERY I OKEANA (Interaction Between the Atmosphere and Ocean), Leningrad, Gidrometeoizdat, 1976.

13. Kuznetsov, A. D., "Investigation of the Accuracy in Determining Atmospheric Humidity from AES by the Numerical Experiments Method," PROBLEMY FIZIKI ATMOSFERY (Problems in Atmospheric Physics), No 15, 1978.

14. Makklen, Ye. P., "Correlation Between Cloud Cover Observed by a Satellite and Vertically Summed Humidity Fields," GIDROMETEOROLOGIYA ZA RUBEZHOM (Hydrometeorology Abroad), No 6, 1967.

15. MATERIALY NABLYUDENIY NAUCHNO-ISSLEDOVATEL'SKIKH DREYFUYUSHCHIKH STANTSIY "SP-4, 5 i 6" 1956/1957 (Observational Data from the Scientific Research Drifting Stations "SP-4, 5 and 6" 1956/1957), Vol II, Leningrad, Morskoy Transport, 1959.

16. Pastushkov, R. S., Nikonov, V. I., Fishchev, N. N., Bobrov, S. G., Babkin, V. N., "Latitude Dependence and Distribution of the Characteristics of Atmospheric Blocking Layers in the ICZ Region in the Eastern Atlantic," TROPEKS-74. T 1. ATMOSFERA, Leningrad, Gidrometeoizdat, 1976.

17. REZUL'TATY NAUCHNO-ISSLEDOVATEL'SKIKH RABOT DREYFUYUSHCHIKH STANTSIY "SEVERNYY POLYUS-4" I "SEVERNYY POLYUS-5" 1955/56 GODA (Results of Scientific Research Work of the Drifting Stations "SP-4" and "SP-5" 1955/56), Vol III, Leningrad, Morskoy Transport.

18. Snitkovskiy, A. I., Trapeznikov, N. B., "Moisture Content in the ICZ," TROPEKS-74. T 1. ATMOSFERA, Leningrad, Gidrometeoizdat, 1976.

19. Snopkov, V. G., "Correlation Between Atmospheric Water Vapor Content and the Characteristics of Air Humidity at the Earth's Surface," METEOROLOGIYA I GIDROLOGIYA (Meteorology and Hydrology), No 12, 1977.

20. Timofeyev, N. A., "Determination of Water Reserves in the Atmosphere Over the Ice-Free Surface of the Oceans," METEOROLOGIYA I GIDROLOGIYA, No 4, 1965.

21. Timofeyev, N. A., "Atmospheric Transparency and Aerosol Turbidity Over the Southern Part of Polygon A," TROPEKS-74. T I. ATMOSFERA, Leningrad, Gidrometeoizdat, 1976.

22. Shatunov, I. A., "Vertical Humidity Profile and Total Atmospheric Moisture Content Along the Profile from 60°N to 60°S," PROBLEMY TSIRKULYATSII V ATMOSFERE I GIDROSFERE ATLANTICHESKOGO OKEANA (Problems in Circulation in the Atmosphere and Hydrosphere in the Atlantic Ocean), Leningrad, Gidrometeoizdat, 1970.

23. Oort, A. H., "Adequacy of the Rawinsonde Network for Global Circulation Studies Tested Through Numerical Model Output," MON. WEATHER REV., Vol 106, No 2, 1978.

UDC 551.465.558

COMPUTATION OF AVAILABLE POTENTIAL ENERGY IN THE NORTHWESTERN PACIFIC OCEAN

Moscow METEOROLOGIYA I GIDROLOGIYA in Russian No 8, Aug 79 pp 63-67

[Article by Candidate of Physical and Mathematical Sciences V. F. Kozlov, L. A. Molchanova and Ye. A. Sergeyeva, Far Eastern State University, submitted for publication 29 November 1978]

Abstract: On the basis of the mean long-term data on density distribution by 1° squares in the northwestern part of the Pacific Ocean in August it was possible to compute the available potential energy (APE) on the assumption of incompressibility of sea water. The computed distribution of surface density of APE correlates with the position of the dynamic axis of the Kuroshio and with bottom relief. The mean volumetric density of APE, according to these computations, is $1.32 \cdot 10^2$ J/m^3.

[Text] According to modern concepts, one of the possible energy sources for the existence of mesoscale eddies in the ocean is the reserve of available potential energy (APE). A part of this energy can be realized by means of the baroclinic instability mechanism [5, 7]. For regionalization of the world ocean on the basis of the degree of intensity of possible eddy formation and also for the purpose of studying the energy resources of the real ocean it is of interest to estimate the distribution of climatic reserves of APE under specific physiographic conditions. Due to the inadequate amount of representative data on the distribution of oceanological characteristics such computations for the real oceans are for the time being made only using a quite coarse grid [2] or for model basins [5]. However, there is a possibility of computing APE in individual parts of the world ocean, about which the necessary information is adequate.

In this article we give an example of computation of APE for a 1° grid in the northwestern part of the Pacific Ocean bounded on the south by a circle of latitude 25°N and on the east by the meridian 160°E. Compressibility of sea water was neglected in order to simplify the computations. The initial data on the distribution of density $\rho(\lambda, \varphi, z)$ and depths $H(\lambda, \varphi)$ were the same as in [3].

Now we will proceed to a description of the computation algorithm. For a column of fluid of the height H and with a unit base the potential energy can be determined in the form

$$E = -g\int_0^H \rho(\lambda, \varphi, z)\, z dz.$$

In the case of stable equilibrium with the density $\overline{\rho}(z)$ the cited formula determines the unavailable potential energy

$$\overline{E} = -g\int_0^H \overline{\rho}(z)\, z dz.$$

The available potential energy is found as the difference

$$\Delta E = E - \overline{E}.$$

Denoting by asterisks the characteristic scales of the corresponding parameters, by means of the relationships $\rho = \rho_\infty - \delta^* \delta'$, z, $H = H^* z'$, H', $\Delta E = E^* \Delta E' = g\delta^* H^{*2} \Delta E'$ we convert to dimensionless variables; removing the primes, we obtain

$$\Delta E = \Pi - \overline{\Pi}, \quad \Pi = \int_0^H \delta z dz.$$

We will stipulate a set of numbers $\overline{\delta}_k$ satisfying the conditions $0 < \overline{\delta}_N < \overline{\delta}_{N-1} < \ldots < \overline{\delta}_1 < \max \delta$. At the i-th station (center of a 1° square) we determine the limits $z_k^{(i)}$ of the "equivalent layers" using the expressions

$$\int_{z_{k-1}^{(i)}}^{z_k^{(i)}} \delta\, dz = \overline{\delta}_k (z_k^{(i)} - z_{k-1}^{(i)}), \quad k = 1, 2, \ldots \tag{1}$$

$$z_0^{(i)} = 0.$$

The system of these equations is solved successively: $z_k^{(i)}$, determined from the k-th equation, is substituted into the following equation, which is then solved relative to $z_{k+1}^{(i)}$. Each of the equations (1) was solved by the "ranging" method. As the initial value $z_k^{(i)}$ we selected the first standard horizon $z_m > z_{k-1}^{(i)}$ and found the value

$$\sigma = \frac{1}{z_m - z_{k-1}^{(i)}} \int_{z_{k-1}^{(i)}}^{z_m} \delta\, dz, \tag{2}$$

which then was compared with stipulated $\overline{\delta}_k$. If σ was greater than $\overline{\delta}_k$ as the next approximation we selected a point to the left of z_m, otherwise, a point to the right of z_m. The process was repeated up to the time that the σ value coincided with $\overline{\delta}_k$ with a stipulated accuracy of ε. In applying this algorithm the integrals (2) were computed analytically with the use of a spline (cubic spline) interpolation of a stipulated (at standard horizons) distribution of disturbance of density δ at each station [4].

Using the constructed $z_k^{(i)}$ curves, we determined the total volumes (with an accuracy to a constant factor) of the equivalent layers

$$V_k = \sum_i (z_k^{(i)} - z_{k-1}^{(i)}) \cos \varphi_i,$$

where summation is extended to the entire considered region and φ_i denotes the latitude of the i-th station. Then we carried out the "overflow" operation for the purpose of constructing the density distribution $\overline{\delta}$ (z) corresponding to a state of stable equilibrium. The boundaries of the equivalent layers in this state were determined from the system of equations

$$\sum_{j=1}^{n} V_j = \tau (\hat{z}_n), \quad n = 1, 2, \ldots, N, \tag{3}$$

where the function τ (z) determines the volume of the part of the ocean situated above the z horizon and is equal to

$$\tau (z) = \sum_i d_i (z) \cos \varphi_i, \quad d_i = \begin{cases} z, & \text{if } z \leq H_i \\ H_i, & \text{if } z > H_i \end{cases}.$$

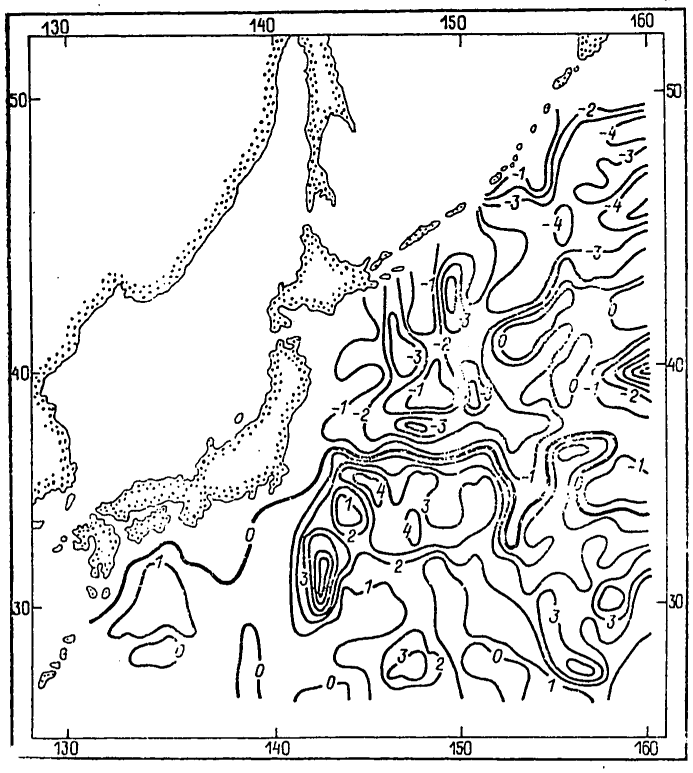

Fig. 1. Computed distribution of surface density of available potential energy Δ E.

By virtue of the piecewise-linear nature of the function $\tau(z)$ equations (3) are easy to solve. If the stations (squares) are numbered in order of increasing bottom depth in them, we obviously have

$$\hat{z}_n = \frac{(H_i - H_{i-1})\left[\sum_{j=1}^{n} V_j - \tau(H_{i-1})\right]}{\tau(H_i) - \tau(H_{i-1})},$$

where H_i and H_{i-1} are such that $\tau(H_{i-1}) \leq \sum_{j=1}^{n} V_j < \tau(H_i)$.

After determining $\hat{z}_n$ the $\overline{\delta}_k$ values were assigned to the horizons

$$\overline{z}_k = \frac{1}{2}(\hat{z}_k + \hat{z}_{k-1}), \quad k = 1, 2, \ldots, N,$$

and it was assumed that $\overline{z}_0 = \hat{z}_0 = 0$ and $\overline{\delta}_0 = \overline{\delta}_{-1}$. Using these data at each station we found the available potential energy $\overline{\Pi}$.

A total of 488 stations participated in the computations. At these we had the mean long-term vertical density distributions for August. Two methods for sampling the $\overline{\delta}_k$ numbers were examined. In the first case as δ_k we used the mean δ values at the k-th standard horizon. In the second case these values were determined from the expressions

$$(z_k - z_{k-1})\,\overline{\delta}_k = \frac{1}{N}\int_0^H \overline{\delta}(z)\,dz,$$

where $\overline{\delta}(z)$ was constructed by the first method and N was equal to the number of standard horizons at the most deep-water station. In both cases the results of computations of Δ E were quite close, differing by a value of the order of ε.

Now we will examine the results of the computations.

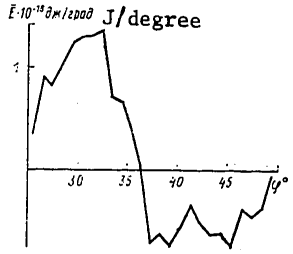

Fig. 2. Computed meridional distribution of APE in one-degree latitude zones.

Figure 1 represents the computed ΔE field; one dimensionless unit corresponds to a surface density of APE equal to $25 \cdot 10^5$ J/m^2. It is interesting to note that the zero equipotential line very precisely corresponds to the mean position of the Kuroshio axis (for example, see [4]). The maximum positive Δ E value, equal to approximately $225 \cdot 10^5$ J/m^2, is attained in

the region of the Idzu-Bonin trench. A minimum value of about $-160 \cdot 10^5$ J/m^2 is discovered in the eastern margin of the computation region in a square with the coordinates 39.5°N, 159.5°E in the region of the northern periphery of the Shatskiy Rise.

The computed ΔE distribution has a quite complex spotty character. However, on the average the surface density of APE decreases from south to north. This can be seen clearly in Fig. 2, which is a graph of the meridional distribution of the APE reserve in one-degree latitude zones.

The total quantity of APE in the considered region was $3.12 \cdot 10^{18}$J, which is approximately 100 times less than the value cited in [2] for the entire Atlantic Ocean. Dividing by the surface area (about 5 million square kilometers), we obtain the mean surface density of APE $\Delta E_{mean} = 6.35 \cdot 10^5$ J/m^2, which agrees in order of magnitude with the estimates obtained for a model ocean in [5]. The mean depth of the region is 4,800 m; therefore, for the mean volume density of APE we obtain a value $1.32 \cdot 10^2$ J/m^3, which is approximately five times less than the corresponding estimate ($7 \cdot 10^2$J/m^3) for the Atlantic [2] and almost twice less than the theoretical estimate for a model ocean ($2.4 \cdot 10^2$ J/m^3), cited in [5]. The somewhat understated value which we obtained for the mean volume density of APE is easily attributed to the quite large mean depths of the considered region, as well as the limited nature of the entire region. Nevertheless, the APE reserve was quite large; as a comparison we recall that the kinetic energy of a cubic meter of water moving translationally with a velocity of 10 cm/sec is 5 J/m^3.

Figures 1 and 2 show that in the considered region the entire APE reserve is concentrated to the south of the Kuroshio, whereas in the northern part there is an APE deficit. In general, the system has a definite energy level [1], which is determined by the mean APE surface value. Only with the active exchange of water masses through the Kuroshio front can there be an evening-out of the ΔE distribution and a general decrease in the energy level. One of the possible mechanisms of such exchange can be related to baroclinic instability. From this point of view it is interesting to compare the computed ΔE distribution with the results of computation of the characteristics of instability of integral circulation in this same region [3]. The mentioned study gives maps of the distribution of sectors of directions of propagation of unstable disturbances for different wavelengths. These maps show that precisely the least unstable zone is the zone of the southern periphery of the Kuroshio, which approximately corresponds to the maximum meridional gradient of zonal density of APE in Fig. 2. Since in both cases the basis of the computations was one and the same mean long-term data, then it is evident, naturally, that in general the Kuroshio is a quite stable dynamic formation which also sustains the drop in energy levels of individual parts of the ocean along both sides of the current itself. An impairment of such an equilibrium can occur as a result of the season-to-season or year-to-year variability of intensity of the subtropical circulation ring, a link in which is the Kuroshio. During

such periods there is a redistribution of part of the APE as a result of meandering and active eddy formation. However, it is not clear whether these phenomena were generated by baroclinic instability or whether their nature is completely different.

We note in conclusion that recently the opinion has been expressed (for example, see [6] and the corresponding discussion) that a study of the stability of averaged circulation in general cannot answer the question as to what might be the sources of existence of real synoptic eddies.

BIBLIOGRAPHY

1. Borisenkov, Ye. P., "Some Energy Properties of a Baroclinic Ocean," IZVESTIYA AN SSSR, FIZIKA ATMOSFERY I OKEANA (News of the USSR Academy of Sciences, Physics of the Atmosphere and Ocean), Vol 12, No 1, 1976.

2. Vulis, I. L., Monin, A. S., "Available Potential Energy in the Ocean," DOKLADY AN SSSR (Reports of the USSR Academy of Sciences), Vol 221, No 3, 1975.

3. Kozlov, V. F., Molchanova, L. A., "Baroclinic Instability of Integral Circulation of the Northwestern Pacific Ocean," METEOROLOGIYA I GIDROLOGIYA (Meteorology and Hydrology), No 7, 1978.

4. Kozlov, V. F., Molchanova, L. A., Bulgakov, S. N., "Method for Multisided Processing of Measured Density Fields in the Ocean," GIDROFIZICHESKIYE ISSLEDOVANIYA SEVERO-ZAPADNOY CHASTI TIKHOGO OKEANA (Hydrophysical Investigations of the Northwestern Part of the Pacific Ocean), Vladivostok, Pacific Ocean Oceanological Institute Far Eastern Scientific Center USSR Academy of Sciences, 1978.

5. Korotayev, G. K., Kosnyrev, V. K., Kuftarkov, Yu. M., "Available Potential Energy and Generation of Mesoscale Eddies in the Ocean," MORSKIYE GIDROFIZICHESKIYE ISSLEDOVANIYA (Marine Hydrophysical Research), Sevastopol', MGI AN UkrSSR, No 4(79), 1977.

6. Nikitin, O. P., "Selection of the Main Flow in the Geophysical Theory of Stability," ISSLEDOVANIYA SINOPTICHESKOY IZMENICHIVOSTI OKEANA (Investigations of Synoptic Variability of the Ocean), Sevastopol', MGI AN UkrSSR, 1977.

7. Gill, A. E., Green, J. S., Simons, A. J., "Energy Partition in the Large-Scale Ocean Circulation and the Production of Mid-Ocean Eddies," DEEP SEA RES., Vol 21, No 7, 1974.

UDC 551.(46.01:464.5)(262.54)

USE OF THE EXPONENTIAL SMOOTHING METHOD FOR PREDICTING THE LONG-TERM VARIATION OF SALINITY IN THE SEA OF AZOV

Moscow METEOROLOGIYA I GIDROLOGIYA in Russian No 8, Aug 79 pp 68-73

[Article by V. N. Bortnik and Candidate of Geographical Sciences A. N. Ovsyannikov, State Oceanographic Institute, submitted for publication 22 December 1978]

Abstract: The authors examine the mathematical basis of the exponential smoothing method. It is shown that the method can be used in the approximate prediction of inertial sea hydrological processes, in particular, the mean annual salinity of sea water, for a period of 2-5 years in advance. In the example of the long-term variation of salinity in the Sea of Azov the article examines the peculiarities of use of the method and its shortcomings. An approximate prediction of salinity of the Sea of Azov for 1978-1980 is given.

[Text] The prediction of variation of sea hydrological elements for several years in advance is a timely problem in oceanography. This problem is acquiring more and more practical significance in the modern stage when on an increasing scale there is an anthropogenic modification of the regime of southern seas -- the Sea of Azov, the Caspian Sea and the Aral Sea. In all these seas the removal of the fresh runoff of rivers is leading to substantial changes in water salinity. A prediction of the future sea salinity values, at least for several years in advance, is necessary for the proper planning of fishing, the quantities of removal and replenishment of fresh water, etc.

Different methods are used for long-term prediction in oceanography [1, 3, 4, 6]. However, the complexity of sea hydrological processes, with the present status of science, for the time being does not make it possible to obtain the precise values of sea hydrological elements for several years in advance. Therefore, in oceanography it is better to speak of an approximate prediction of the surmised long-term values of hydrological elements, stipulating the conditions under which the determined predictable values can be observed.

During recent years in economic science the exponential smoothing method is used for predicting the output of industrial production for several years in advance. This method was developed in general form by R. G. Brown [7] and was put into practical use by H. Grunwald [9], Yu. L. Selivanov and D. I. Kleandrov [5], G. S. Kil'dishev and A. A. Frenkel' [2]. In this article we consider the possibility of using this method for an approximate prediction of the mean annual water salinity values for the Sea of Azov. The Sea of Azov was selected because here, during the last 20 years, in connection with the uniformly increasing intake of the runoff of the Don and Kuban' Rivers, there has been a monotonic increase in water salinity. The article also is of methodological importance, and therefore the computation method is set forth in adequate detail.

Essence of the Exponential Smoothing Method

The essence of the method is that a long-term empirical series is smoothed by a weighted moving mean in which the weights conform to the exponential law. This ensures a reliable description of the process at the end of the smoothing interval, where the weights are maximum. If the temporal variation of the sea hydrological elements, especially water salinity, has a definite inertia, in which the process during the predicted period transpires under the same conditions as in the period to be analyzed, the moving exponential mean can serve as a tool for an approximate forecast. This, on the one hand, is a serious limitation on the method applicable to the long-term variation of sea hydrological elements, since the probability, for example, that the increase in water salinity observed during recent years in the Sea of Azov will have the same character in the future as well is small. On the other hand, the method takes into account the basic structure of the available empirical series and is capable of showing its future trend. No more can be expected from this method. A prediction of salinity is made using expansion of the initial long-term empirical series into a Taylor series. As indicated by Brown and Mayer [4], any derivative of this series can be expressed through linear combinations of exponential means with computation of recurrent corrections to the coefficients of the equation.

The exponential mean of the k-th order for the y_t series has the expression

$$S_t^{[k]}(y) = \alpha S_t^{[k-1]}(y) + (1-\alpha)\, S_{t-1}^{[k]}(y), \qquad (1)$$

where α is the smoothing parameter $(0 < \alpha < 1)$.

Each new exponential mean is equal to the preceding plus a fraction of the difference between the new terms of the series and the preceding smoothed values of this series. Equation (1) is a linear combination of all past observations; the weights of the preceding values decrease in a geometrical progression. Thus, the derivatives in the Taylor expansion are obtained from the equations

$$S_t^{[1]}(y) = \alpha y_1 + (1-\alpha)\, S_{t-1}^{[1]}(y), \qquad (2)$$

$$S_t^{[2]}(y) = \alpha S_t^{[1]}(y) + (1-\alpha)\, S_{t-1}^{[2]}(y),$$
$$\cdots\cdots\cdots\cdots\cdots\cdots \qquad (2)$$
$$S_t^{[k]}(y) = \alpha S_t^{[k-1]}(y) + (1-\alpha)\, S_{t-1}^{[k]}(y).$$

In order to express the coefficients of the trend equation through the exponential means using the theorem [4], we obtain a system of equations relating the coefficients a_0, a_1 and a_2 to the exponential means $S_t^{[1]}(y)$, $S_t^{[2]}(y)$ and $S_t^{[3]}(y)$. For example, for a quadratic model, where the trend is expressed by a second-degree parabola

$$y_t = a_0 + a_1 t + \frac{1}{2} a_2 t^2, \qquad (3)$$

the system of equations has the form

$$S_t^{[1]}(y) = \hat{a}_0 - \frac{1-\alpha}{\alpha}\hat{a}_1 + \frac{(1-\alpha)(2-\alpha)}{2\alpha^2}\hat{a}_2,$$
$$S_t^{[2]}(y) = \hat{a}_0 - \frac{2(1-\alpha)}{\alpha}\hat{a}_1 + \frac{(1-\alpha)(3-2\alpha)}{\alpha^2}\hat{a}_2, \qquad (4)$$
$$S_t^{[3]}(y) = \hat{a}_0 - \frac{3(1-\alpha)}{\alpha}\hat{a}_1 + \frac{3(1-\alpha)(4-3\alpha)}{2\alpha^2}\hat{a}_2.$$

The coefficients $\hat{a}_0$, $\hat{a}_1$, $\hat{a}_2$ for each year in the actual series for the predicted years are computed using the following formulas

$$\hat{a}_0 = 3\,[S_t^{[1]}(y) - S_t^{[2]}(y)] + S_t^{[3]}(y),$$

$$\hat{a}_1 = \frac{\alpha}{2(1-\alpha)^2}\,[(6-5\alpha)\,S_t^{[1]}(y) - 2(5-4\alpha)\,S_t^{[2]}(y) \qquad (5)$$
$$+ (4-3\alpha)\,S_t^{[3]}(y)],$$

$$\hat{a}_2 = \frac{\alpha^2}{(1-\alpha)^2}\,[S_t^{[1]}(y) - 2\,S_t^{[2]}(y) + S_t^{[3]}(y)].$$

Prognostic extrapolation of the empirical series is accomplished using formula (3).

The mathematical error in the forecast is equal to

$$\sigma_y \cong \sigma_\varepsilon \sqrt{2\alpha + 3\alpha^2 + 3\alpha^3 t^2}, \qquad (6)$$

where σ_ε is the mean square error, computed using the deviations of the empirical values from the trend line.

It can be seen from formula (1) that for carrying out the computations we first stipulate the initial conditions S_{t-1}^{k}, which are computed using formulas (4). In this case the coefficients $\hat{a}_0$, $\hat{a}_1$ and $\hat{a}_2$ are taken from the trend equation (3), computed by the least squares method.

The accuracy of the extrapolation is dependent on the proper selection of the α parameter. If α is close to 1, the last values of the empirical series will be more taken into account in the forecasting. If α is close to 0, almost all terms in the empirical series are taken into account. In computations on an electronic computer the α parameter can be selected quite precisely and it is first obtained from the formula

$$\alpha = \frac{2}{m+1}, \tag{7}$$

where m is the smoothing interval.

The smoothing interval is dependent on the fundamental periodicity and length of the long-term empirical series, but when $m \geqslant 10$ about 87% of the weight is assigned to the last terms of the series.

Computation Algorithm and Results

In order to compute the changes in the mean salinity of the Sea of Azov we took an empirical series of its mean annual values from 1957 through 1973. Using this series, by the least squares method we calculated the parabolic trend:

$$\bar{y}_t = 11{,}5175 - 0{,}1394\ t + 0{,}0114\ t^2. \tag{8}$$

The mean square error of deviations of the values of the series from the trend is $\sigma = 0.08$. Then, using formula (4) for the series from 1957 through 1970 we calculated the initial conditions with the values $\alpha = 0.1818$ (m = 10) and with $\alpha = 0.3333$ (m = 5). Using the successive approximations method, extrapolating the series to 1973 and comparing it with the actual values, we selected the precise value m = 6.5 ($\alpha = 0.2667$).

It should be noted that the choice of the m parameter (and this means α as well) is accomplished best of all using an empirical series divided into two parts. A model of the second part of the series is computed from the first part of the series for different m values. For different m values we find the deviations of the computed values in the second part of the series from the empirical values and determine the dispersion of these deviations. The m value for which the minimum dispersion is obtained is used for the forecast. The initial conditions computed with m = 6.5 were equal to: $S_t^{[1]}(y) = 12.1044$; $S_t^{[2]}(y) = 12.8636$; $S_t^{[3]}(y) = 13.7950$. Using these initial conditions, beginning with 1957, employing formula (2) we obtain $S_t^{[1]}(y)$, $S_t^{[2]}(y)$, $S_t^{[3]}(y)$, $\hat{a}_0$, $\hat{a}_1$ and $\hat{a}_2$ for each year. The computed salinity values y_t^* were determined using formula (3). The predicted salinity values from 1973 through 1980 can be obtained by a dual method: by computing $\hat{a}_0$, $\hat{a}_1$, $\hat{a}_2$ for each prediction year on the basis of the values $S_t^{[1]}(y)$, $S_t^{[2]}(y)$, $S_t^{[3]}(y)$ relating to 1973, or considering them recurrently. The computed and predicted y_t^* values are cited in Table 1. The extrapolated y_t^* values here were computed on the basis of 1973 conditions.

Table 1

Successive Computation of Salinity by Exponential Smoothing Method

Год Year	y_t	$\bar{y}_t$	$y_t - \bar{y}_t$	$S_t^{[1]}(y)$	$S_t^{[2]}(y)$	$S_t^{[3]}(y)$	$\hat{a}_0$	$\hat{a}_1$	$\hat{a}_2$	y_t^*	$y_t - y_t^*$
1958	11,1	11,3	—0,2	11,8099	12,5826	13,4717	11,1536	—0,1886	0,0154	11,0	0,1
1959	11,2	11,2	0	11,6259	12,3275	13,1666	11,0619	—0,1460	0,0182	10,9	0,3
1960	11,5	11,1	0,4	11,5043	12,1080	12,8843	11,0734	—0,0825	0,0228	11,0	0,5
1961	11,4	11,1	0,3	11,4952	11,9446	12,6337	11,2855	0,0268	0,0317	11,3	0,1
1962	11,8	11,1	0,7	11,4778	11,8201	12,4167	11,3899	0,0773	0,0336	11,5	0,3
1963	11,3	11,1	0,2	11,5584	11,7503	12,2390	11,6633	0,1657	0,0392	11,8	—0,5
1964	11,1	11,1	0	11,4922	11,6815	12,0904	11,5224	0,1054	0,0290	11,6	—0,5
1965	10,7	11,2	—0,5	11,3822	11,6017	11,9600	11,3017	0,0304	0,0184	11,3	0,4
1966	10,9	11,3	—0,4	11,2110	11,4975	11,8367	10,9772	—0,0624	0,0070	10,9	0
1967	11,2	11,4	—0,2	11,1361	11,4011	11,7205	10,9254	—0,0532	0,0072	10,9	0,3
1968	10,9	11,5	—0,6	11,1611	11,3371	11,6183	11,0903	0,0194	0,0139	11,1	—0,2
1969	11,8	11,6	0,2	11,0968	11,2730	11,5262	10,9976	—0,0030	0,0102	11,0	0,8
1970	11,9	11,8	0,1	11,2817	11,2753	11,4593	11,4783	0,1533	0,0252	11,6	0,3
1971	12,1	12,0	0,1	11,4572	11,3238	11,4232	11,8233	0,2332	0,0308	12,1	0
1972	12,2	12,2	0	11,6206	11,4030	11,4178	12,0707	0,2636	0,0307	12,3	—0,1
1973	12,6	12,4	0,2	11,7885	11,5058	11,4413	12,2895	0,2759	0,0288	12,6	0

It is infeasible to make a forecast for a long period because the existing "latent" polyharmonic component of the long-term time series for salinity in the Sea of Azov, dependent on long-range climatic factors, sooner or later will introduce a substantial correction into the predicted values which cannot be taken into account by the considered method. Table 1 shows that the last three years (1970-1973) are described by a mathematical model with a maximum error ±0.1°/oo. It can be expected that the predicted salinity values from 1974 through 1980 will have the same error. But this is only in a case if there is persistence of the hydrometeorological conditions exerting an influence on the change in salinity of the Sea of Azov during 1957-1973 (nonreturn removal of fresh-water runoff with an increase from 9 to 12 km^3, annual fresh-water runoff in the range 18-21 km^3). With adherence to the hydrometeorological conditions exerting the strongest influence on salinity of the Sea of Azov, especially at the end of the computation interval (1970-1973), the approximate forecast from 1974 through 1980 looks as follows (Table 2).

Table 2

Actual and Predicted Salinity Values in Sea of Azov

Элемент 1	1974	1975	1976	1977	1978	1979	1980
S°/oo эмпирич. 2	12,9	13,1	13,7	13,3	—	—	—
S°/oo расчетн. по ряду 1957—1973	12,9	13,2	13,6	14,0	14,4	14,9	15,4
σ°/oo 3	0,07	0,07	0,08	0,10	0,11	0,12	0,14
S°/oo расчетн. по ряду 1957—1977	—	—	—	—	13,9	14,2	14,5
σ°/oo	—	—	—	—	0,06	0,07	0,07

KEY:

1. Element
2. Empirical
3. Computed from series...

The table shows that prediction of salinity in the Sea of Azov in 1974, 1975 and 1976 was justified with an accuracy to ±0.1°/oo, and the forecast for 1977 has an error of 0.7°/oo, which, to be sure, is unsatisfactory. The reason for the marked decrease in salinity in 1977 was a considerable increase in fresh-water runoff (by almost 10 km^3) as a result of high levels in rivers. Thus, the climatic factors disrupted the monotonic increase in salinity of the Sea of Azov; therefore, the forecast for 1978-1980 will be incorrect. As already mentioned, the considered method does not make it possible to predict this sort of change. Despite this, the exponential smoothing method will without question find use in oceanography for the extrapolation of different kinds of hydrometeorological trends having a stable tendency. Using this method it is possible to find the reasons for the deviations of the computed values from the observed values and give them a physical interpretation. In our case, for example, with persistence of the hydrometeorological conditions of 1970-1973 (close to the mean climatic conditions of these years for the

Sea of Azov basin; removal of runoff increasing somewhat from year to year; mean runoff in the range 18-21 km^3) the forecast for 1974-1976 was justified, whereas in 1977 the sea salinity should be 14°/oo. However, an increase in the fresh water runoff by 10 km^3 decreased the salinity value by 0.7°/oo. This important numerical dependence can be used in further computations. It must be noted that considerable deviations of the actual salinity values from the computed trend as a result of the influence of sharp changes in background conditions not taken into account by this method do not change the detected overall tendency of the process, but only somewhat shift this period in time. For example, a refined forecast for 1978-1980, using the more prolonged factual series for 1957-1977 (Table 2), gives approximately these same values of the annual increments of sea salinity.

It should also be stated that the exponential smoothing method henceforth can be improved applicable to the problems of predicting sea hydrological processes.

BIBLIOGRAPHY

1. Alekhin, Yu. M., STATISTICHESKIYE PROGNOZY V GEOFIZIKE (Statistical Forecasts in Geophysics), Leningrad, Izd-vo LGU, 1963.

2. Kil'dishev, G. S., Frenkel', A. A., ANALIZ VREMENNYKH RYADOV I PROGNOZIROVANIYE (Analysis of Time Series and Prediction), Moscow, Statistika, 1973.

3. Maksimov, I. V., GEOFIZICHESKIYE SILY I VODY OKEANA (Geophysical Forces and Waters of the Ocean), Leningrad, Gidrometeoizdat, 1970.

4. Sarukhanyan, E. I., Smirnov, N. N., "Application of the Genetic Method to the Prediction of Long-Term Water Temperature Variations in the Barents Sea," OKEANOLOGIYA (Oceanology), Vol 10, No 4, 1970.

5. Selivanov, Yu. L., Kleandrov, D. I., "Prediction of the Macroeconomic Structure by the Generalized Exponential Smoothing Method," POVYSHENIYE EFFEKTIVNOSTI OBSHCHESTVENNOGO PROIZVODSTVA I PROBLEM EKONOMICHESKOY REFORMY (Increase in the Effectiveness of Social Production and Problems in Economic Reform), Moscow, Izd-vo IE AN SSSR, 1968.

6. "Present-Day and Future Water and Salt Balances of the Southern Seas of the USSR," TRUDY GOIN (Transactions of the State Oceanographic Institute), No 108, 1972.

7. Brown, R. G., SMOOTHING, FORECASTING AND PREDICTION OF DISCRETE TIME SERIES, Prentice Hall, Englewood Cliffs, N. Y., 1963.

8. Brown, R. G., Mayer, R. F., "The Fundamental Theorem of Exponential Smoothing," OPERATIONS RESEARCH, Vol 9, No 5, 1961.

9. Grunwald, H., "The Correlation Theory for Stationary Stochastic Processes Applied to Exponental Smoothing," STATISTICA NEERLANDICA, Vol 19, No 2-3, 1965.

UDC 628.394:556.166"321"

PREDICTION OF THE QUALITY OF RIVER WATER DURING THE PERIOD OF SPRING HIGH WATER

Moscow METEOROLOGIYA I GIDROLOGIYA in Russian No 8, Aug 79 pp 74-77

[Article by Doctor of Chemical Sciences F. Ya. Rovinskiy and Candidate of Technical Sciences Z. L. Sinitsyna, Institute of Applied Geophysics, submitted for publication 25 December 1978]

Abstract: A study is made of a method for predicting the quality of river water during the period of spring high water for rivers whose runoff during this period is formed for the most part by slope water flowing from the watershed. The runoff coefficient of ingredients used in the computations, obtained under natural conditions, makes it possible in the prediction to limit oneself to data on the reserve of ingredients in the watershed only in the snow cover. The method is used in predicting the concentration of ingredients in river water averaged for the high-water period and the distribution of the concentration with time.

[Text] The prediction of the quality of river water during the period of the spring high water is an independent and important problem in practical respects, methodologically unrelated to prediction during low-water periods [3].

Spring high water is a characteristic peculiarity of the regime of most lowland rivers in the USSR and can constitute up to 80% of the annual volume of runoff [7]. The water discharges during the time of high water increase a hundredfold, which is caused by the entry of melt water from the watershed. For most of the unregulated rivers in the middle zone of the European USSR the water runoff during the period of the spring high water is formed for the most part (90% or more) due to the slope waters of the watershed and will determine the quality of river water during this period.

The melt waters flowing from the watershed contain different substances which have accumulated during the winter in the snow cover, and also falling with rain and entering from the ground in the watershed as a result of interaction

of the downflowing water and the underlying surface. In this case for rivers or reaches of rivers in which there is absolutely no discharge of unpurified waste water or if it is discharged in an insignificant quantity, the mean concentration of the i-th ingredient at the lowest-lying station in the watershed during the period of the spring high water can be determined from the expression

$$\overline{C_i} = \frac{U_i}{W}, \tag{1}$$

where U_i is the quantity of the i-th ingredient entering into the river from the area of the watershed with the surface waters; W is the volume of the slope waters.

The quantity of the i-th ingredient entering the river from the area of a watershed with melt waters is

$$U_i = f_i N_i^{\Sigma}, \tag{2}$$

where N_i^{Σ} is the reserve of the i-th ingredient in the watershed before melting of the snow; f_i is the fraction of the i-th ingredient of its total reserve entering with the melt water into the river channel or the coefficient of runoff of the i-th ingredient. Hence

$$\overline{C_i} = \frac{f_i N_i^{\Sigma}}{W}. \tag{3}$$

The f_i and N_i^{Σ} values are determined experimentally; the water volume W is predicted.

The reserve of the i-th ingredient in the watershed N_i^{Σ} consists of its quantity accumulating in the snow cover falling with the rain during the period of snow melting and the reserve of this ingredient in the soil layer, from which the ingredient can enter into the downflowing water in the process of its interaction with the underlying surface.

The quantity of liquid precipitation during the period of snow melting for rivers of the middle zone of the European USSR is usually small in comparison with the water reserve in the snow [1]; therefore, its contribution to contamination of the watershed during this period must be considered insignificant.

A determination of the reserve of ingredients in the soils of a watershed is made difficult by the choice of the necessary depth of the layer in which it is necessary to estimate this reserve. On the basis of the results of laboratory experiments [5] it can be assumed that the ingredients are washed out of the upper layer of the soil, but the depth of this layer is dependent on a whole series of factors, such as the type of soil, nature of the watershed, slope, etc., an examination of which is beyond the scope of this paper.

A determination of the runoff coefficient for ingradients from the watershed is made experimentally in natural watersheds or in runoff areas set up on the watershed. A determination is made of the reserve of ingredients in the

snow cover in the experimental watershed or runoff area prior to the onset of snow melting and runoff of ingredients from these areas. The runoff coefficient f_i is conveniently expressed in fractions of the reserve of the i-th ingredient in the snow cover. The coefficient f_i obtained under natural conditions actually reflects the process of formation of the quality of melt water flowing from the watershed, including due to the underlying surface. The use of this coefficient in prediction of the mean concentration of the i-th ingredient in river water makes it possible to limit ourselves to the reserve of the i-th ingredient only in the snow cover, that is

$$\overline{C}_i = \frac{f_i N_i^{\text{CH}}}{W}, \tag{4}$$

[CH = snow] where N_i^{snow} is the reserve of the i-th ingredient in the snow cover prior to the onset of snow melting.

In an investigation of the runoff of ^{90}Sr [4] and some other substances [6] from the watershed with the melt water we found that the runoff coefficient for these ingredients increases with an increase in the water runoff, to wit:

$$f_i = f'_i y, \tag{5}$$

where f'_i is a proportionality factor characterizing the fraction of the i-th ingredient (of its reserve in the snow cover) flowing down with 1 mm of water, y is the layer of water runoff.

Replacing the reserve of ingredients in the snow cover and the volume of slope water by the corresponding expressions

$$N_i^{\text{snow}} = \overline{C}_i^{\text{snow}} x F \text{ and } W = yF, \tag{6}$$

where $\overline{C}_i^{\text{snow}}$ is the mean concentration of the i-th ingredient in the snow water, x is the water reserve in the snow prior to the onset of snow melting, F is the area of the watershed, and substituting (5) and (6) into (4), we obtain the mean concentration of the i-th ingredient at the lowest-lying station on the river during the period of the spring high water

$$\overline{C}_i = f'_i \overline{C}_i^{\text{CH}} x. \tag{7}$$

[CH = snow]

On the basis of the results of investigations in two watersheds in the basin of the Moskva River during the period of the spring high water we established a dependence between the concentration of petroleum products, iron and cobalt and the water discharges in the river at the lowest-lying station (Fig. 1) in the form

$$\frac{C_i(t)}{\overline{C}_i} = \rho_i \frac{Q(t)}{\overline{Q}}, \tag{8}$$

where $Q(t)$ and $\overline{Q}$ are the water discharges at the time t and the mean slope runoff for the period; ρ_i is a proportionality factor determined from Fig. 1.

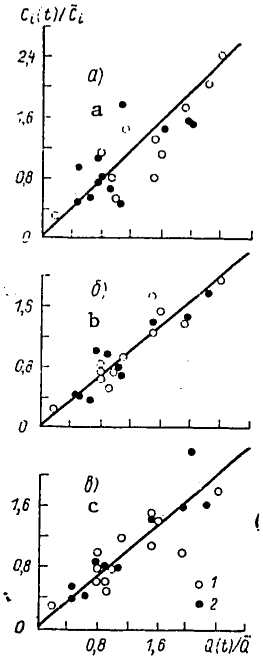

Fig. 1. Dependence between concentration of the ingredient and water discharge. a) petroleum products; b) iron; c) cobalt, 1) watershed 1: Moskva River, Rublevo station; 2) watershed 2, Severka River, Pokrovskoye station

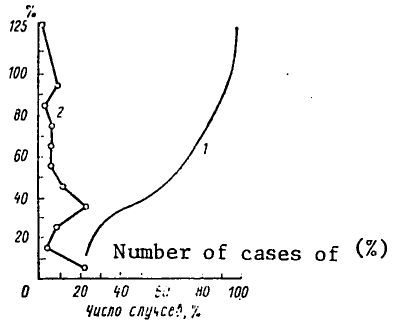

Fig. 2. Probability (1) and frequency of recurrence (2) of deviations of computed concentrations from actual values during period of spring high water in 1975

It was found that the value of the ρ_i coefficient is equal for petroleum products to 0.92, for iron and cobalt -- 0.83.

Using dependence (8) and substituting the value of the mean concentration $\overline{C}_i$ from expression (7), it is possible to compute the change in the concentration of the mentioned ingredients with time.

$$C_i(t) = \rho_i f_i \overline{C}_i^{\text{сн}} \, x \frac{Q(t)}{\overline{Q}}. \qquad (9)$$

In accordance with the described method we carried out an analysis of the content of some ingredients in the Moskva River in the upper reach at the lowest-lying station Rublevo during the spring high water of 1975, the run-off in which is 70% formed due to slope water from the unregulated watershed basin.

The deviations of the computed mean concentrations from the measured values (in percent) are:

Petroleum products	-43	Chromium	+7
Phenols	+53	Antimony	+32
Surface-active agents	-5	Cobalt	-18
Iron	-45		

The satisfactory convergence of the computed and experimental data confirms the assumption made in the computations that the water quality in the Moskva River in its upper reach is formed for the most part by slope waters in the watershed.

Using the computed mean concentration of ingredients $\overline{C}_i$, the value of the ratio of water discharges $Q(t)/\overline{Q}$ at Rublevo station in 1975 and the coefficient ρ_i, determined for the watershed of the Severka River (right-hand tributary of the Moskva River, unregulated water flow, watershed area 792 km^2), we obtained the distribution of the content of petroleum products, iron and cobalt at Rublevo station with time in accordance with dependence (9). An analysis of the curves of the frequency of recurrence and probability of the error in the computed concentrations in comparison with the actual values indicated that the maximum frequency of recurrence of error corresponds to the range of errors 0-10 and 30-40%. In 70% of the cases the error in the computed concentrations is less than 50% of the actual value (Fig. 2).

Using this method we made a prediction of the water quality at the Rublevskaya water-intake station during the period of the spring high water of 1976. For this purpose prior to the onset of snow melting we determined the reserve of ingredients in the snow cover in the watershed, for which we took snow samples and determined the content of ingredients in them. In the computations we used the experimentally determined coefficients f'_i [6]. The deviation of the mean values from the observed values during the period for phenols, surface-active substances and iron was 14, 40 and 25% respectively. [The samples were taken and analyzed by the MosvodokanalNIIproyeky Institute.] The predicted and actual values of the maximum iron content coincided.

BIBLIOGRAPHY

1. Appolov, B. A., Kalinin, G. P., Komarov, V. D., KURS GIDROLOGICHESKIKH PROGNOZOV (Course on Hydrological Forecasts), Leningrad, Gidrometeoizdat, 1974.

2. RESURSY POVERKHNOSTNYKH VOD SSSR, T 10, KNIGA I, VERKHNE-VOLZHSKIY RAYON (Surface Water Resources of the USSR, Vol 10, Book I. Upper Volga Region), Moscow, Gidrometeoizdat, 1973.

3. Rovinskiy, F. Ya., Koloskov, I. A., Iokhel'son, S. B., Voznesenskiy, G. F., Sinitsyna, Z. L., "Balance Model of Contamination of the Moskva River," METEOROLOGIYA I GIDROLOGIYA (Meteorology and Hydrology), No 11, 1976.

4. Rovinskiy, F. Ya., Morozova, G. K., Sinitsyna, Z. L., Sinitsyn, N. M., "Transfer into Water and Migration Capacity of Radionuclides in the Peaceful Application of Atomic Energy," RADIOEKOLOGIYA VODNYKH ORGANIZMOV (Radioecology of Water Organisms), Riga, "Zinatiye," 1973.

5. Rovinskiy, F. Ya., Sinitsyna, Z. L., Cherkhanov, Yu. P., "On the Problem of the Migration of ^{90}Sr from the Soils With Surface Waters," POCHVOVEDENIYE (Soil Science), No 18, 1976.

6. Sinitsyna, Z. L., Cherkhanov, Yu. P., Koloskov, I. A., "Runoff of Some Contaminating Substances from a Watershed During the Spring," TRUDY IEM (Transactions of the Institute of Experimental Meteorology), No 9(83), 1978.

7. Chebotarev, N. P., UCHENIYE O STOKE (Science of Runoff), Moscow, Izd-vo MGU, 1962.

UDC 631.6:556.542

INVESTIGATIONS OF THE WATER, HEAT AND SALT BALANCES IN AMELIORATED LANDS

Moscow METEOROLOGIYA I GIDROLOGIYA in Russian No 8, Aug 79 pp 78-84

[Article by Professor A. A. Sokolov and Doctor of Technical Sciences S. I. Kharchenko, State Hydrological Institute, submitted for publication 20 February 1979]

Abstract: A study is made of the problems involved in organizing water-balance stations on ameliorated lands and the makeup of hydrometeorological observations at these stations.

[Text] Investigations at the State Hydrological Institute and at other organizations, carried out during the course of the last 15-20 years in irrigated and drained lands, indicated that rational control of water, heat and salt regimes of irrigated and drained fields, ensuring the obtaining of high yields, maintenance of a good meliorative state and a high fertility of the soils to be improved, and also the rational use of water resources, can be carried out only on the basis of a joint analysis and detailed allowance for all the elements of the water, salt and thermal balances of the soil active layer and also the intensity of moisture exchange in the aeration zone.

At the State Committee on Hydrometeorology and the USSR Water Management Ministry specialists have been assigned the task of creating a fundamentally new specialized network of water balance stations on irrigated and drained lands. In the years immediately ahead plans call for establishing 16 water balance stations: 10 in irrigated fields (Khersonskaya, Semikarakorskaya, Saratovskaya, Maryyskaya, Khorezmskaya, Karshinskaya, Golodnostepskaya, Amurskaya) and rice plantations (Kubanskaya, Khankayskaya) and 6 in drained lands and lands with drainage-moistening amelioration work in the humid zone (Rovnenskaya, Novgorodskaya, Vitebskaya, Nerovskaya, Meshcherskaya, Tyumenskaya).

The principal tasks of the water balance stations are a detailed study of the entire complex of elements of the water and salt balances of the aeration zone and the water-bearing layer, heat balance, and also the intensity of

the moisture-heat-salt exchange between the aeration zone and the water-bearing layer, ground water regime, salt regime of the soils, quality of river and irrigation water.

The principal characteristics of the established WBS will be as follows:
1) The WBS investigations will be carried out complexly, that is, all types of hydrological, hydrogeological, meteorological and other observations will be matched in area and will be carried out simultaneously by an integrated method and using instruments of a definite accuracy;
2) Investigations of all elements of the water, heat and salt balances and the factors determining them will be carried out simultaneously in different structural components of the ameliorated system (field, extended area, region or contour).

This approach to the investigations will make possible all the types of collected information to be collated and the programs for obtaining these data can be matched with the amelioration and other investigations carried out in this region.

The theoretical basis for the organization of field investigations and stationary observations at WBS are the equations for the water, salt and heat balances, which depending on the problems to be solved are used for a separate agricultural field, melioration system, territory or basin.

The balance equations used in the practical work of WBS include a large number of components [2, 3]. For example, the general water balance equation for an undrainable field for the soil layer from the surface to the water-resistant surface has the following form:

$$P + M + R_{пп} + R_{пр} + R_{пг} - R_{п} - R_{к} - R_{г} - E_{т} - E_{к} + \\ + \Delta S + Q_1 - Q_2 = 0. \quad (1)$$

For a drained field:

$$R_{п} + R_{к} + R_{р} + R_{г} = R_{кол} + R_{гк}. \quad (1')$$

The water balance equation for the water-bearing layer (ground water) for an undrained field from the impermeable water surface to the ground water table is:

$$\Delta S_{гр} + R_{пг} - R_{г} - f_{р} + f_{п} + f_{к} - K + Q_1 - Q_2 = 0. \quad (2)$$

For a drained field:

$$R_{г} = R_{г\,кол} + R_{гк}. \quad (2')$$

[Note: For equivalents of Russian notations see top of next page.]

RUSSIAN NOTATIONS:

И = i(rrigation)	ИИ = in i (inflow - irrigation)
Р = p(recipitation)	ИР = in p (inflow - precipitation)
Г = g(round water)	ИГ = in g (inflow - ground water)
К = c(anal)	ГКОЛ = col(lector runoff)
ИОВ = surf	ГК = c(ollector-drainage network)

The water balance equation for the aeration zone for the layer from the surface to the ground water level is

$$P + M + R_{\text{ин}} + R_{\text{пр}} - R_{\text{и}} - R_{\text{р}} - R_{\text{к}} - E_{\text{т}} - E_{\text{к}} - f_{\text{и}} - f_{\text{к}} - f_{\text{р}} - K + \Delta W + \Delta S_{\text{пов}} = 0. \quad (3)$$

Here P is precipitation; M is the irrigation norm; $R_{in\ i}$, $R_{in\ p}$, $R_{in\ g}$ are the inflows onto the field surface by irrigation water, precipitation and ground water; R_i, R_p, R_g, R_c are the runoffs from the field of irrigation water, precipitation, ground water, runoff (discharge) from canals; E_T is the optimum evaporation from an irrigated field (evapotranspiration); E_{col} is evaporation from the water surface of canals and other water bodies; ΔS is the accumulation of moisture on the surface ΔS_{surf}, in the aeration zone ΔW and in the water-bearing layer ΔS_g; Q_1 and Q_2 are the receipts of ground water in the deeper horizons and their feeding from below by head water; f_p, f_i, f_c is the infiltration of precipitation, irrigation water and filtering from canals; K is the flow of ground water into the aeration zone (capillary feeding from below); R_{col} is the collector runoff; $R_{g\ col}$ is the ground component of the collector runoff; $R_{g\ c}$ is the runoff of ground water below the bottom of the collector-drainage network.

A still greater number of components must be taken into account in an analysis of the water-salt (4) and heat (5) balances:

$$\Delta S_{\text{гр}} C_{\Delta s_{\text{гр}}} + R_{\text{пг}} C_{R_{\text{пг}}} - R_{\text{г}} C_{R_{\text{г}}} + f_{\text{р}} C_{f_{\text{р}}} + f_{\text{п}} C_{f_{\text{п}}} + f_{\text{к}} C_{f_{\text{к}}} + Q_1 C_{Q_1} - Q_2 C_{Q_2} = 0, \quad (4)$$

$$P C_{\text{р}} + M C_{\text{м}} + R_{\text{ип}} C_{R_{\text{ип}}} + R_{\text{пр}} C_{R_{\text{пр}}} - R_{\text{п}} C_{R_{\text{п}}} - R_{\text{р}} C_{R_{\text{р}}} - R_{\text{к}} C_{R_{\text{к}}} - f_{\text{п}} C_{f_{\text{п}}} - f_{\text{к}} C_{f_{\text{к}}} - f_{\text{р}} C_{f_{\text{р}}} + \Delta W C_{\Delta W} + \Delta S_{\text{пов}} C_{\Delta s_{\text{пов}}} + C_{\text{у}} = 0, \quad (5)$$

where

$C_{\text{р}}$, $C_{\text{м}}$, $C_{P_{\text{ип}}}$, $C_{R_{\text{пр}}}$, $C_{R_{\text{пг}}}$, $C_{R_{\text{п}}}$, $C_{R_{\text{к}}}$, $C_{R_{\text{р}}}$, $C_{R_{\text{г}}}$, $C_{\Delta s_{\text{пов}}}$, $C_{\Delta W}$, $C_{\Delta s_{\text{г}}}$, C_{Q_1}, C_{Q_2}, $C_{\text{у}}$

is the concentration of salts (respectively) in precipitation, irrigation water, inflow of irrigation water, precipitation, ground water, surface runoff of irrigation water, from canals, precipitation, runoff of ground water, in water held at the surface in the aeration zone and in the water-bearing

layer, and also in overflowing and head waters, in fertilizers, C_{f_i}, C_{f_c}, C_{f_p} are the concentrations of salts in the infiltration flow of irrigation waters, from the canal, and from precipitation.

The heat balance equation is

$$R=P+B+V \tag{6}$$

or

$$E=\frac{R-P-B}{L}, \tag{6'}$$

where R is the radiation balance of the active surface, P is the heat flow in the surface layer of the atmosphere, V are the heat expenditures on evaporation, representing the product of the latent heat of evaporation L and the evaporation value E itself.

For the practical use of the cited equations, as we see, it is necessary to have a quite reliable measurement of a large number of parameters entering into them and their changes in time and in space.

For this purpose the irrigation, drainage or drainage-moistening systems in which WBS are established, should be outfitted with modern hydraulic structures making it possible to determine the inflow and outflow of irrigation waters (or diversion of moisture excesses from overmoistened lands), all sources of surface, underground (ground water) and collector-drainage runoff and the runoff of the river-water receiver within the limits of the melioration system.

Water balance stations must be outfitted with instruments for measurement and continuous registry of precipitation, ground water levels, temperature and air humidity, radiation balance, filtering of ground water into the aeration zone, evaporation from the water surface and transpiration of different agricultural crops, etc.

In order to obtain this research information it is necessary to carry out, in a number of experimental fields or control sectors, whose number can vary in dependence on the distribution and nature of the soils, the formulated production tasks and the adopted crop rotation. The number can be from 2-3 to 10-12. In more complex cases the investigations are carried out in typical (key) sectors, situated in different irrigation or drainage systems.

As an example, Fig. 1 shows the typical distribution of observation points at one of the WBS situated in irrigated lands.

In order to evaluate and predict the meliorated state of fields it is necessary, simultaneously with study of elements of the water and heat balances, to carry out investigations of the soil cover (peculiarities of genesis,

hydrophysical, chemical and physicochemical properties), and also the ground water regime (including head waters) and their quality. As an independent complex problem we should mention study of the relationship between surface and ground water with waters in the aeration zone. In this connection, the investigations in the WBS experimental or control sectors must be mutually tied in with observations of rivers which are sources of water or receivers of water, which makes it possible to study the influence of melioration measures on the regime, balance and quality of waters in the river basin.

For this purpose there must be more frequent hydrometric measurements of water runoff in a river in different reaches, and also hydrogeological observations in boreholes near the channel and in the drainage basin as a whole.

The WBS program provides for observations ensuring study of the water regime of surface water sources and ground waters, and also the water balance of the aeration zone and the water-bearing layer in agricultural fields, ameliorated areas and river basins with well-developed melioration. At the same time, a study will be made of the mineralization of ground and surface waters, and also soil solutions, the salt composition of the soils, its temporal dynamics and the distribution of soils in area. This will make it possible to determine the salt balance of agricultural fields, ameliorated systems and river basins, and on this basis formulate a prediction of their long-range changes. The principal objective in study of the radiation balance, the turbulent flux of moisture and the heat flux into the soil is the detection of the energy resources of moisture and salt exchange in ameliorated agricultural fields.

The created network of water balance stations on ameliorated lands is intended for solution of a series of important practical problems related to increasing the effectiveness of agriculture in ameliorated lands and the rational use of water and land resources:

-- validating the norms for water requirements and water diversion and return waters for irrigated lands and lands with drainage-moistening melioration;
-- monitoring the ameliorated state of lands in irrigated and drained sectors and development of a method for predicting the levels of ground water, salinization and desalinization of soils;
-- evaluation and prediction of changes in the chemical and nutrient regime, hydrophysical properties of soils under the influence of melioration and development of methods for using this information in the planning and use of drainage and drainage-moistening melioration work;
-- evaluation of the moisture supply for arid and semimoist (swampy) soils, determining the reasons why areas become swampy, determining the degree of swampiness and validating the principles for the drainage of swampy soils in a humid zone, the drainage of overmoistened and saline soils in an arid zone;
-- evaluation and prediction of the influence of melioration on the environment, change in water regime, balance and quality.

The most important task of the WBS is the routine supply of water and agricultural agencies with information on precipitation, runoff, evaporation, ground water level, water diversion, hydrophysical and chemical properties

of soils and other characteristics necessary for planning, construction and operation of melioration systems.

The water balance stations must be part of the control network of stations and posts of the USSR State Committee on Hydrometeorology. This is new and complex work for the administrations of the Hydrometeorological Service. It requires much preparation.

In this connection, a task of the administrations of the Hydrometeorological Service is active participation, jointly with agencies of the USSR Water Management Ministry, in the planning and construction of WBS, the training of personnel in the field of meliorative hydrology, an increase in the level of hydrometeorological support of agriculture on drained and irrigated lands.

At the present time the agencies of the USSR Water Management Ministry are carrying out much work for improvement and increase in the technical level of amelioration work. In particular, in carrying out drainage work extensive use is being made of enclosed drainage, a changeover is taking place from drainage by gravitational flow by the regulation of rivers receiving drainage waters to drainage by means of machine pumping, with pumping stations for the diversion of water into receiving rivers, drainage-moistening systems are being created, and the task is being formulated of creating and maintaining the optimum water, air, heat, gas and nutrient regime of the soil and the surface air layer during the entire growing season. In the next 20 years systems will be created for the automated control of water, air, salt, heat and nutrient regimes for the soil, ensuring a considerable increase in the productivity of agricultural production. For this purpose it is necessary not only to increase the level of the systems for collecting, storing, processing and dissemination of information on the environment, but also to improve methods for the scientific generalization of this information and the validation of more modern melioration procedures.

In order to validate drainage-moistening melioration work and automatic control of water, air, heat and salt regimes there must be continuous information (at 24-hour intervals) on the excesses of moisture and inadequacies of water consumption, which can be obtained on the basis of a study of elements of the water, heat and salt balances at WBS.

Figure 2 shows the 10-day values for the excesses of moisture and shortages in water requirements for plants (Kingisepp hydrometeorological station in Leningradskaya Oblast) in a field occupied by grain crops in an arid,(1), moderately moist (3) and moist (2) year [1].

This graph shows that during the course of the entire growing season the moisture excesses during all years alternate with water requirement inadequacies. In moist and moderately moist years the moisture excesses prevail over the shortages in water requirements. In an arid year, on the other hand, the water supply requirements are greater than the moisture excesses.

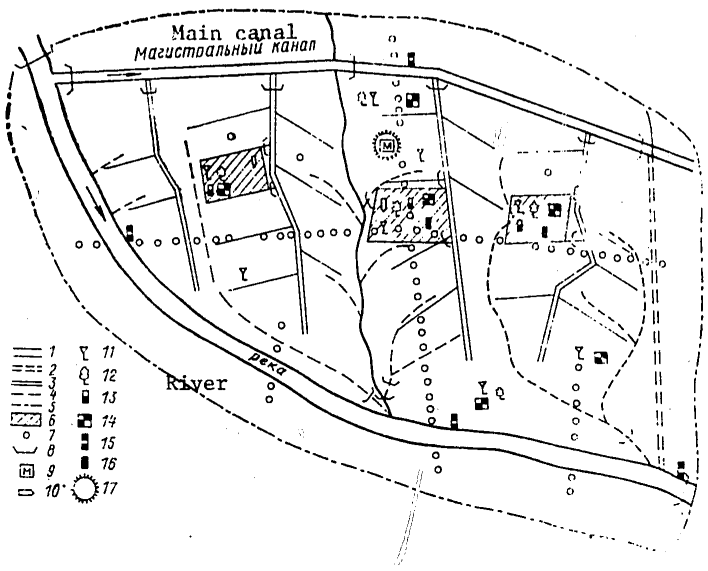

Fig. 1. Diagram of placement of instruments and equipment in experimental fields and extended areas in irrigation system. 1) main canal, 2) catastrophic discharge, 3) irrigation distributor, 4) collector, drain, 5) boundary of experimental area, 6) experimental field, 7) hydrogeological borehole, 8) hydrometric post, 9) meteorological station, 10) runoff area, 11) precipitation gage point, 12) point for phenological observations, 13) lysimeters, 14) point for measuring soil moisture content, 15) water-measuring post, 16) water balance sector, 17) field point for the collection and storage of information and water management complex automatic control system.

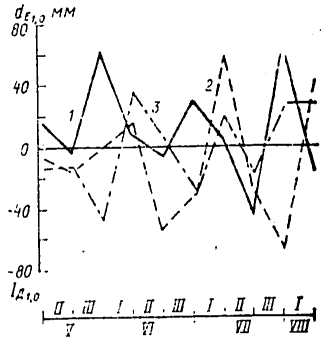

Fig. 2. Ten-day values of moisture excess $I_{10\text{-day}1.0}$ and shortages of water consumption d_E of grain crops for hydrometeorological station Kingisepp in Leningradskaya Oblast.

Table 1

Mean Long-Term and Probable Values of Ten-Day and Seasonal Values of Moisture Excesses and Water Requirement Inadequacies for Mean Depth of Ground Water 1.0 m

1 Станция, область	2 Период расчета	3 Месяц	4 Декада	5 Избытки влаги, мм				8 Недостатки водопотребления, мм			
				6 средняя многолетняя величина	7 различной обеспеченности			6 средняя многолетняя величина	7 различной обеспеченности		
					25%	50%	75%		25%	50%	75%
Кингисепп Ленинградской области 8	1958—1975 гг.	V	1	9,6	12,7	9,0	5,4	10,5	13,3	9,8	6,7
			2	4,6	6,4	4,3	2,6	9,2	11,7	8,6	5,9
			3	12,2	16,1	11,5	6,8	10,6	13,5	9,8	6,8
		VI	1	5,8	7,9	5,4	3,2	11,4	14,5	10,6	7,3
			2	8,9	11,7	8,4	5,0	8,6	10,9	8,0	5,5
			3	7,8	10,3	7,3	4,4	6,9	8,8	6,4	4,4
		VII	1	5,7	7,5	5,4	3,2	13,6	17,3	12,6	8,7
			2	16,9	22,3	15,9	9,5	9,9	12,6	9,2	6,3
			3	13,1	17,3	12,5	7,3	21,5	27,3	20,0	13,8
		VIII	1	6,4	8,4	6,0	3,6	15,5	19,7	14,4	9,9
		V—VIII		91,0	120,0	85,5	51,0	117,7	149,6	109,4	75,3

KEY:
1. Station, oblast
2. Computation period
3. Month
4. Ten-day period
5. Moisture excesses, mm
6. Mean long-term value
7. With different probability
8. Kingisepp, Leningradskaya Oblast

This indicates that in order to create optimum conditions for plant cultivation in a particular field in the course of one growing season it is necessary to both irrigate the crops and divert excess moisture from the field. In such cases the arrangements for regulating moisture (techniques and apparatus for irrigation and moisture diversion) must be extremely universal because moisture excesses extremely frequently alternate with shortages in water requirements.

Statistical data on moisture excesses and water requirement shortages over a long-term period are given in Table 1 for the Kingisepp hydrometeorological station. These data indicate that the alternation of moisture excesses with shortages of water requirements are observed annually and in the course of the entire growing season. These same phenomena to one degree or another are also observed in other oblasts of the Nonchernozem zone. Therefore, an increase in the yield of agricultural crops in the Nonchernozem zone is possible only by means of constructing structures for the complex regulation

of the life conditions for plants and especially the diversion of excess moisture and the irrigation of fields which can function successfully only when using continuous information on elements of the water, heat and salt balances.

BIBLIOGRAPHY

1. VOPROSY MELIORATIVNOY GIDROLOGII (Problems in Meliorative Hydrology), TRUDY GGI (Transactions of the State Hydrological Institute), No 251, 1978.

2. METODY RASCHETA VODNYKH BALANSOV. MEZHDUNARODNOYE RUKOVODSTVO PO ISSLEDOVANIYAM I PRAKTIKE (Methods for Computing Water Balances. International Manual on Research and Practical Work), edited by A. A. Sokolov and T. G. Chapmen, Leningrad, Gidrometeoizdat, 1976.

3. Kharchenko, S. I., GIDROLOGIYA OROSHAYEMYKH ZEMEL' (Hydrology of Irrigated Lands), Leningrad, Gidrometeoizdat, 1978.

UDC 556.535.6(282.254.44)

METHOD FOR DETERMINING THE RUNOFF OF ENTRAINED SEDIMENTS IN RIVERS USING DATA ON THEIR ACCUMULATION IN BACKWATERS

Moscow METEOROLOGIYA I GIDROLOGIYA in Russian No 8, Aug 79 pp 85-90

[Article by V. S. Lapshenkov and T. A. Boguslavskaya, Novocherkasskiy Engineering-Melioration Institute, submitted for publication 20 November 1978]

Abstract: The authors give a method for determining the runoff of bottom sediments in rivers using data on their accumulation in backwaters (in the example of the Malo-Kabardinskiy backwater on the Terek River). The applicability of the V. N. Goncharov and Ya. A. Nikitin formulas for determining the runoff of entrained sediments is demonstrated.

[Text] The entrained sediments in mountain rivers in mountain and foothill reaches constitute a frequently small part of the solid runoff. But this part is decisive in predicting the clogging up of the upper reaches of reservoirs and study of the dynamics of "underflooding" by ground water and water accumulation under snow, in determining the most important parameters of rock slides, bridges and other river structures. The runoff of entrained sediments determines the intensity of the positive deformation of the channel; their grain size and fractional composition determine the slopes and and current velocities of the flow, the potential depths of local erosion near individual structures and other morphological elements of the flow and channel in the sector of accumulation. It is also known that the measurement of runoff and the fractional composition of bottom sediments by hydrometric methods is extremely difficult and therefore this is not done by the stations of the Hydrometeorological Service.

What has been stated above makes clear that it is essential to organize measurements of the runoff of bottom sediments, at least in river reaches where hydraulic complexes create backwaters and reservoirs. These measurements are useful both directly in the operation of already constructed structures, and also will be useful in the planning of structures on this same river or on other rivers under similar conditions. At the same time it is obvious

that the method and scope of field investigations must conform to a very definite method for the analysis of data.

In the manual METHODS FOR MEASURING DISCHARGES OF SEDIMENTS AND STUDY OF THE DEFORMATION OF RIVER CHANNELS AND INVESTIGATION OF SOLID RUNOFF [3] our formulas expressing the pattern of accumulative processes in reservoirs are also recommended for solution of the inverse problem: for determining their runoff. In this article we determine the runoff of entrained sediments in the reach at Kotlyarevskaya station on the basis of the actual accumulation of sediments in the backwater of the Malo-Kabardinskiy hydraulic complex. Determination of the runoff norm for entrained sediments in this reach is extremely necessary for predicting the accumulation of sediments in the planned Tersko-Urukhskoye Reservoir.

Earlier it was demonstrated in [1, 2] that the processes of silting and sediment accumulation in reservoirs and backwaters for the most part have the following regularity:

[$\pi = \lim$]
$$V = V_n (1 - e^{-\frac{t}{E}}), \tag{1}$$

where V is the volume of the upper reach silted or clogged by entrained sediments, V_{lim} is the maximum siltable, and in the analysis of clogging, the maximum cloggable volume of the upper reach; t is the time of silting (choking up or clogging); E is a characteristic of siltability or clogability of a reservoir or backwater;

$$E = \frac{V_n}{\varepsilon' G}, \tag{2}$$

where G is the mean annual volume of runoff of suspended (in the case of silting) or entrained (in the case of clogging) sediments in volumetric measurement; ε' is the fraction of deposits of sediments in the reservoir or backwater at the onset of their accumulation:

$$\varepsilon' = \frac{\rho_0 - \rho'}{\rho_0} = \frac{S_0 - S'}{S_0}, \tag{3}$$

ρ_0, S_0 are the turbidity of the flow and the discharge of sediments (suspended or entrained) respectively at the entry into the reservoir (reflecting the ordinary runoff of sediments); ρ', S' are the turbidity of the flow and discharge of sediments respectively, passed through the hydraulic complex into the lower reach at the beginning of its operation.

Two computation equations were derived for solving the formulated problem on the basis of formula (1). In the absence of necessary data the volume of the maximum siltable or maximum cloggable volume of the reservoir can be determined on the basis of the volumes of silting at different times using the formula

[$\pi = \lim$]
$$V_n = \frac{V_1^2}{2V_1 - V_2} \quad (\text{when } t_2 = 2t_1), \tag{4}$$

where t_1 and t_2 is the time of accumulation of sediments; V_1 and V_2 are the volumes of accumulation of sediments corresponding to this time.

On the basis of data on the actual accumulation of sediments the characteristic of siltability (or sediment accumulation) is determined as:

$$E = -t\frac{\lg e}{\lg(1-\eta_v)}, \tag{5}$$

where η_v is the relative volume of silting or clogging:

[π = lim]

$$\eta_v = \frac{V}{V_n}.$$

Now we will examine application of the method for analysis of data on accumulation of suspended and entrained sediments in a specific example. The factual data cited below on the accumulation of sediments in the upper reach or backwaters of the Malo-Kabardinskiy hydraulic complex were taken from a study by V. F. Shul'ga [5]. There is also some information not contradicting Shul'ga's data in a study by G. A. Ter-Abramyants [4].

The Malo-Kabardinskiy hydraulic complex was put into operation in 1929; creating a level rise, on the Terek River it formed a backwater whose length at the beginning of operation was 790 m. According to data from the Administration of the Hydrometeorological Service, the water discharges in the region of the hydraulic complex vary from 40 to 1400 m^3/sec; the mean annual runoff of suspended sediments is 3.4 million tons, and for bottom sediments -- 426 thousand tons (G. A. Ter-Abramyants reports that there are no data on the runoff of bottom sediments).

The hydraulic complex includes: a concrete spillway dam with a height of 2.59 m and a length of 288.5 m, a flushing water gate and a canal water intake, situated on the right shore, and also a left-shore limiting dam with a length of more than 3 km. In the backwater the velocities were considerable and only the large sandy fractions were deposited from among the suspended sediments. The deposition of the entrained sediments caused an increase in the flow slope within the limits of the backwater and the extension of the backwater upstream as much as 4 km.

Seven measuring points were developed and permanently established over a distance of 3,178 m in the backwater. Measurements at these points were made in 1936, 1948 and in 1955. It was demonstrated in a study by Shul'ga that as a result of sediment accumulation there was a rise in levels. The volume of sediment accumulation was: from 1929 through 1936, according to data published by D. G. Shaposhnikov -- 485,000 m^3, from 1929 through 1948, according to Shul'ga's data -- 727,000 m^3 and from 1929 through 1955 -- 747,000 m^3. The volume of deposits during the first seven years was 116% of the initial capacity of the backwater, whereas by 1955 it had increased to 179%

and the backwater extended beyond the limits of the area of effective measurements by Kotlyarevskaya station, being situated 3,178 m above the dam.

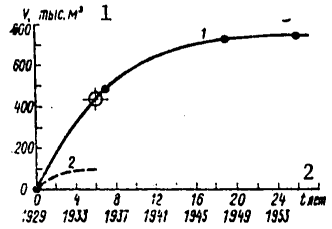

Fig. 1. Increase in volume of accumulated sediments in backwater of Malo-Kabardinskiy hydraulic complex on Terek River. 1) total volumes, 2) only silting volumes.

KEY:
1. thousands of m^3
2. years

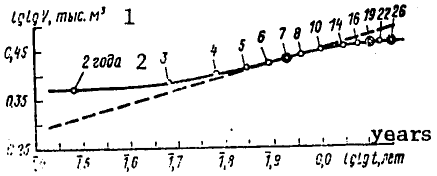

Fig. 2. Dynamics of volumes of accumulation of suspended and entrained sediments during silting and sediment accumulation in backwater of Malo-Kabardinskiy hydraulic complex. The figures on the curve denote the operating time in years, beginning from 1929. The double circle shows points of actual measurements.

KEY:
1. thousands of m^3
2. years

The dynamics of the volume of accumulated sediments is shown in Fig. 1 (it is given in the articles of Shul'ga and Ter-Abramyants, but the points of actual measurements were joined by a broken line, not by a curve).

First of all we note that the cited curve reflects the total of both silting and other sediment accumulation. The article gives no information on silting time, the volumes of silting or the fractional composition of the sediments passing through the dam. Only one thing is clear: whenever silting occurred, at this same time the runoff of bottom sediments in the backwater is fully retarded. Accordingly, during the first years of operation the volume of the

accumulated sediments must be not less than 426,000 tons annually (according to Shul'ga's data). But it follows from an analysis of the curve in Fig. 1 that there cannot be such a great runoff of entrained sediments in the river since the total volume of accumulation of entrained and suspended sediments did not exceed 100,000 m^3 annually. Evidently, taking these same factors into account, Ter-Abramyants rejected data on the runoff of sediments.

There are considerable difficulties here in separating the sediments accumulated in the backwater into "suspended" and "bottom." In this example we take advantage of the fact that from the time of the transit movement of suspended sediments the accumulation of the entrained sediments conformed to the dependence (1), whereas before this time silting occurred in accordance with the same regularity (1) (with its own parameters) and sediment accumulation:

$$V = V_{зл} + V_{зв} = V_{п.\ зл}\left(1 - e^{-\frac{t}{t_{зл}}}\right) + Gt. \qquad (6)$$

[ЗЛ = silt(ing); П. ЗЛ = max silt(ing)]

Table 1

Volumes of Silting and Sediment Accumulation in Axes of Double Logarithms

		t лет 1										
		1	2	4	6	7	8	10	14	19	22	26
2	V тыс. $м^3$	100	175	308	423	485	529	595	680	727	742	747
	lg lg t	$-\infty$	1,479	1,78	1,892	1,928	1,957	0,000	0,004	0,107	0,128	0,151
	lg lg V	0,301	0,352	0,399	0,420	0,430	0,436	0,444	0,452	0,458	0,458	0,458

KEY:

1. years
2. thousands of m^3

The curve in Fig. 2 has a different curvature, and accordingly, a different pattern of accumulation of sediments: first it is turned convexly downward, and then upward. The dashed line, drawn through the inflection point, separates these sectors and is tangent to both parts of the curve. Such a graphic construction, with further analytical evaluation, makes it possible to find the time of ending of silting of the backwater: it can be seen that six years after beginning of operation of the backwater the silting ended. In the seventh and eighth years the intensity of sediment accumulation remained almost the same as in the preceding years (the slope of this segment of the curve is equal to the slope of the tangent). Moreover, due to the ever-increasing part of transport of bottom sediments, the intensity of sediment accumulation is decreasing.

This determination of this moment in time agrees with Shul'ga's data on channel deformation in the lower pool (see Fig. 7 in her mentioned work): as a result of the intensive total erosion of the channel for a length of 1-3 km the water levels in the lower pool decreased by 2.62 m (late in 1933) and only toward 1937 was a reverse trend noted and the levels increased by 30 cm. The latter occurred due to the entry of entrained sediments into the lower pool; although these sediments consisted of fine fractions, they stopped the further erosion of the channel, whose slope as a result of erosion was much less than formerly.

Using the curve in Fig. 1 we determine that during six years in the backwater there was an accumulation of 435,000 m^3 of suspended and entrained sediments. This point can be used as the initial point in an analysis of the process only of sediment accumulation. The maximum cloggable volume of the pool is determined using formula (4). At arbitrarily selected moments in time (for example, t_1 = 5 years, and t_2 = 10 years, that is, at the scale in Fig. 1, this will be 11 and 16 years), using the curve we will determine the volume of the deposits 623,000 and 700,000 m^3 respectively. But taking into account the sediments accumulated during the first six years, the volume of silting for 5 and 10 years, beginning in 1935, will be 188,000 and 265,000 m^3 respectively. According to these data, the maximum cloggable volume of the pool is equal to

$$V_{\max\ clog} = \frac{188\,000^2}{2 \cdot 188\,000 - 265\,000} = 319\,000\ м^3.$$

The characteristic of cloggability of the backwater is determined using formula (5). For example, using data for 10 years the fraction of sediment accumulation is 265 000:319 000 = 0.830

$$E = -10\,\frac{0{,}434}{\lg(1-0{,}83)} = 5{,}64 \quad \text{years}$$

Now we will check these parameters by computations using formula (1); for this case it is written in the form

$$V = 319\,000 \cdot (1 - e^{-\frac{t}{5{,}64}}).$$

The results of the computations are given in Table 2, from which it can be seen that the results of the computations have a high accuracy.

Table 2

Volumes of Deposits of Entrained Sediments in Backwater

	t лет 1								
	7	9	11	13	16	19	21	24	26
$t_р$, лет 2	1	3	5	7	10	13	15	18	20
$V_{эм}$, тыс. $м^3$ 3	51,7	131,5	187,5	227,0	265,0	287,0	297,0	306,0	310,0
$V_{эм}+435 \cdot 10^3$, тыс. $м^3$ 4	486,7	566,5	622,0	662,0	700,0	722,0	732,0	741,0	745,0
$V_ф$, тыс. $м^3$ 5	485,0	—	—	—	—	727,0	—	—	747,
Разность, % 6	+0,35	—	—	—	—	—0,69	—	—	—0,2

KEY TO TABLE 2

1. Years
2. t_{comp}, years
3. V_{clog}, thousands of m^3
4. V_{clog}...thousands of m^3
5. V_{act}, thousands of m^3
6. Difference, %

The runoff of entrained sediments can be computed using formula (2):

$$G = \frac{V_{п.\,зн}}{\varepsilon' E_{зн}} = \frac{319\,000}{1{,}0 \cdot 5{,}64} = 56{,}6 \text{ thousands } m^3.$$

[п. З Н = max clog; З Н = clog]

With a volumetric density of the deposits 1.9-2.0 tons/m^3 the runoff of entrained sediments in the Terek River at Kotlyarevskaya station was determined as the value 108-113 thousand tons/year. Here it should be noted that earlier, as a result of special investigations, the mean long-term runoff of entrained sediments was as follows
-- using the V. N. Goncharov formula -- 129 thousand tons/year
-- using the G. I. Shamov formula -- 49.5 thousand tons/year
-- using the Ya. A. Nikitin formula -- 97 thousand tons/year.

Here we should note the quite good agreement of the results of determination of the runoff of entrained sediments, computed using data on their accumulation in the backwater and using the Ya. A. Nikitin and V. N. Goncharov formulas.

The determined runoff of entrained sediments also makes it possible to determine the characteristics of silting which occurred in the pool during the first six years of its operation. These six years the runoff of the entrained sediments was completely held in the pool and the volume of their deposits was $56.6 \cdot 10^3 \cdot 6 = 339.6$ thousand m^3. Accordingly, the maximum siltable volume of the pool $(435-340) \cdot 10^3 = 95$ thousand m^3.

The siltability characteristic is determined using formula (5). For example, during two years of operation the volume of accumulation of sediments in the pool was 175 thousand m^3. During these same two years the retention of entrained sediments in the pool was $56.6 \cdot 10^3 \cdot 2 = 113.2$ thousand m^3; the volume of silting was $(175-113.2) \cdot 10^3 = 61.8$ thousand m^3. The silting fraction is 61.8:95.0 = 0.652. The siltability characteristic of the backwater is

$$E = -2 \frac{0{,}434}{\lg(1 - 0{,}652)} = 1{,}9 \text{ years.}$$

We will determine the silting volumes during the first years:

$$V_{silt} = 95000\,(1 - e^{-\frac{t}{19}}).$$

Table 3

Volumes of Silting During First Years of Operation of Hydraulic Complex

	1 t лет					
	1	2	3	4	5	6
2 $V_{нак}$, тыс. $м^3$	39,0	61,7	75,3	83,5	88,0	91,2

KEY:
1. years
2. V_{silt}, thousand m^3

The fraction of suspended sediments precipitating in the pool at the beginning of silting was (using formula (2))

$$\varepsilon'' = \frac{95 \cdot 10^3}{1{,}9 \cdot 3400 \cdot 10^3} = 0{,}0147,$$

that is, only 1.47% of the suspended sediments were deposited in the backwater.

The method, demonstrated in a specific example, made it possible to determine the mean annual runoff of sediments in the Terek River at Kotlyarevskaya station. At the same time it was demonstrated that the formulas published by Ya. A. Nikitin and V. N. Goncharov for determining the runoff of entrained sediments give extremely reliable results under the conditions prevailing in the Terek.

BIBLIOGRAPHY

1. Lapshenkov, V. S., "Analysis of Silting of the Chir-Yurtskoye Reservoir on the Sulak River," TRUDY NIMI (Transactions of the Novocherkasskiy Engineering-Melioration Institute), Vol XIII, No 5, Novocherkassk, 1974.

2. Lapshenkov, V. S., "Some Results of Processing Data on Silting and Deposition of Sediments in the Backwaters of Hydraulic Complexes," VOPROSY GIDROTEKHNIKI (Problems in Hydraulic Engineering), No 2, Tashkent, Izd-vo AN UzSSR, 1961.

3. METODIKA IZMERENIYA RASKHODOV NANOSOV I IZUCHENIYE DEFORMATSIY RECHNYKH RUSL I ISSLEDOVANIYE TVERDOGO STOKA (Method for Measuring the Discharges of Sediments and Study of River Channels and Investigation of Solid Runoff), Council of Economic Mutual Assistance, Budapest, 1972.

4. Ter-Abramyants, G. A., "Investigation of Reforming of the Backwater of the Malo-Kabardinskiy Hydraulic Complex," ZAILENIYE VODOKHRANILISHCH I BOR'BA S NIM (Silting of Reservoirs and Preventive Measures), Moscow, Kolos, 1970.

5. Shul'ga, V. F., "Investigations of Head Structures in Irrigation Systems," TRUDY NIMI, Vol VII, Rostov-na-Donu, 1961.

UDC 551.50:633.18(477)

METHOD FOR PREDICTING THE MEAN OBLAST YIELD OF RICE IN THE UKRAINE

Moscow METEOROLOGIYA I GIDROLOGIYA in Russian No 8, Aug 79 pp 91-94

[Article by V. M. Prosunko and Professor Yu. I. Chirkov, Ukrainian Scientific Research Hydrometeorological Institute, submitted for publication 29 November 1978]

Abstract: The authors derive an equation for multifactor correlation between rice yield and the density of the plant stand and the mean air temperature for interphase periods, making it possible to prepare a prediction of the mean oblast yield of this crop. The advance time for such a forecast is about two months before the onset of crop harvesting.

[Text] In the practice of agrometeorological servicing of agriculture extensive use is being made of forecasts of the yield of different agricultural crops, prepared differentially for each oblast. Such an approach to the prediction of productivity of individual crops makes possible a more complete allowance for the regional peculiarities of soil-climatic conditions and the agricultural methods and procedures used in cultivation in different agricultural regions (hydrometeorological regime, soil fertility, range of varieties, crop rotation, methods for working the soil, etc.) in prognostic models.

Prognostic models of rice yield have been formulated applicable to the conditions prevailing in the Northern Caucasus [4, 7], Volga region [2], Far East [13] and Central Asia [1].

In this article we present the results of investigations which make it possible to develop a method for predicting the mean oblast yield of rice cultivated in the southern Ukraine. The initial data used were materials from the Central Statistical Administration on the mean oblast yield for 1951-1979 and data from agrometeorological observations during this period at hydrometeorological stations situated in rice-growing regions of the Ukrainian SSR.

Variations in the yield of agricultural crops in each geographic region in which the agricultural techniques and equipment used in cultivation and the seed varieties are the same are a result of variation of weather conditions [3, 6, 10].

The cultivation of rice in our country is carried out under conditions of optimum moistening. This is achieved by the flooding of rice paddies with water during the entire growing cycle. As indicated by the studies of different researchers [1, 2, 4, 7, 13], the limiting climatic factor exerting a dominating influence on the formation of the rice yield is the thermal regime.

The integral and most stable biological index of rice productivity, as for other agricultural crops [12, 14 and others], is the density of the productive stand.

The mentioned points served as a basis for developing a method for predicting the mean oblast rice yield. As the multiple correlation predictors included in the program for computations on an electronic computer we selected the following productivity indices for rice: density of stems with ears, characterizing the potential possibilities of the crop, and the mean air temperature for the interphase periods of development "sprouting - leaf tube formation" and "leaf tube formation - heading of panicles," which reflects the conditions for growth and development. The basis for selecting the enumerated independent variables in the prognostic model of the yield was their information content and significance, determined in pair correlation with the mean oblast rice yield. The correlation coefficients between the yield and the mean air temperature values during the mentioned periods are 0.52 and 0.64 respectively. The closeness of the correlation between the rice yield and the density of the productive stand is characterized by a correlation ratio 0.70.

As the dependent variable in the rice yield model we used the ratio of the absolute value of the mean oblast yield (y) to its statistical maximum (Y_{max}), which was computed for each oblast with a probability 99.9% by the Gumbel' method [5]. As indicated in [3, 6], the replacement of the yield value by the ratio y/Y_{max} makes it possible to take into account such factors constantly acting on the yield, characterizing the regional peculiarities of individual regions of crop cultivation as soil fertility, agricultural techniques and equipment, seed varieties and productivity of climate. This also makes it possible to increase the volume of the sample for the statistical processing of data by means of combining data for different oblasts [11], which is extremely important in the case of short observation series.

As a result of multiple correlation of the dependent variable y/Y_{max} and the enumerated predictors we obtained the following linear regression equation:

$$y = Y_{max}\ (0{,}325\, x_1 + 0{,}018\, x_2 + 0{,}023\, x_3 - 0{,}250)$$

$$R = 0{,}703 \pm 0{,}003 \qquad S_y = \pm 4{,}6 \text{ centners/hectare,} \qquad (1)$$

where y is the mean oblast yield (limits of variation from 20 to 60 centners/hectare); Y_{max} is the statistical maximum of the rice yield, equal to 65.0 centners/hectare for Krymskaya Oblast and 60.7 centners/hectare for Khersonskaya Oblast; x_1 is the mean (oblast) number of stems with panicles, divided by 1000 (limits of change from 200 to 900 stems per 1 m^2); x_2, x_3 are the mean (oblast) air temperatures for the interphase periods of rice development "sprouting - leaf tube formation" and "leaf tube formation - heading of panicles," limits of change 17-23 and 19-25°C).

The probability of the deviations between the yield computed using equation (1) and the actual yield, not exceeding the admissible computation error ($0.67\Delta\sigma$ = 4.4 centners/hectare), with the volume of the sample being 28 annual cases, was 82%. The deviations between the actual and computed data considerably exceeded the admissible error in computations in those years whose summer months were characterized by a marked negative heat anomaly. This relates to 1973 and 1976. These years are characterized by a marked temperature anomaly observed in the European USSR during the entire growing season. In particular, in Khersonskaya Oblast the heat deficit in comparison with the norm for June, July and August was about 150°C in 1973 and more than 200°C in 1976. A decreased thermal regime at the beginning of the growing season caused a poor bushiness of the plants, as a result of which the density of the rice stand after leaf tube formation did not exceed 360-400 stems per 1 m^2. In a subsequent period in the growing season a heat inadequacy had a negative effect on formation of the reproductive organs, as a result of which in the maturing of the rice there was a great number of underdeveloped spikelets, bareness of the panicle and puniness of the grain. According to observational data for the Kherson agrometeorological station, the weight of 1000 grains in 1973 was 26.4 g and was 4.3 g less than in 1975, favorable with respect to the thermal regime. At the same time, the number of underdeveloped spikelets was 10 times greater than in the compared year. In 1976 the rice sowing in the observation sector at the agrometeorological station was mowed for hay due to the poor appearance of the panicles and nonmaturing of the grain. On the basis of an evaluation of the influence of the heat shortage on the yield we developed a scale of corrections by which it is necessary to decrease the computed yield in years with a marked negative temperature anomaly. The values of the corrections, expressed in percent of the computed yield value, are given in Table 1.

The magnitude of the correction is dependent on the deviation of the sum of mean annual air temperature in June or July from the norm ($\Delta\sum t$). This deviation

[Φ = act]
$$\Delta\Sigma t = (t_\phi - t_N)\, n, \qquad (2)$$

where t_{act} is the mean (oblast) mean monthly air temperature in the current year; t_N is the mean long-term value for mean monthly air temperature (norm); n is the number of days per month.

In 1977, after rice ear emergence, that is, with an advance time of about two months before the harvest, an experimental forecast was made of the mean oblast yield of this crop for Krymskaya and Khersonskaya Oblasts. From the

forecast it was expected that the yields would be 43.9 and 38.0 centners/hectare respectively, whereas after the harvest the actual rice yield for this territory was 43.5 and 35.5 centners/hectare. The forecast was 100% justified since the deviation of the predicted yield from the actual yield did not exceed the admissible error in computations and the relative error

$$(\delta = \frac{Y_{comp} - Y_{act}}{Y_{act}} 100)$$

was 1% for Krymskaya Oblast and 7% for Khersonskaya Oblast.

Table 1

Correction to Predicted Mean Oblast Rice Yield in Case of Negative Anomaly of Mean Monthly Air Temperature in June and July

Отклонение суммы среднесуточных температур от нормы, °C 1	2 Величина поправки в % к прогнозируемой урожайности	
	3 июнь	4 июль
31—40	6	3
41—50	8	4
51—60	10	5
61—70	12	6
71—80	14	7
81—90	16	8
91—100	18	9

KEY:

1. Deviation of sum of mean daily temperatures from norm, °C
2. Magnitude of correction in % of predicted yield
3. June
4. July

The method for agrometeorological forecasting of the mean oblast yield of rice, developed using data from the rice-growing oblasts of the Ukrainian SSR, can also be recommended for other rice-growing zones. In order to do this it is necessary to compute the statistical yield maxima and carry out a preliminary checking of the accuracy of computations on the basis of factual data during the last 10 years for the purpose of ascertaining the systematic error, which is eliminated by a change in the free term in equation (1). It must be remembered that the value of the statistical yield maximum is usually 8-10% greater than the actual maximum value of the mean oblast yield. If in subsequent years, as a result of improvement of agricultural techniques and equipment for the cultivation of rice, its actual yield attains or exceeds the statistical maximum, the latter must be recomputed.

BIBLIOGRAPHY

1. Abdulayev, Kh. M., "Method for Evaluating Agrometeorological Conditions for Development and Formation of the Rice Yield in Uzbekistan and Tadzhikistan," TRUDY SARNIGMI (Transactions of the Central Asian Regional Scientific Research Hydrometeorological Institute), No 40(121), 1977.

2. But, V. I., "Influence of Weather Conditions on Rice Yield in Astrakhanskaya Oblast," METEOROLOGIYA I GIDROLOGIYA (Meteorology and Hydrology), No 7, 1974.

3. Grushka, I. G., "Method for Long-Range Forecasting of Mean Oblast Yield of Winter Barley in the Ukraine," TRUDY UkrNIGMI (Transactions of the Ukrainian Scientific Research Hydrometeorological Institute), No 72, 1968.

4. Gulimova, N. V., "Heat Supply for Forming of the Rice Yield in the Northern Caucasus," TRUDY GIDROMETTSENTRA SSSR (Transactions of the USSR Hydrometeorological Center), No 85, 1971.

5. Gumbel', E., STATISTIKA EKSTREMAL'NYKH ZNACHENIY (Statistics of Extremal Values), Moscow, Mir, 1965.

6. Dmitrenko, V. P., "Models for Computing the Yield of Agricultural Crops With Allowance for Hydrometeorological Factors," METEOROLOGIYA I GIDROLOGIYA (Meteorology and Hydrology), No 5, 1971.

7. Leleko, Z. A., "Method for Predicting Kray Rice Yield," TEZISY DOKLADOV VSESOYUZNOGO NAUCHNO TEKHNICHESKOGO SOVESHCHANIYA "SOVERSHENSTVOVANIYE METODOV PROGNOZA UROZHAYA ZERNOVYKH KUL'TUR" (Summaries of Reports at the All-Union Scientific and Technical Conference "Improvement of Methods for Predicting the Yield of Grain Crops"), Moscow, 1977.

8. METODICHESKIYE UKAZANIYA PO PROVEDENIYU OPERATIVNYKH ISPYTANIY NOVYKH METODOV GIDROMETEOROLOGICHESKIKH PROGNOZOV (Systematic Instructions on Carrying Out Routine Tests of New Methods for Hydrometeorological Forecasts), Leningrad, Gidrometeoizdat, 1977.

9. Pannikov, V. D., KUL'TURA ZEMLEDELIYA I UROZHAY (Agricultural Crops and Yield), Moscow, Kolos, 1974.

10. Pasov, V. M., "Climatic Variability of Yield of Winter Wheat," METEOROLOGIYA I GIDROLOGIYA (Meteorology and Hydrology), No 2, 1973.

11. Polevoy, A. N., Myzina, T. I., METODICHESKIYE UKAZANIYA PO SOSTAVLENIYU AGROMETEOROLOGICHESKOGO PROGNOZA SREDNEOBLASTNOY UROZHAYNOSTI YAROVOGO YACHMENYA V NECHERNOZEMNOY ZONE YeTS (Systematic Instructions on Preparation of an Agrometeorological Forecast of the Mean Oblast Yield of Spring Barley in the Nonchernozem Zone of the European USSR), Moscow, Gidrometeoizdat, 1976.

12. Ilanova, Ye. S., AGROMETEOROLOGICHESKIYE USLOVIYA I UROZHAYNOST' OZIMOY PSHENITSY (Agrometeorological Conditions and Yield of Winter Wheat), Leningrad, Gidrometeoizdat, 1975.

13. Chernysheva, L. S., "Prediction of the Rice Yield in Primorskiy Kray," TRUDY DVNIGMI (Transactions of the Far Eastern Scientific Research Hydrometeorological Institute), No 48, 1974.

14. Chirkov, Yu.I., AGROMETEOROLOGICHESKIYE USLOVIYA I PRODUKTIVNOST' KUKURUZY (Agrometeorological Conditions and Corn Productivity), Leningrad, Gidrometeoizdat, 1969.

UDC 551.(509.3:524)

DESCENDING FLUX OF LONG-WAVE RADIATION AT THE 50-mb LEVEL

Moscow METEOROLOGIYA I GIDROLOGIYA in Russian No 8, Aug 79 pp 95-98

[Article by Candidate of Physical and Mathematical Sciences L. R. Dmitriyeva-Arrago and L. V. Samoylova, Main Geophysical Observatory, submitted for publication 2 August 1978]

Abstract: The authors computed the descending fluxes of long-wave radiation at the 50-mb level for latitude zones from 0 to 70°N each 10°. The article gives a comparison of the results of two variants of computations with different transmission functions with allowance for water vapor, carbon dioxide and ozone. The comparison indicated that the results of the computations differ by approximately a factor of 1.5-2. In the zonal variation the fluxes have a maximum in the middle latitudes.

[Text] Computations of fluxes of long-wave radiation in models with a great vertical resolution are carried out for the troposphere and stratosphere. As the upper boundary condition use is made of an equality of the descending current at the upper boundary of the atmosphere to zero [9].

In computations for the stratosphere it is necessary to take into account the absorption of radiation by ozone, carbon dioxide and water vapor. In models with few levels computations of radiation transfer are made approximately. Allowance for the influence of ozone is difficult because in the stratosphere there are usually no computation levels or there is only one such level. In order to avoid this difficulty the fluxes of long-wave radiation can be computed in advance for some level lying above the computation levels or for the last computation level in the model. In such a case it is possible to use climatic data on the profile of temperature and humidity, on the total content of ozone and carbon dioxide. The computed values of the descending flux can be used as a boundary condition for computing the long-wave flux in the troposphere on the basis of data on temperature and humidity, obtained using a hydrodynamic model.

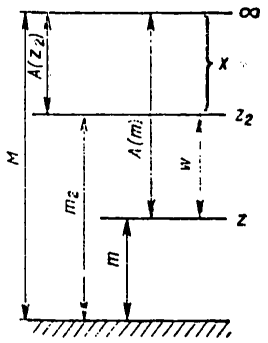

Fig. 1. Diagram of notations.

However, it is necessary to take into account the difference in the spectral composition of the incident radiation from the radiation of an ideally black body and use a modified transmission function [10].

In such a case for computing the descending flux A(z) it is possible to use a formula derived in [10]

$$A(z) = \int_{m}^{m_2} E(\varphi)\frac{dD'}{d\varphi}(z - m)\,d\varphi + A(z_2)\,D'(m_2 - m,\ M - m_2). \tag{1}$$

Here m_2 is the absorbing mass in the layer from the earth's surface to the level z_2, for which the flux is computed on the basis of climatic data, M is the effective absorbing mass of the entire column of the atmosphere, m is the effective absorbing mass in the layer from the earth's surface to some level z lying below z_2 (see Fig. 1), $E = \sigma T^4$ is the radiation function, D' is the modified integral transmission function, computed using the formula

$$D'(w, x) = \frac{D(w) - D(w + x)}{1 - D(x)}, \tag{2}$$

where $w = m_2 - m, \quad x = M - m_2,$

$$m = \int_0^z \rho_w \left(\frac{p}{p_0}\right)^n dz, \tag{3a}$$

$$M = \int_0^\infty \rho_w \left(\frac{p}{p_0}\right)^n dz, \tag{3b}$$

ρ_w is the density of the absorbing gas, n is an exponent taking into account the influence of nonuniformity of pressure in the atmosphere on absorption. For water vapor n = 0.5, for carbon dioxide n = 0.8, for ozone n = 0.25 [13], p_0 = 1000 mb, D(x) is the integral transmission function for ideally black radiation.

As the stratospheric computation level we chose the 50-mb level. The descending flux at the level z_2 is computed using a formula from [9]

$$A(z_2) = \int_{m_2}^{M} E(T)\, dD(\varphi, m_z). \tag{4}$$

where m_2 and M are determined using formulas (3a), (3b).

The computations were made on the basis of quite detailed data on the vertical distribution of temperature, ozone and humidity in the layer between p = 50 mb and p = 0.1 mb for different circles of latitude in January [13]. The humidity value was stipulated approximately [12]. Since available information on the descending flux of long-wave radiation at the level 50 mb is extremely fragmentary [1, 2, 4], it was of interest to carry out two variants of the computations with different transmission functions in order to obtain the possible interval of differences of this flux. We selected the following transmission functions:

1) The F. N. Shekhter function [11], taking into account absorption by water vapor, carbon dioxide and ozone:

$$D(H_2O,\ CO_2, O_3) = D(H_2O, CO_2) - A(O_3), \tag{5}$$

where

$$D(H_2O, CO_2) = D^*(m_H) - \Delta D, \tag{6}$$

$$D^*(m_H) = 0{,}471\, e^{-0{,}695\sqrt{m_H}} + 0{,}529\, e^{-8{,}94\sqrt{m_H}}, \tag{7}$$

ΔD is the correction for more accurate allowance for CO_2, represented below:

m_H	0,0001	0,0003	0,001	0,003	0,01	0,03	0,1	0,3	1	3
$100\Delta D$	7,4	8,2	8,5	8,9	9,2	7,4	5,2	2,2	0,2	0,0

$A(O_3)$ is the absorption function for ozone, represented below, where $m(O_3)$ is the ozone content in a column from the upper boundary to the z-level

$m(O_3)$	0,01	0,03	0,06	0,1	0,2	0,4	0,6
$100\ (A\ O_3)$	0,4	0,9	1,6	2,3	3,3	4,1	4,4

In this transmission function an allowance for absorption by carbon dioxide was made approximately, using the relationships between the quantity of water vapor and carbon dioxide in the atmosphere. As the input value for the function $D(H_2O, CO_2)$ we use the effective water vapor content in the atmosphere m_H.

2) The Kh. Yu. Niylisk function [7]

$$D(w^*, u^*, m^*) = 0{,}001\,(\Delta D_1(w^*, u^*) + \Delta D_2(w^*, m^*)), \tag{8}$$

where w^*, u^*, m^* are the effective absorbing masses of water vapor, carbon dioxide and ozone.

ΔD_1 is a function taking into account absorption by water vapor and carbon dioxide, ΔD_2 is a function taking into account absorption by water vapor and ozone.

The computation formula (4) was written in a form convenient for approximate computations

$$A(m_k) = \sum_{i=1}^{k} E(T_{i-1/2}) \times \left(D\left(\sum_{j=i+1}^{k} \Delta w_j\right) - D\left(\sum_{j=i}^{k} \Delta w_j\right)\right). \tag{9}$$

Here the k denotes the total number of layers into which the main layer $M - m_k$ is broken down

$$E(T_{i-1/2}) = \sigma T_{i-1/2}^4,$$

where $T_{i-1/2}$ is the temperature in the middle of the i-th layer, Δw_j is the effective mass of the absorbing gas present in the j-th layer, computed using the following formulas:

for ozone [8]

$$\Delta w_{O_3 i} = 69{,}1\ \bar{q}_{O_3}\,(p_i^{5/4} - p_{i-1}^{5/4}), \tag{10}$$

where $\bar{q}_{O_3\,i}$ is the mean ratio of the ozone mixture for the i-th layer, g/g, p_i is pressure at the upper boundary of the i-th layer, p_{i-1} is pressure at the lower boundary of the i-th layer;

for carbon dioxide [5]

$$\Delta w_{CO_2 i} = 146\left(\left(\frac{p_{i+1}}{p_0}\right)^{1{,}8} - \left(\frac{p_i}{p_0}\right)^{1{,}8}\right); \tag{11}$$

for water vapor [3]

$$\Delta w_{H_2O} = 0{,}01\left(\frac{e_i}{\sqrt{p_i}} + \frac{e_{i+1}}{\sqrt{p_{i+1}}}\right) \times (p_{i+1} - p_i), \tag{12}$$

where e_i is water vapor elasticity, mb.

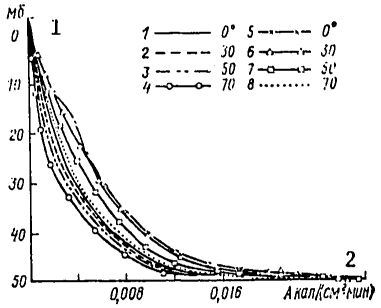

Fig. 2. Vertical distribution of descending flux of long-wave radiation for different latitude zones (1-4 -- Kh. Niylisk transmission function; 5-8 -- F. N. Shekhter transmission function).

KEY:

1. mb
2. A cal/(cm^2·min)

Table 1

Descending Flux of Long-Wave Radiation at 50-mb Level in cal/(cm^2·min)

Широта, *град* Latitude, degrees							
0	10	20	30	40	50	60	70
0,0142 0,0258	0,0146 0,0262	0,0154 0,0277	0,0150 0,0271	0,0155 0,0280	0,0155 0,0280	0,0143 0,0259	0,0124 0,0226

On the basis of formulas (9)-(12), with the use of (4)-(8), we carried out computations for mean zonal initial data relating to latitudes from $\varphi = 0°$ to $\varphi = 70°$, each 10°. The results of the computations are given in Fig. 2 and in Table 1.

Figure 2 shows the vertical profile of the flux of descending radiation for four latitudes zones for both variants of the computations. Table 1 gives the latitudinal variation of the descending flux of long-wave radiation, computed with allowance for its absorption by ozone, water vapor and carbon dioxide with the use of the Shekhter and Niylisk transmission functions.

A comparison shows that the results of the computations differ by a factor of approximately 1.5-2. In the latitudinal distribution all the values of the flux decreased toward the pole and equator and increase in the middle latitudes. For example, at Murmansk station in winter the measured flux at the 50-mb level is 0.08-0.1 cal/(cm^2·min). At the same time the data in

Table 1 (line 2) are quite close to the computations made in [1] for a dry cold atmosphere where the flux values were obtained at an altitude 10 km -- A = 0.038 cal/(cm^2·min).

BIBLIOGRAPHY

1. Ginzburg, A. S., Niylisk, Kh. Yu., "Comparison of Different Methods for Computing the Field of Long-Wave Radiation," TEPLOOBMEN V ATMOSFERE (Heat Exchange in the Atmosphere), Moscow, 1972.

2. Ginzburg, A. S., Yershov, A. G., Semenchenko, B. A., Feygel'son, Ye. M., "Fluxes of Thermal Radiation at the Center of the Equatorial Atlantic According to Computations and Measurements on the Scientific Research Ship 'Akademik Kurchatov'," TRUDY MEZHDUVEDOMSTVENNOY EKSPEDITSII TROPEKS-74 (Transactions of the Interdepartmental Expedition Tropeks-74), T 1, ATMOSFERA (Atmosphere), 1976.

4. Dmitriyeva-Arrago, L. R., "Computation of Gains of Long-Wave Radiation Under Cloudy Conditions," TRUDY GGO (Transactions of the Main Geophysical Observatory), No 197, 1968.

5. Kagan, R. L., "Computations of Fluxes of Thermal Radiation in the Cloudless Atmosphere," TRUDY GGO, No 174, 1965.

6. Kondrat'yev, K. Ya., LUCHISTYY TEPLOOBMEN V ATMOSFERE (Radiant Heat Exchange in the Atmosphere), Leningrad, Gidrometeoizdat, 1956.

7. Niylisk, Kh. Yu., "Determining the Intensity of Long-Wave Radiation in the Atmosphere," Tartu, AN ESSR, IFA, No 3, 1962.

8. Khrgian, A. Kh., FIZIKA ATMOSFERNOGO OZONA (Physics of Atmospheric Ozone), Leningrad, Gidrometeoizdat, 1973.

9. Shekhter, F. N., "Computation of Radiant Heat Fluxes in Atmosphere," TRUDY GGO, No 22, 1950.

10. Shekhter, F. N., "Computation of the Radiant Heat Influx," TRUDY GGO, No 187, 1966.

11. Shekhter, F. N., "On Radiation Diagrams," TRUDY GGO, No 150, 1964.

12. Mastenbrook, H. J., "Water Vapor Observations at Low, Middle and High Latitudes During 1964 and 1965," NAVAL RESEARCH LABORATORY REPORT 6447, 1966.

13. Rodgers, Clive D., "The Radiative Heat Budget of the Troposphere and Lower Stratosphere," Massachusetts Institute of Technology, Report No 42, 1967.

UDC 551.576.11

ROLE OF RADIATION IN THE FORMATION OF STRATIFORM CLOUDS

Moscow METEOROLOGIYA I GIDROLOGIYA in Russian No 8, Aug 79 pp 98-99

[Article by Doctor of Physical and Mathematical Sciences Ye. M. Feygel'son, Institute of Physics of the Atmosphere, submitted for publication 27 November 1978]

Abstract: The author comments on an article by Professor L. T. Matveyev entitled "Reasons for Cloud Formation" [2].

[Text] The author of [2] assumes that he was able to demonstrate the secondary role of radiation in the thermal regime and formation of St-Sc-Ac clouds and recommends that in the corresponding numerical models in the first approximation the radiation factor be neglected.

Such a recommendation inevitably leads to a contradiction with the physical laws of thermal radiation.

The fact is that a cloud radiates as a black body and the atmosphere above the clouds has a far lesser emissivity. Therefore, the flux of descending thermal radiation increases sharply, intersecting the upper boundary of the cloud. A "thermal pit" is created which in the upper parts of model inhomogeneous cloud layers ensures a cooling of about 10°/day [4]. For these same physical reasons the flux of ascending radiation, passing through the lower boundary of the cloud layer, here creates a zone of heating of about 1°C/day.

These radiation losses and the heat source near the cloud boundaries are not only computed, but are also clearly detected using data from measurements of radiation fluxes. It goes without saying that in real clouds the radiation effects are smoothed (in part due to instrument inertia); nevertheless, they attain several degrees per day [4].

The intensity of cooling and heating is dependent on the size of the cloud droplets, the position of the cloud boundaries, the distribution of temperature and water vapor content outside the cloud, and most importantly of all, the liquid water content gradient dw/dz near the boundaries [4].

The radiation effect of St-Sc-Ac clouds is much greater than the similar effect of Ns-As clouds because, according to the data published by L. T. Matveyev, dw/dz near the upper boundary in the first case is much greater than in the second [3].

In our opinion, there is no need to ask whether or not radiant heat exchange exerts an influence on the cloud-formation process. Other questions are more logical: what physical mechanisms arise as a result of the formation of such a powerful "thermal pit," how do they lead to its smoothing and what is the resultant effect?

It is possible that these questions at least in part have been answered by L. T. Matveyev, who demonstrated that in clouds turbulent exchange is intensified in comparison with that in the surrounding space [3].

Now we will further discuss the direct argumentation of article [2].

1. The "results of computation of temperature change (ΔT) after 10 hours, caused by absorption and emission of infrared radiation," cited on page 25, in actuality represent the difference $T' - T$, where T is the temperature computed in the L. T. Matveyev cloud-formation model [3] without allowance for radiation, and T' is temperature in the same model with addition of a radiation "block."

The cited numbers ($\Delta T = +0.3°C$ near the lower boundary of the cloud and $\Delta T = -0.2°C$ near its upper boundary) do not at all mean a real increase or decrease in the temperature at the boundaries after 10 hours. The radiation only changed the reaction of temperature to other forms of heat exchange by the indicated -- not small -- values.

2. The radiation heating at the lower boundary of the cloud layer was almost an order of magnitude less than the cooling at the upper boundary. Therefore, the first, against the background of other forms of heat exchange, may not be manifested and will not lead to an anticorrelation of temperatures at the boundaries.

3. The aircraft sounding, whose data were used in [2], was carried out during the daytime when the "thermal pit" effect, if not completely, was half reduced by heating of the cloud by solar radiation [5].

4. If a comparison was made of temperature changes at the cloud boundaries after 12 hours from the onset of cloud formation, the sought-for anticorrelation of temperatures would probably be discovered under the condition that other forms of heat exchange during this time retained their intensity. However, in the forming cloud layers considered in [2] the changes after 12 hours in liquid-water content and other factors mentioned above can lead to both an intensification and to an attenuation of radiation effects, and independently in the neighborhood of each boundary.

This objection against the argumentation in [2] is basic; a similar discussion is given on p 12 in [4].

We point out in conclusion that the author of this note does not insist and never has insisted on a first and foremost role of radiant heat exchange in the cloud formation process. What we are talking about is the need for creating closed models in which all forms of moisture and heat exchange would interact. Models of this kind are being created and as a rule take radiation into account [1].

BIBLIOGRAPHY

1. Buykov, M. V., CHISLENNOYE MODELIROVANIYE OBLAKOV SLOISTYKH FORM. OBZOR (Numerical Modeling of Stratiform Clouds. Review), Obninsk, 1978.

2. Matveyev, L. T., "Reasons for Cloud Formation," METEOROLOGIYA I GIDROLOGIYA (Meteorology and Hydrology), No 8, 1978.

3. Matveyev, L. T., KURS OBSHCHEY METEOROLOGII. FIZIKA ATMOSFERY (Course in General Meteorology. Physics of the Atmosphere), Leningrad, Gidrometeoizdat, 1976.

4. Feygel'son, Ye. M., LUCHISTYY TEPLOOBMEN I OBLAKA (Radiant Heat Exchange and Clouds), Leningrad, Gidrometeoizdat, 1970.

5. Feygel'son, Ye. M., Krasnokutskaya, L. D., POTOKI SOLNECHNOGO IZLUCHENIYA I OBLAKA (Fluxes of Solar Radiation and Clouds), Leningrad, Gidrometeoizdat, 1978.

UDC 551.576.1(234.9)

HELICAL CLOUDS IN THE EL'BRUS REGION

Moscow METEOROLOGIYA I GIDROLOGIYA in Russian No 8, Aug 79 pp 99-102

[Article by T. N. Bibikova, Moscow State University, submitted for publication 4 December 1978]

Abstract: The article gives an example of a rare form of helical clouds in the mountains of the Central Caucasus, in the El'brus region. The helical clouds developed during the flowing of a WSW flow around El'brus in the presence of a jet stream in the upper troposphere.

[Text] In mountainous regions circulations are manifested in the form of special types of local weather with the development of definite cloud systems, in particular, wave orographic systems consisting of lenticular clouds of the type Ac lent.

Numerous observations carried out in different regions of the earth made it possible to prepare a detailed description of many varieties of orographic clouds [2, 5]. However, in nature it is possible to encounter such forms as are not contained in special atlases of mountainous cloud types.

For example, on 3 August 1964, in the mountains of the Central Caucasus, in the neighborhood of El'brus, there were clouds of a rare helical form. Figure 1 shows three successive photographs of these clouds for 1200, 1210 and 1230 hours respectively. The photographs were taken from Epchik Pass (2296 m above sea level). Henceforth all elevations will be given from sea level.

Due to the exceptional form of the clouds we will briefly discuss the conditions for their genesis and development.

On 3 August the weather in the Caucasus was governed by a low-gradient pressure field and therefore during the first half of the day it was cloudless in the mountains of the Central Caucasus. At 1200 hours the first cloud appeared in the El'brus region; it rapidly began to change its configuration and a spiral twist was formed (Fig. 1a). At 1210 hours it developed a distinct helical form (Fig. 1b). Then along the line of sight a similar cloud developed which seemed to be considerably smaller on the photograph

due to its greater distance. The clouds retained their configuration for 17 minutes. At 1220 hours similar helical clouds began to form in greater number and by 1230 hours a whole series of helical clouds was formed (Fig. 1c).

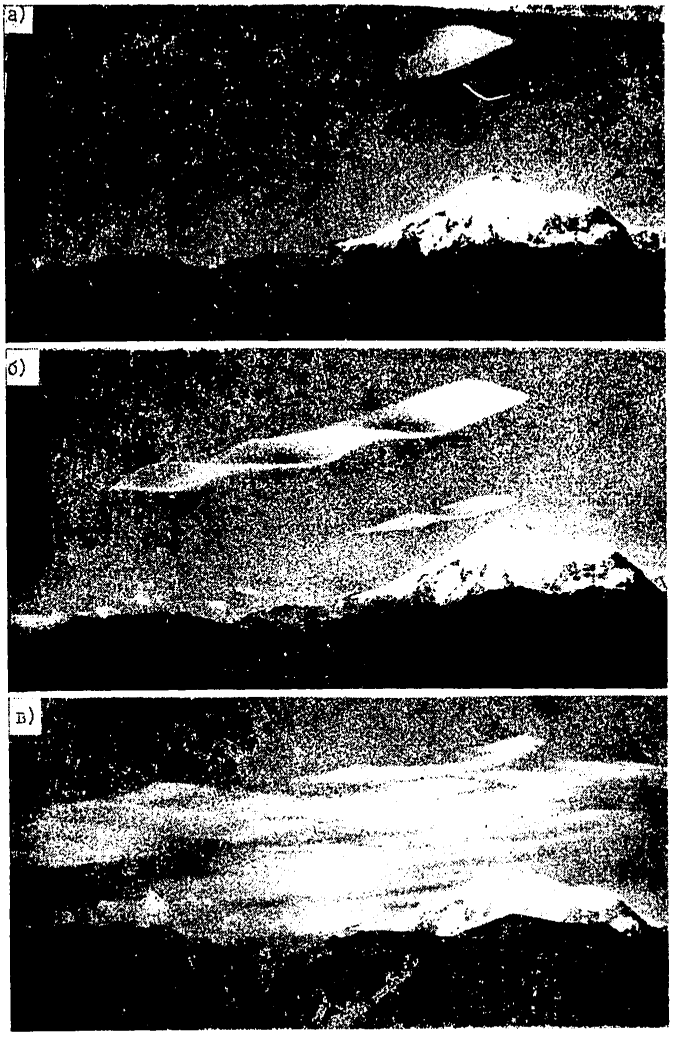

Fig. 1. Helical clouds in the El'brus region. Photographs taken from Epchik Pass on 3 August 1964. 1) 1200 hours; b) 1210 hours, c) 1230 hours.

An analysis of the photographs revealed that the clouds had a distinctly orographic nature since their windward part remained in place (despite a considerable wind velocity in the cloud layer) and seemingly was "tied" to a definite local relief. Only the leeward part of the cloud was rapidly drawn out and twisted. Unfortunately, the photographs were taken from one point and the position of the clouds and their dimensions can be obtained by stipulating the corresponding altitude of the lower base. For this purpose we used data from radiosonde observations at the nearest points: Sukhumi, Mineral'nyye Vody, Tbilisi and data from pilot balloon observations at Nal'chik station. By comparing these data with the orography, it was possible to advance some well-founded hypotheses.

The central part of the Main Caucasus Range is oriented from NW to SE and has mean elevations of 3500-4000 m. Individual peaks attain 4500-5500 m. The highest point is El'brus, in whose region the helical clouds developed. El'brus rises to 5633 m.

Figure 2a shows the vertical profiles of temperature and wind from the windward (Sukhumi station) and leeward (Mineral'nyy Vody station) sides of the range on the basis of radiosonde data for 0900 hours. Figure 2a shows that the wind direction in the oncoming flow had a stable WSW direction (232-253°) in the layer from 4000 m to the tropopause. If it is taken into account that the direction perpendicular to the range averages 230°, it becomes clear that the wind direction in the oncoming flow was deflected from the perpendicular direction not more than 25°. Thus, the wind shear was caused for the most part only by a change in wind velocity with altitude. The greatest vertical gradient of wind velocity was observed at altitudes from 9000 to 10 000 m (6 m/sec per 100 m) and from 10 000 to 11 000 m (12 m/sec per 100 m). In addition, in the layer 11 000-14 000 m there was a jet stream whose axis passed through the El'brus region (the wind velocity on the jet stream axis attained 45 m/sec). The tropopause was situated at an altitude of 14 270 m, that is, the upper boundary of the jet stream was situated near the lower boundary of the tropopause.

The variation of temperature with altitude in the oncoming flow was as follows: in the layer 1000-1500 m the vertical temperature gradient was small -- 0.3°C/100 m. At altitudes 2600-2800 m there was an isothermic layer, and above, in the layer from 3000 to 3840 m, there was again a reduced vertical temperature gradient -- γ = 0.33°C/100 m. Thus, in the lower layers of the atmosphere there was increased stability, which aloft was replaced by strong instability. In the layer from 4000 to 9000 m the vertical temperature gradient was close to a dry adiabatic gradient (γ = 0.85°C/100 m). Again, still higher, there was a layer with a small temperature gradient, that is, from 9000 to 11 000 m γ = 0.25°C/100 m. In general, the temperature variation with altitude in the windward flow (Mineral'nyye Vody station) was similar to the temperature variation in the leeward flow.

The relative humidity in the oncoming flow changed little with altitude and in the layer from 3000 m to the tropopause itself averaged 20%. In the leeward flow the relative humidity values were somewhat greater (by not more than 15%), nevertheless remaining small.

Knowing the tilt of the photograph, the focal length of the objective and the enlargement of the photograph, it is possible to construct the plane position of the clouds using the laws of perspective geometry. The results of such a construction gave the following. [Construction from a photograph taken at 1210 hours.] The clouds were formed behind El'brus, on its leeward side (on the northern side). If 9000 m is used as the altitude of the lower base, the length of the first (closest to Epchik Pass) helical cloud was 16 000 m, and the second -- 9000 m. The distance between the helical clouds in the direction perpendicular to the flow was 7000 m. The "pitch" for the larger cloud was 600 m. The rotation of this "screw" was to the right. This can be seen particularly clearly in the frames of the motion picture survey of these clouds.

We also stipulated the altitude of the lower base of these helical clouds at 11 000 m. The results of the corresponding computations are presented below.

Dimensions (km) of Helical Clouds for Altitudes of the Lower Base 9 and 11 km

Altitude of lower cloud base.....	9	11
Length of first cloud.....16		19
Length of second cloud.....	9	11
Distance between clouds (perpendicular to flow).....	7	8.5
Pitch of "screw".....	6	7

Comparing the computations of the corresponding parameters for two different altitudes, we note that they vary on the average by 20%.

Thus, an examination of the photographs of helical clouds together with an analysis of data from vertical sounding of the atmosphere make it possible to draw some conclusions:

1. The helical clouds were formed during the flow of a perpendicular SW wind around El'brus.

2. The presence of a jet stream at altitudes 11 000-13 000 m, in all probability, is characteristic for helical air movements in the upper troposphere and helical clouds are indicators of these movements.

3. Clouds developed in a flow having thick layers with small vertical temperature gradients.

In conclusion it should be said that in the recent literature it is more and more common to find articles indicating a helical nature of air movement in the mountains. Thus, investigations carried out at the Central Aerological Observatory in the mountains of Central Asia in the neighborhood of Tashkent using equal-altitude balloons made it possible to detect a helical structure of the flow at altitudes 10 000-12 000 m [3].

Summarizing everything which has been said, and also proceeding on the basis of the conclusions which we drew earlier in a study of orographic clouds in the Crimea [1] and the experimental results obtained by Shmeter and Pinus [4], we made the assumption that the helical clouds developed near a layer with the maximum wind shear under an inversion. In our opinion, the most probable altitude can be considered the altitude 9000 m (if it is also taken into account that the elevation of the underlying surface in the cloud region is more than 5000 m).

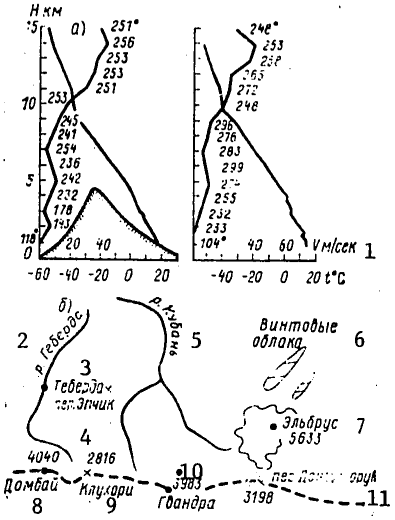

Fig. 2. Results of observations of orographic helical clouds on 3 August 1964. a) vertical profiles of temperature and wind according to radiosonde data for stations Sukhumi (at left) and Mineral'nyye Vody (at right) (the wind direction is given in degrees reckoned clockwise from the direction to the north. The direction of the perpendicular to the main line of the range is about 230°); b) horizontal position of clouds under the condition that the lower base of the helical clouds is at an altitude 9000 m.

KEY:

1. V m/sec
2. Teberda River
3. Teberda
4. Epchik Pass
5. Kuban' River
6. Helical clouds
7. El'brus
8. Dombay
9. Klukhori
10. Gvandra
11. Dongus-orun Pass

This fact is also confirmed by the studies of Angell, et al., who discovered sectors of spiral circulation in the Los Angeles region over the southern spurs of the Sierra Nevada. The vertical and horizontal dimensions of sectors with spiral circulation were 600-1000 m [6].

BIBLIOGRAPHY

1. Dyubyuk, A. F., Bibikova, T. N., "Conditions for the Formation of Cloud Cover in Dependence on Orography," TRUDY GGO (Transactions of the Main Geophysical Observatory), No 171, 1965.

2. Musayelyan, Sh. A., VOLNY PREPYATSTVIY V ATMOSFERE (Obstacle Waves in the Atmosphere), Leningrad, Gidrometeoizdat, 1962.

3. Patsayeva, V. A., "Investigation of Orographic Disturbances in the Atmosphere Using Equal-Altitude Balloons," TRUDY TsAO (Transactions of the Central Aerological Observatory), No 59, 1964.

4. Pinus, N. Z., Shmeter, S. M., ATMOSFERNAYA TURBULENTNOST', VYZVAYUSHCHAYA BOLTANKU SAMOLETOV (Atmospheric Turbulence Causing Aircraft Bumping), Moscow, Gidrometeoizdat, 1962.

5. Alaka, M., "The Airflow Over Mountains," WMO, TECHNICAL NOTE, No 34, 1960.

6. Angell, J. R., Pack, D. H., Holxworth, G. G., Dickson, G. R., "Tetroon Trajectories in an Urban Atmosphere," J. APPL. METEOROL., Vol 5, No 5, 1966.

UDC 551.(461.25+465.755)

USE OF THE HIGH-ALTITUDE PRESSURE FIELD FOR INCREASING THE ADVANCE TIME FOR SHORT-RANGE FORECASTS OF SEA LEVEL

Moscow METEOROLOGIYA I GIDROLOGIYA in Russian No 8, Aug 79 pp 102-104

[Article by V. I. Andryushchenko, Arctic and Antarctic Scientific Research Institute, submitted for publication 1 November 1978]

Abstract: The author proposes a procedure for using steering current rules for increasing the advance time of predictions of surge variations in sea level.

[Text] Predictions of aperiodic variations of sea level are an important component part of the system for hydrometeorological support of marine operations. The effectiveness of planning of the latter is essentially dependent on the advance time of the forecasts. However, the advance time of most prognostic methods developed both in our country and abroad does not surpass the time interval separating the cause from the effect. The length of this interval is different for different points, but its optimum value does not evidently exceed 27 hours. It is possible to achieve an objective increase in the advance time of level forecasts without making a synoptic forecast for this purpose by means of use of additional information in the form of actual AT_{500} charts related to the time of preparation of the forecast.

In routine synoptic practice in the analysis and prediction of weather extensive use is made of the steering current rule, according to which the movement of pressure systems and fronts occurs along the isohypes at AT_{500} in the direction of the high-level wind. The rate of movement of pressure systems is proportional to the velocity of the high-level wind or the density of the isohypses at AT_{500}. Since the variability of high-pressure fields is considerably less than the variability of the surface pressure fields, this circumstance is effectively used for prediction of movement of surface pressure formations.

Applicable to level predictions, the steering current rule can be used for transforming the coordinates of points at which atmospheric pressure is read from the surface weather chart. The sense of this transformation is to read pressure at that part of the surface chart from which with the

greatest probability it is possible to expect movements of any pressure formation. Thus, if in the prognostic regression equation as the predictors we use the pressure differences or the coefficients of expansion of the pressure field, in addition to that advance time for which the particular equation was computed, the transformation of coordinates of the points makes it possible to obtain an additional advance time. The length of this additional advance time is naturally determined as the minimum time interval T during which the moving pressure system (such as a cyclone) can overcome the distance between the centers of action of the surface pressure field. The centers of action (there are usually two) are those field regions, being situated in which a medium-scale cyclone causes the greatest rise or fall at the investigated point. They are easily determined by simple averaging of the surface pressure fields relating to the times of extremal level values.

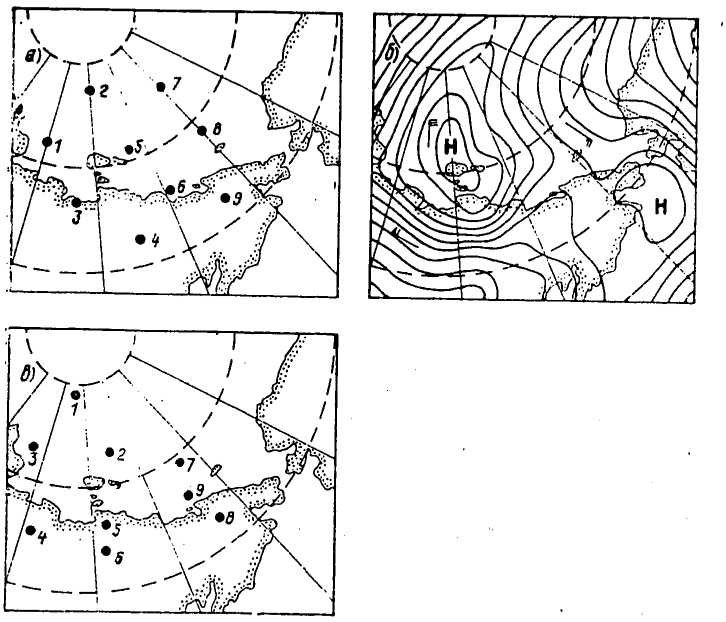

Fig. 1. Example of transformation of coordinates at which surface atmospheric pressure is read. a) initial grid of points, b) AT_{500} chart 19 August 1972, c) transformation of grid points.

The principle for the transformation of coordinate points can be represented in the following way. Each point of the working grid is matched with the middle of a unit segment oriented along the normal to the isohypses at AT_{500}. Then it is displaced along the isohypses in the direction opposite the steering current (high-altitude wind) at a distance proportional to the number of isohypses intersecting the unit segment. As a unit segment it is

possible to take a part of the distance between the centers of action of the surface pressure field, for example, a half.

Since the greatest path which a cyclone can overcome during the time T is equal to the distance between the centers of action in the pressure field, the ratio of this distance to the maximum number of isohypses intersecting it at AT500 gives a distance unit corresponding to one isohypse. In order that the obtained distance unit correspond to the length of a unit segment, it must be increased by as many times as the unit segment is less than the distance between the centers of action of the pressure field. For routine work it is most convenient that the distance be expressed in degrees of latitude.

An example of transformation of coordinates of the points is illustrated in Fig. 1, in which the initial grid of points after being superposed on AT500 and transformation of the coordinates of points acquires a new form (Fig. 1c). The operation of transformation of the coordinates of points makes possible an indirect allowance for the probable movement of the pressure formations acting at the level, but their possible evolution is not taken into account. The influence of this shortcoming can be somewhat lessened by adding to the pressure read from the surface chart by means of transformation of the grid of points the value of its tendency, performing this addition algebraically.

Testing of the proposed scheme for increasing the advance time of level forecasts at the bar of the Kolyma River gave fairly good results and at the present time this scheme is being used successfully in routine practical work in the eastern regions of the Arctic.

UDC 556.013

LAW OF DISTRIBUTION OF SUM OF RANDOM VALUES WITH TYPE-III PEARSON PROBABILITY DENSITIES IN HYDROLOGY

Moscow METEOROLOGIYA I GIDROLOGIYA in Russian No 8, Aug 79 pp 104-107

[Article by Candidate of Technical Sciences I. V. Busalayev, Kazakh Scientific Research Institute of Power, submitted for publication 12 February 1979]

Abstract: The author has derived a general, completely rigorous formula for the composition of γ-distributed hydrological random values suitable for any number of components. This formula can be used in deriving different approximate or asymptotic expressions convenient for hydrological computations. On its basis (with specific values of the parameters) it is easy to determine the approximation error. The formula is useful for hydrological and water management applications.

[Text] Despite a half-century of experience of use of the type-III Pearson distribution in hydrology, some of its important properties have still not been clarified. In particular, a formula for the composition of distributions of this type in a general case remains unknown. [For the first time the type-III Pearson curve was used in hydrology by Foster in 1924 and later in the 1930's by D. L. Sokolovskiy, S. N. Kritskiy and M. F. Menkel'.]

In our article [3] an attempt was made to answer this question. We derived an approximate formula, convenient for use and generalization, but not entirely rigorous and precise.

In this brief communication, which can be regarded as a continuation of the mentioned article, we derive and demonstrate a composition formula entirely correctly and examine some corollaries from it useful for hydrological computations.

Assume that the random values x_i, distributed in conformity to the law

$$g_i(x_i) = Ce^{-\gamma_i x_i} x_i^{\alpha_i - 1},$$

are independent and in addition,

$$\gamma_1 < \gamma_2 < \ldots < \gamma_n < \infty \quad (i=1, 2, \ldots, n),$$

it being required that the distribution of their sum be determined

$$y = \sum_{i=1}^{n} x_i.$$

For the mentioned densities we find their Laplace transform

$$L\{g_i(x); p\} = \left(\frac{\gamma_i}{p+\gamma_i}\right)^{a_i},$$

which, with some assumptions (positiveness of x_i and monotony of L) unambiguously determines the distribution [7].

By virtue of the multiplicity property, the Laplace transform of the sum of the independent random values is equal to the product of the corresponding transforms of the terms [6]

$$L\{P(y); p\} = \left(\frac{\gamma_1}{p+\gamma_1}\right)^{a_1} \ldots \left(\frac{\gamma_n}{p+\gamma_n}\right)^{a_n}. \tag{1}$$

The probability density function of the indicated sum of random values can now be determined using an inverse transform of expression (1). In order to accomplish this we will rewrite formula (1) in the following equivalent form:

$$L\{P(y); p\} = \gamma_1^{a_1}\left(\frac{1}{p+\gamma_n-(\gamma_n-\gamma_1)}\right)^{a_1} \cdot \gamma_2^{a_2}\left(\frac{1}{p+\gamma_n-(\gamma_n-\gamma_2)}\right)^{a_2} \ldots \tag{2}$$

$$\ldots \gamma_n^{a_n}\left(\frac{1}{p+\gamma_n-(\gamma_n-\gamma_n)}\right)^{a_n}.$$

Then, using the known pair of Laplace transforms [1, 5]

$$t^{\gamma-1}\Phi_2[\beta_1, \ldots, \beta_n; \gamma; \lambda_1 t, \ldots, \lambda_n t] \doteq \frac{\Gamma(\gamma)}{p^{\gamma}}\left(1 - \right.$$

$$\left. -\frac{\lambda_1}{p}\right)^{-\beta_1} \ldots \left(1-\frac{\lambda_n}{p}\right)^{-\beta_n}.$$

where Φ_2 is a degenerate hypergeometric function of n variables [2, 4].

We will multiply the original by $e^{-\lambda_n t}$, in connection with which in the transform we will have $p + \lambda_n$ instead of p. After some simple transformations, also taking into account that in our case $\beta_1 + \ldots + \beta_n = \gamma$, we will have

$$e^{-\lambda_n t}\, t^{\gamma-1}\Phi_2(\beta_1, \ldots, \beta_n; \gamma; \lambda_1 t, \ldots, \lambda_n t) \doteq \tag{3}$$

$$\doteq \frac{\Gamma(\gamma)(p+\lambda_n)^{\gamma}}{(p+\lambda_n)^{\gamma}}\left(\frac{1}{p+\lambda_n-\lambda_1}\right)^{\beta_1}\cdots\left(\frac{1}{p+\lambda_n-\lambda_n}\right)^{\beta_n}. \tag{3}$$

Comparing the derived expression (3) with formula (2), using the inverse transform we find the density distribution function for the sum of gamma-distributed independent random values in the most general form:

$$P(y)=\frac{\gamma_1^{a_1}\cdots\gamma_n^{a_n}}{\Gamma(a_1+\ldots+a_n)}e^{-\gamma_n y}\,y^{a_1+\ldots+a_n-1}\times \tag{4}$$

$$\times\Phi_2[a_1,\ldots,a_n;\ a_1+\ldots+a_n;\ (\gamma_n-\gamma_1)y,\ldots,(\gamma_n-\gamma_n)y].$$

We will show that the necessary normalization conditions are also satisfied:

$$\int_0^{\infty}P(y)\,dy=\frac{\gamma_1^{a_1}\cdots\gamma_n^{a_n}}{\Gamma(a_1+\ldots+a_n)}\int_0^{\infty}e^{-\gamma_n y}\,y^{a_1+\ldots+a_n-1}\Phi_2[a_1,\ldots,a_n;\ a_1$$

$$+\ldots+a_n;\ (\gamma_n-\gamma_1)y,\ldots,(\gamma_n-\gamma_n)y]\,dy=$$

$$=\frac{\gamma_1^{a_1}\cdots\gamma_n^{a_n}}{\Gamma(a_1+\ldots+a_n)}\frac{\Gamma(a_1+\ldots+a_n)}{\gamma_n^{a_1+\ldots+a_n}}\times$$

$$\left(1-\frac{\gamma_n-\gamma_1}{\gamma_n}\right)^{-a_1}\cdots\left(1-\frac{\gamma_n-\gamma_n}{\gamma_n}\right)^{-a_n}=1.$$

Thus, formula (4) in actuality represents the sought-for density of the sum of γ-distributed random values.

Now we will examine some special cases:

a) With $\gamma_1=\gamma_2=\ldots=\gamma_n=\gamma$ all the variables in the hypergeometric function become equal to zero and $\Phi_2=1$ and we obtain the known result

$$P(y)=\frac{\gamma^{a_1+\ldots+a_n}}{\Gamma(a_1+\ldots+a_n)}e^{-\gamma y}\,y^{a_1+\ldots+a_n-1}.$$

b) Assume that n = 2; then, since $(\gamma_2-\gamma_2)y=0$, in the numerator the parameter a_2 disappears and from the general formula we have

$$P(y)=\frac{\gamma_1^{a_1}\gamma_2^{a_2}}{\Gamma(a_1+a_2)}e^{-\gamma_2 y}\,y^{a_1+a_2-1}\,{}_1F_1[a_1,\ a_1+a_2;\ (\gamma_2-\gamma_1)y]. \tag{5}$$

where ${}_1F_1$ is a degenerate hypergeometric Kummer function.

The mentioned distribution of the sum $y=x_1+x_2$ can be obtained in direct computations [3].

For this same reason, with n = 3, we obtain the probability density function, expressed through a hypergeometric function of two variables

$$P(y) = \frac{\gamma_1^{a_1}\gamma_2^{a_2}\gamma_3^{a_3}}{\Gamma(a_1+a_2+a_3)} e^{-\gamma_3 y} y^{a_1+a_2+a_3-1} \times$$
$$\times \Phi_2[a_1, a_2; a_1+a_2+a_3; (\gamma_3-\gamma_1)y, (\gamma_3-\gamma_2)y].$$

c) Proceeding from the general formula, it is also possible to obtain some other equivalent expressions for density. For example, substituting into the exponent γ_{min} or the sum of all γ_i, we will have

$$P(y) = \frac{\gamma_1^{a_1} \cdot \ldots \cdot \gamma_n^{a_n}}{\Gamma(a_1+\ldots+a_n)} e^{-\left(\sum_i \gamma_i\right) y} y^{\sum_i a_i - 1} \Phi_2[a_1, \ldots, a_n; \quad (6)$$
$$a_1+\ldots+a_n; \left(\sum_i \gamma_i - \gamma_1\right) y, \ldots, \left(\sum_i \gamma_i - \gamma_n\right) y].$$

This expression is convenient in that with sufficiently large n ($n \to \infty$) it can be expressed through one variable.

In actuality, if it is assumed that

$$\lim_{n\to\infty} \frac{\gamma_i}{\sum_i \gamma_i} = 0, \quad i = 1, \ldots, n$$

(any of γ_i at the limit is quite small in comparison with the entire sum), then, using a formula from [4, 8]

$$\Phi_2[a_1, \ldots, a_n; a_1+\ldots+a_n; x, \ldots, x] = \Phi_2[a_1+\ldots+a_n; a_1+\ldots+a_n; x],$$

we obtain

$$\Phi_2\left[a_1, \ldots, a_n; a_1+\ldots+a_n; \left(\sum_i \gamma_i - \gamma_1\right) y, \ldots, \left(\sum_i \gamma_i - \gamma_n\right) y\right] =$$
$$= \Phi_2\left[a_1+\ldots+a_n, a_1+\ldots+a_n \left(\sum_i \gamma_i - \gamma_i\right) y\right] = e^{\left(\sum_i \gamma_i - \gamma_{max}\right) y}.$$

Hence, substituting the exponent

$$e^{\left(\sum_i \gamma_i - \gamma_{max}\right) y}$$

into formula (6), we find that at the limit with $n \to \infty$ there is satisfaction of the equation

$$P(y) = Ce^{-\gamma_{max} y} y^{a_1+\ldots+a_n-1}.$$

The general formulas (4) and (6) can be easily generalized for describing the linear form of the random values conforming to a gamma-distribution

$$y = b_1 x_1 + \ldots + b_n x_n, \; b_i > 0. \quad (7)$$

In accordance with the similarity rule the Laplace transform of the probability density function of the i-th term from (7) is equal to the expression

$$L\{g_i(b_i x_i); p\} = \frac{1}{b_i}\left(\frac{\gamma_i}{p/b_i + \gamma_i}\right)^{a_i} = \frac{(\gamma_i b_i)^{a_i}}{b_i}\left(\frac{1}{p + \gamma_i b_i}\right)^{a_n}.$$

Since the probability density function of a linear form (7) (in the case of a nondependence of the random values, which is assumed) corresponds to the product of the Laplace transforms, we will have, after small transformations

$$L\{P(y); p\} = \frac{(b_1\gamma_1)^{a_1} \cdot \ldots \cdot (b_n\gamma_n)^{a_n}}{b_1 \ldots b_n}\left(\frac{1}{p + \gamma_n - (\gamma_n - \gamma_1 b_1)}\right)^{a_1} \ldots$$

$$\ldots \left(\frac{1}{p + \gamma_n - (\gamma_n - \gamma_n b_n)}\right)^{a_n}.$$

Hence, similar to the preceding, we obtain

$$P(y) = C\,\frac{(b_1\gamma_1)^{a_1} \cdot \ldots \cdot (b_n\gamma_1)^{a_n}}{\Gamma(a_1 + \ldots + a_n)\, b_1 \ldots b_n}\, e^{-\gamma_n y}\, y^{a_1 + \ldots + a_n - 1} \times \qquad (8)$$

$$\times \Phi_2[a_1, \ldots, a_n; a_1 + \ldots + a_n; (\gamma_n - \gamma_1 b_1) y, \ldots, (\gamma_n - \gamma_n b_n) y],$$

where C is a normalization factor.

A conclusion of practical importance for hydrological applications follows from this formula: if the coefficients b_i are assumed to be equal to γ_n/γ_i, we obtain (since in this case in formula (8) $\Phi_2 = 1$) the γ-distribution.

The established fact affords the possibility for programmed modeling of γ-distributed hydrological series with the stipulated parameters γ and a on an electronic computer. In this respect it is particularly convenient to use a formula of the type (6) with an exponent expressed through

$$\sum_{i=1}^{n} \gamma_i.$$

It is sufficient to multiply the initial series by the coefficients

$$\sum_{i} \gamma_i/\gamma_i,$$

in order to construct from them a Pearson series with stipulated characteristics.

Thus, we confirmed that the derived formulas (4), (6), (8) are extremely useful for both theoretical examinations and for practical computations. On their basis it is possible to construct different types of approximate or asymptotic expressions and also investigate the limiting properties of density when $n \to \infty$. In specific computations, using it one can then estimate the approximation error for a definite combination of parameters.

BIBLIOGRAPHY

1. Beytmen, G., Erdeyn, A., TABLITSY INTEGRAL'NYKH PREOBRAZOVANIY (Tables of Integral Transforms), Vol I, Moscow, Nauka, 1969.

2. Beytman, G., Erdeyn, A., VYSSHIYE TRANSTSENDENTNYYE FUNKTSII (GIPERGEOMETRICHESKIYE FUNKTSII, FUNKTSII LEZHANDRA) (Higher Transcendental Functions (Hypergeometric Functions, Legendre Functions)), Moscow, Nauka, 1965.

3. Busalayev, I. V., "Composition Formula for Distribution Curves of Hydrological Parameters (Type-III Pearson)," METEOROLOGIYA I GIDROLOGIYA (Meteorology and Hydrology), No 8, 1977.

4. Gradshteyn, I. S., Ryzhik, I. M., TABLITSY INTEGRALOV, SUMM, RYADOV I PROIZVEDENIY (Tables of Integrals, Sums, Series and Products), Moscow, Fizmatizdat, 1962.

5. Ditkin, V. A., Prudnikov, A. P., SPRAVOCHNIK PO OPERATSIONNOMU ISCHISLENIYU (Handbook on Operational Calculus), Moscow, Vysshaya Shkola, 1965.

6. Prokhorov, Yu. V., Rozanov, Yu. A., TEORIYA VEROYATNOSTEY (Theory of Probabilities), Moscow, Nauka, 1973.

7. SPRAVOCHNIK PO TEORII VEROYATNOSTEY I MATEMATICHESKOY STATISTIKE (Handbook on the Theory of Probabilities and Mathematical Statistics), Kiev, Naukova Dumka, 1978.

8. Appell, P., Kampe de Feriet M., FONCTIONS HYPERGEOMETRIQUES ET HYPERSPHERIQUES, POLYNOMES d'HERMITE, Gauthier-Villars, 1926.

UDC 551.(508.769:571)

LIDAR MEASUREMENTS OF ATMOSPHERIC HUMIDITY

Moscow METEOROLOGIYA I GIDROLOGIYA in Russian No 8, Aug 79 pp 108-114

[Article by Doctor of Physical and Mathematical Sciences V. M. Zakharov, S. F. Kalachinskiy, Candidate of Physical and Mathematical Sciences O. K. Kostko, G. A. Krikunov and I. S. Zhiguleva, Central Aerological Observatory, submitted for publication 2 January 1979]

Abstract: The article gives a description of laser ranging apparatus developed by the authors for determining humidity of the lower troposphere. The authors analyze the results of measurements of humidity of the lower troposphere obtained during 1976-1977 at the laser sounding station at the Central Aerological Observatory in Dolgoprudnyy.

[Text] Introduction. The development of remote methods for determining the humidity field in the lower troposphere is necessary for a number of reasons. As is well known, gas and aerosol contaminants, propagating from the sources of effluent, interact with the humidity field, which to a considerable degree can determine the distribution of contaminating substances in the atmosphere and as a result, lead to the formation later of chemical reactions of the new components. These processes are of the greatest interest in the air basin of industrial centers, where regular radiosonde measurements most frequently are impossible. The results of humidity measurements in the lower troposphere, obtained by remote methods, can also be used for the purposes of weather forecasting, since these measurement methods can supply a great mass of statistical data. Remote measurement methods make it possible to determine humidity on any sounding path, which is necessary for solving some practical problems. Finally, joint measurements of the distribution of humidity and aerosols in the atmosphere make it possible to investigate their joint influence on atmospheric transparency, and accordingly, on the radiative transfer of heat in the atmosphere. The enumerated problems stimulated the development of the remote laser sounding method and the creation of apparatus for determining the humidity profile in the lower troposphere.

Measurement Method

As the remote method for determining atmospheric humidity we selected the "spontaneous combination scattering method" (SCS) for the scattering of laser radiation on water vapor. In using the SCS method the backscattering signal from scattering on water vapor is compared with a signal caused by SCS on molecular nitrogen. In the processing of sounding data this makes it possible to exclude some instrument coefficients, and with simultaneous reception at two SCS wavelengths, exclude instability of laser radiation. The distribution of the water vapor concentration ρ_{H_2O} with altitude H is determined by the following expression from [4]:

$$[\text{CKP} = \text{SCS}] \quad \rho_{H_2O}(H) = \rho_{N_2}(H) \frac{N_{\text{CKP},1}(H)\,\sigma^0_{\pi\,\text{CKP},2}\,K_{12}K_{22}\eta_2 \exp\left\{-\int_0^H \varepsilon_2(H')\,dH'\right\}}{N_{\text{CKP},2}(H)\,\sigma^0_{\pi\,\text{CKP},1}\,K_{11}K_{21}\eta_1 \exp\left\{-\int_0^H \varepsilon_1(H')\,dH'\right\}}, \tag{1}$$

where $N_{SCS}(H)$ is the backscattering signal caused by SCS, K_1 is the transmission coefficient for the optical receiving system and the interference filter, K_2 is the transmission coefficient for the selecting filter, η is the quantum efficiency of the photomultiplier, ε is the attenuation index, σ^0_{SCS} is the SCS backscattering cross section, ρ_{N_2} is the concentration of molecular nitrogen, the subscripts 1 and 2 denote the wavelengths of SCS on water vapor and molecular nitrogen respectively. Since sounding in most cases was carried out with high values of the meteorological range of visibility, then it was assumed that

$$\frac{q_{377,7}}{q_{397,5}} = 1 \qquad \left(q = \exp\left\{-2\int_0^H \varepsilon(H')\,dH'\right\}\right).$$

The maximum error in the estimates due to this assumption on the entire sounding path does not exceed 5% (see end of article).

Thus, expression (1) can be written in the form

$$\rho_{H_2O}(H) = \rho_{N_2}(H) \frac{N_{\text{CKP},1}(H)\,\sigma^0_{\pi\,\text{CKP},2}\,K_{12}K_{22}\eta_2}{N_{\text{CKP},2}(H)\,\sigma^0_{\pi\,\text{CKP},1}\,K_{11}K_{21}\eta_1}. \tag{2}$$

Formula (2) includes the ratio of the SCS cross sections for H_2O and N_2. An analysis of data in the literature [4] indicated that as the SCS cross sections it is possible to use the mean values $\sigma^0_{\pi\,SCS\,2} = 3.05\cdot10^{-30}$ cm^2/sr, $\sigma^0_{\pi\,SCS\,1} = 7.62\cdot10^{-30}$ cm^2/sr. The quantum efficiency of the photomultiplier for wavelengths 377.7 (N_2) nm and 397.5 nm (H_2O) nm was assumed to be identical $\eta_1 = \eta_2$; the remaining coefficients entering into expression (2) were determined experimentally.

In the processing of the experimental lidar and radiosonde data we also used the known formulas from [8]

$$\rho_{H_2O}\ (z/м^3) = \frac{M}{A}\ 10^6\ \rho_{H_2O}\ (см^{-3}) =$$

$$= 2{,}99 \cdot 10^{-17}\ \rho_{H_2O}\ (см^{-3}),$$

$$\rho_{H_2O}\ (z/м^3) = \frac{216{,}7}{T}\ e, \qquad (3)$$

$$E\ (мб) = 6{,}107 \cdot 10^{\frac{7{,}6326\ t}{241{,}9 + t}},$$

$$\rho\ (см^{-3}) = 7{,}35 \cdot 10^{18}\ \frac{p}{T},$$

where M is molecular weight, A is the Avogadro number, T is temperature in °K, t is temperature in °C, E is the elasticity of saturating vapor, e is the partial pressure of water vapor in mb, p is pressure in mb.

Instrumentation

In the measurements we used a lidar with the following principal parameters:

Laser emission power at a wavelength 347.2 nm	0.06 J
Diameter of receiving antenna	0.5 m
Angle of field of view of receiving system	28 min
Transmission coefficient of optical system	0.7
Transmission coefficients of filters:	
interference at 397.5 nm	0.23
interference at 377.7 nm	0.1
selecting at 397.5 nm	0.56
selecting at 377.7 nm	0.26
Coefficient of suppression of signal at 347.2 nm by 377.7 and 397.5 nm not less than 10^8.	

Using a system for the electronic processing of laser information it is possible to:
-- measure the SCS of laser radiation by atmospheric components at different altitudes;
-- measure the total energy of laser radiation during a stipulated operating time;
-- count the number of laser pulses.

The structural diagram of the electronic processing system is shown in Fig. 1. Measurement of laser radiation energy is accomplished using the FEK-22 (3), an energy recorder (9) and an "accumulating counting rule" (15). The FEK-09 (2) performs the function of a source of starting current pulses controlling operation of the entire system.

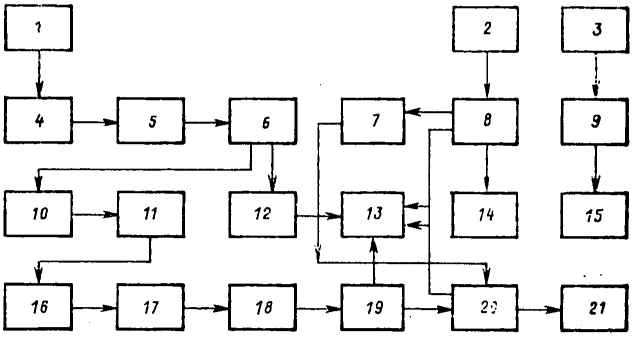

Fig. 1. Structural diagram of system for the electronic processing of laser information. 1) FEU-71; 2) FEK-09; 3) FEK-2; 4) low-noise emitter follower; 5) preamplifier; 6) divider; 7) multiphase generator of strobe pulses; 8) stand-by generator of nanosecond pulses; 9) recorder of energy of sounding pulse; 10) limiter; 11) differentiating circuit; 12) emitter follower; 13) dual trace, four-input storage oscillograph; 14) counter of number of sounding pulses; 15) "accumulating counting rule"; 16) wide-band measuring amplifier; 17) threshold device; 18) stand-by generator of nanosecond pulses; 19) divider; 20) pulse time analyzer; 21) recorder.

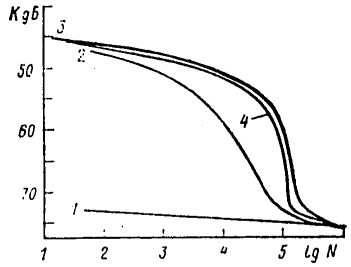

Fig. 2. Integral counting curve for FEU-71. 1) input noise of electronic channel; 2) FEU dark noise; 3) signal + noise with threshold levels of illumination of photocathode.

The frequency characteristic of the FEU-71 output in a dynamic regime falls in the range 0-250 MHz. The low-noise emitter follower (4) is intended for matching the FEU output with the input resistance of the preamplifier, having a transmission band 400 MHz and an input noise temperature 450°K. The signals are fed through the divider (6) and the emitter follower (12) to a

storage oscillograph (13), functioning in a stand-by regime. The signals are also fed from a divider (6) to a limiter (10), then to a differentiating circuit (11), where the pulsed signals are shaped in duration and amplitude and in such a form are fed to the input of a wide-band measuring amplifier (16), where they are amplified to the amplitude necessary for the threshold device (17), which is intended for the cutoff of diode noise of the photomultiplier and the radionoise penetrating to the input of the electronic channel.

The stand-by generator of nanosecond pulses (18) is triggered by pulses passing through the threshold device (17) and sends to the output standard pulses with a duration of 5 nsec, which with respect to time of receipt correspond to the photoelectronic pulses of the FEU-71. These pulsed signals are fed through the divider (19) to the oscillograph (13), where they can be compared in time with the pulses from the emitter follower (12) and also to the input of the pulse time analyzer (20). The pulse time analyzer (20) is controlled by a multiphase generator of strobe pulses (7) and distributes the pulsed signals arriving at its input by channels.

The width of each channel corresponds to the thickness of the analyzed layer of the atmosphere and is 150 m. The total number of channels in the analyzer is 16. The state of the analyzer channels is monitored by the oscillograph (13) and the information accumulated in the channels is registered on punch tape using a recorder (21). The information loss in the pulse analyzer (20) is not more than 2%. The main loss of information occurs in the threshold device (17) and is dependent on the transfer coefficient of the amplification channel to the threshold device. The wide-band measuring amplifier (16) has a fixed level of the transfer coefficient which can vary in the limits 70 db with an accuracy to ±0.5 db. The presence of such an amplifier in the system makes it possible to determine the integral counting curve of the photomultiplier and select a working point on the plateau of this characteristic curve.

Figure 2 shows the integral counting characteristic curve used in the FEU-71 system.

The curve 1 determines the dependence of the intensity of noise and radio interference of the input of the amplification channel at the output of the threshold device (17) on the amplification factor of the measuring amplifier (16), with current fed to the photomultiplier, curve 2 -- dark current of the FEU-71, curves 3 and 4 -- intensity of the signals and the dark current with threshold values of photocathode illumination. The threshold value of illumination was attained using neutral filters. As the light source use was made of an AL103V photodiode, placed in the plane of the telescope aperture opening. The strength of the photodiode working current was 2 ma. The plateau of the integral counting characteristic curve for the photomultiplier is found with values of the amplification factor 58-70 db. The error in measurements on the plateau of the integral counting characteristic curve with instability of the total transfer coefficient 10% is 6%. The

actual instability of the transfer coefficient for the amplification channel in the used system is not more than 7%.

Experimental Results

A determination of humidity by lidar was made beginning in 1974 at Dolgoprudnyy. The results of laser sounding were compared with radiosonde data. The registry and processing of data are automated and the results are fed out by an electronic computer in the form of tables of the profile of absolute atmospheric humidity measured by the lidar, radiosonde data and the elasticity of saturating vapor E. With simultaneous registry of the aerosol scattering signal at a wavelength 347.2 nm or 694.3 nm we compute the correlation coefficient R and the error in the correlation coefficient σ_R using the formulas

$$R = \frac{\sum_{i=1}^{n} [\rho^i_{H_2O}(H) - \overline{\rho}_{H_2O}(H)][N^*_{Ai}(H) - \overline{N}^*_A(H)]}{n\sqrt{\sigma^2_{\rho_{H_2O}}\sigma^2_{N^*_A}}}, \quad (4)$$

where $\sigma_R = \frac{1-R^2}{\sqrt{n}}$; $N^*_A(H) = \frac{\sigma_\pi(H)}{\sigma_\pi(H_{max})}$;

$n \simeq 50 \div 60$;

n is the number of records of the profiles of aerosol scattering σ_π and SCS (H_2O), $\sigma^2_{\rho_{H2O}}$ and $\sigma^2_{N^*_A}$ are the dispersions for ρ_{H2O} and N^*_A.

Among the total number of laser sounding sessions we selected and analyzed 96 sessions carried out under conditions of high atmospheric transparency. In this case the errors caused by different atmospheric transparency at the SCS wavelengths were minimum.

In 46 sounding sessions simultaneously at wavelengths 694.3 nm (16 sessions) and 347.2 nm (30 sessions) we registered the backscattering signal and using formula (4) we computed the R and σ_R values. In 38 cases there was a correlation ($R \geq 0.5$), of which for 31 sounding sessions the correlation was close ($R > 0.7$). There is no substantial difference between sounding at 694.3 nm and 347.2 nm, which once again is evidence of absence of parasitic optical interference, which could lead to the observed structure of atmospheric humidity.

For comparison of the results of lidar sounding and radiosonde data, for each of the sessions we computed the mean square differences

$$\tilde{\Delta}_{\rho_{H_2O}} = \sqrt{\frac{1}{n}\sum_{i=1}[\rho_{1i}(H) - \rho_{3i}(H)]^2}$$

in the entire range of altitudes and computed the differential curves of the statistical distribution of differences

$$\Delta\rho^{*}_{H_2O}(H) = \rho_{H_2O,\,\text{л}}(H) - \rho_{H_2O,\,\text{з}}(H),$$

where $\rho_{H2O,\,lid}$ and $\rho_{H2O,\,rad}$ are the absolute humidities according to lidar and radiosonde measurements.

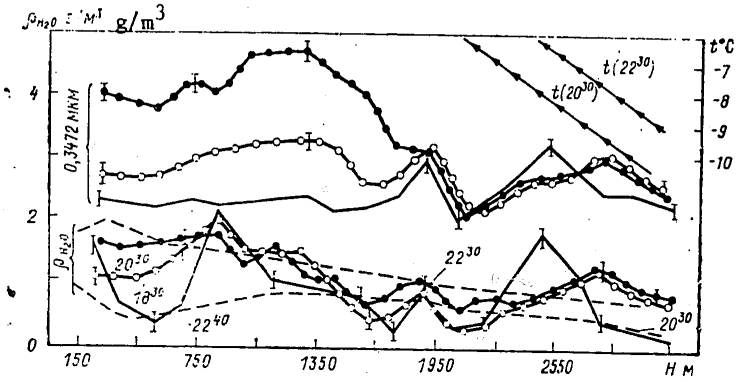

Fig. 3. Results of lidar and radiosonde measurements of humidity and aerosol scattering at wavelength 347.2 nm. 14 December 1977, Dolgoprudnyy.

In 96 sounding sessions: in 13 sessions -- $\Delta\tilde{\rho}_{H2O,\,lid} \leqslant 0.5$ g/m^3, in 46 sessions -- 0.5 g/m$^3 \leqslant \tilde{\rho}_{H2O} \leqslant 1.0$ g/m^3 and in 37 sessions -- $\Delta\tilde{\rho}_{H2O} > 1.0$ g/m^3. Most frequently high $\Delta\tilde{\rho}_{H2O}$ values are characteristic for high values of measured atmospheric humidity. For the purpose of determining the vertical scatter of lidar and radiosonde data we constructed differential curves of the statistical distribution $\Delta\rho_{H2O}(H)$ in the altitude range up to 2 km with an interval 150 m. At low altitudes about 75% of the $\Delta\rho^{*}_{H2O}$ values fall in the limits of errors in lidar measurements. With an increase in altitude the scatter of lidar and radiosonde data increases. However, for all altitudes the lidar and radiosonde data on humidity measurement coincide within the limits of the total errors in the results obtained by different methods.

As an example of joint measurements, Fig. 3 shows three humidity and aerosol backscattering profiles obtained after two hours. Figure 3 illustrates the correlation of profiles and characterizes typical radiosonde and lidar measurement profiles.

Among the 96 analyzed sounding sessions 38 were carried out at a negative temperature at the earth's surface (t_{min} = -16.8°C), 58 -- at a positive temperature (t_{max} = 30.8°C). The atmospheric temperature for all sounding sessions varied in a wide range; in many cases, according to radiosonde data, the temperature changed sign with altitude. High correlation coefficients are characteristic for both positive and negative temperatures.

The laser sounding sessions carried out show that with any atmospheric temperature the humidity profile, determined by the lidar, as a rule has extrema. The humidity profile obtained using radiosonde data in most cases

is monotonic, which is attributable to inertia of the radiosonde sensor, not capable of registering sharp gradients of water vapor concentration. It is characteristic that the profiles of atmospheric humidity measured with a lidar with an interval 1-2 hours do vary but the peculiarities of the vertical distribution of the concentration of water vapor remain as before.

It should be noted that in lidar experiments there is measurement of absolute humidity in the atmosphere. The generally accepted point of view is that there is a correlation between relative humidity and aerosols in the atmosphere [3]. Computations of the relative humidity profile on the basis of data from lidar measurements ρ_{H_2O} and radiosonde measurements of temperature indicated that there is a good correlation between the relative humidity profile and the ρ_{H_2O} profile.

Measurement Errors

In writing expression (2) we assumed that the ratio of the exponential terms in (1) is equal to unity. The computations made by the authors for different meteorological ranges of visibility in the surface layer of the atmosphere in specific aerosol models indicated that under conditions of high atmospheric transparency (meteorological range of visibility not less than 20 km) the error due to the different transparency does not exceed 5%. For lesser altitudes the error varies in the range 2-4%, which agrees with similar estimates by the authors in [1], using somewhat differing aerosol models.

In passing, we note that the computations which we made indicate that there is no justification for using a laser with a radiation wavelength of 266 nm for a rigorous quantitative determination of the contaminants (also including for water vapor determination) by the SCS method. In the spectral region 260-300 nm there is much absorption of radiation by such components as O_3, NO_2, H_2O, SO_2, HNO_3. The concentration of these components can vary in a wide range. Computations indicate that only as a result of different absorption by ozone within the limits of the first kilometer the error due to different transparency can be up to 20%. An increase in total absorption on the path due to other components considerably increases the errors in determining concentrations by the SCS method.

The second sources of errors is governed by the errors in determining the coefficient

$$[\text{CKP} = \text{SCS}] \quad K = K_{12}K_2\eta_2\sigma_\pi^0 \text{ SCS},\ 2/K_{11}K_{21}\eta_1\sigma_\pi^0 \text{ SCS},1$$

The minimum error in determining the σ^0_{SCS} values for strong lines is not more than 10%. The minimum accuracy in determining the

$$K_{12}K_{22}\eta_2/K_{11}K_{21}\eta_1$$

ratio during laboratory calibration does not exceed 20%. The maximum systematic error, determined by the accuracy in K, is 25%. This error is constant with altitude and introduces a shift in the atmospheric humidity profile.

In humidity measurements by the SCS method in a signal caused by SCS on water vapor there will be partial presence of a signal caused by SCS on the liquid phase of H_2O. For the exciting line 347.2 nm the center of the line for the liquid phase is situated at 394.6 nm, the spectral half-width of the line is equal to 64° [7], and the SCS cross section for the liquid phase exceeds by a factor of 7 the cross section for the vapor phase [6]. An analysis of the spectral contour of the filter and the SCS line (394.6 nm) indicated that for the used filters during sounding of the transparent atmosphere the contribution of the signal from the liquid phase did not exceed 1% in the SCS signal from H_2O vapor.

Finally, the random errors in measuring humidity are determined by the errors in measuring signals caused by SCS. Using the criteria for selecting the distribution [2], it was demonstrated that with the used instrument parameters the distribution of the photoreadings conforms to Poisson statistics. Using the standard formulas of the theory of errors, in each sounding session we computed the dispersion of photoelectrons.

Taking into account the comments made above, we determined the total errors $\Delta\rho_{H2O}/\rho_{H2O}$. With minimum values for humidity and the meteorological range of visibility, equal to 20 km, the values $\Delta\rho_{H2O}/\rho_{H2O}$ for 1 km are 12%, for 2 km -- 18%, for 3 km -- 33%. This same error decreases with an increase in atmospheric humidity, and, for example, for a humidity of 3 g/m^3 for 3 km is 24%. Naturally, the cited values characterize the mean errors, which vary in each experiment in dependence on atmospheric conditions and the number of sounding pulses.

At positive temperatures the mean square error in determining relative humidity of the lower troposphere by radiosondes is approximately 4-5% [5]. The estimates which were made indicate that relative humidity can be computed with approximately the same error making lidar measurements of ρ_{H2O} and radiosonde temperature measurements.

BIBLIOGRAPHY

1. Arshinov, Yu. F., Danichkin, S. A., "Influence of Atmospheric Transparency on the Accuracy of Humidity Measurements Using Combination Scattering Spectra," IZVESTIYA AN SSSR, FIZIKA ATMOSFERY I OKEANA (News of the USSR Academy of Sciences. Physics of the Atmosphere and Ocean), Vol 11, No 4, 1975.

2. Astafurov, V. G., Glazov, G. N., "Statistics of Photoreadings and Regimes for the Registry of an Atmospheric Lidar Signal," TEZISY DOKLADOV III VSESOYUZNOGO SIMPOZIUMA PO RASPROSTRANENIYU LAZERNOGO IZLUCHENIYA V ATMOSFERE (Summaries of Reports at the Third All-Union Symposium on the Propagation of Laser Radiation in the Atmosphere), Tomsk, IOA SO AN SSSR, 1975.

3. Georgiyevskiy, Yu. S., Rozenberg, G. V., "Humidity as a Factor in Aerosol Variability," IZVESTIYA AN SSSR, FIZIKA ATMOSFERY I OKEANA, Vol 9, No 2, 1973.

4. Zakharov, V. M., Kostko, O. K., METEOROLOGICHESKAYA LAZERNAYA LOKATSIYA (Meteorological Laser Sounding), Leningrad, Gidrometeoizdat, 1977.

5. NABLYUDENIYA NA GIDROMETEOROLOGICHESKOY SETI SSSR (Observations in the USSR Hydrometeorological Network), edited by O. A. Gorodetskiy, Leningrad, Gidrometeoizdat, 1970.

6. Romanov, N. P., Shuklin, V. S., "Spectrum, Indicatrix and Section of Combination Scattering of Liquid Water," TEZISY DOKLADOV 3-go VSESOYUZNOGO SIMPOZIUMA PO LAZERNOMU ZONDIROVANIYU ATMOSFERY (Summaries of Reports at the Third All-Union Symposium on Laser Sounding of the Atmosphere), Tomsk, IOA SO AN SSSR, 1974.

7. Sushchinskiy, A. M., SPEKTRY KOMBINATSIONNOGO RASSEYANIYA MOLEKUL I KRISTALLOV (Spectra of Combination Scattering of Molecules and Crystals), Moscow, Nauka, 1969.

8. Khrgian, A. Kh., FIZIKA ATMOSFERY (Atmospheric Physics), Leningrad, Gidrometeoizdat, 1969.

UDC 556.08

METHOD AND APPARATUS FOR MEASURING WATER VELOCITY OR DISCHARGE IN OPEN SHALLOW-DEPTH FLOWS

Moscow METEOROLOGIYA I GIDROLOGIYA in Russian No 8, Aug 79 pp 114-116

[Article by M. I. Biritskiy, Central Scientific Research Institute of Complex Use of Water Resources, submitted for publication 4 December 1978]

Abstract: The article describes apparatus introducing changes into measurements by microcurrent meters by the "five-point" method when determining velocity or discharge in open flows with a depth up to 3 m and reducing the amount of time spent on measurements. It consists of five measurement converters, rods and a pulse-counting unit. The measurement converters are rigidly attached on the racks of a rod which mesh with a multioutput reducer. The pulse-counting unit consists of five amplifiers, frequency dividers (division by 2), MES-54 counters, and also a timer, a synchronizer for switching the counters and timer on and off.

[Text] Hydrometric current meters and microcurrent meters have come into wide use for measuring averaged velocities in open flows. The mean velocity on the vertical in the cross section of a water flow is determined at one, two, three or five points. The error in the method when making measurements with a hydrometric current meter for determining averaged velocity on the vertical at one point is not lower than ±5%, at two and three points -- ±(2-4%), and in the case of five points -- ±2% [5]. The last of the employed methods is the most precise, but requires the most time. At the Central Scientific Research Institute of Complex Use of Water Resources USSR Water Management Ministry specialists have developed apparatus [1, 2] introducing changes into measurements by the five-point method and reducing time expenditures on measurements.

It consists of measurement converters, rods and a pulse-counting unit.

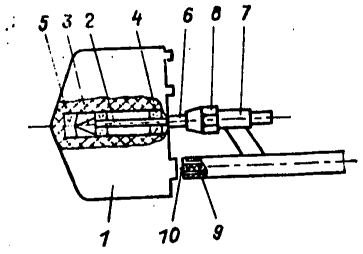

Fig. 1. Measurement converter.

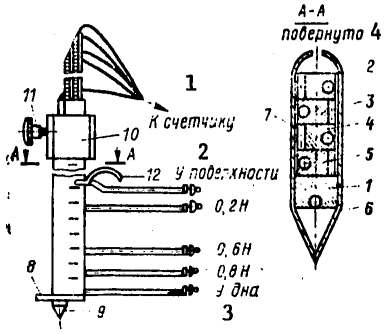

Fig. 2. Rod.

KEY:

1. To counter
2. At surface
3. At bottom
4. A-A/turned

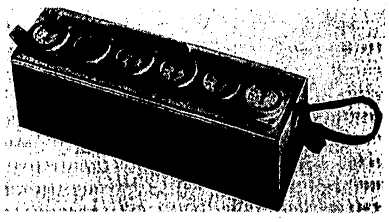

Fig. 3. Pulse-counting unit.

Design of measurement converter and principle of its operation. The primary measurement converter is a two-blade screw 1, fabricated from plastic, with a console suspension, consisting of the axis 2 and the limiter 3, radial bearings (ruby watch jewels) 4, and an agate thrust bearing 5. The axis 2 is attached in a pipe 6, which is inserted into the holder 7 and held tight by the nut 8 (Fig. 1). The holder 7 is attached to an electrode 9, within which there is an insulated electrode 10. Coaxially placed electrodes 9, 10

and a blade with a projection form an intermediate measuring converter. The electrodes have a cleaned end and are connected to the rear edge of the screw blade with projection for a distance less than 1 mm. The electrode 9 is connected to the positive terminal of the current source and the electrode is connected to the negative terminal. The screw blade is designed with a geometric pitch 46 mm [4, 3]. One rear edge of the blade is designed with a projection situated opposite the electrodes 9, 10; the other is designed with two projections situated symmetrically relative to the electrodes, which is ensured by balancing of the screw.

This design of the measuring converter made it possible to broaden the range of measured velocities and substantially lessen polarization phenomena.

With movement of the liquid the screw blade rotates and a diffusion layer, whose thickness is less than one millimeter, is formed at the ends of the electrodes. When the rear edge of the screw with the projection is opposite the electrodes, the resistivity in the circuit of the electrodes changes and current pulses are shaped. With the passage of the blade with two projections about the electrodes a current pulse is not shaped. The number of revolutions of the screw blade during a definite time is a measure of velocity.

The rod (Fig. 2) consists of a fixed shaft 1, four moving shafts 2-5, left and right "jaws" of the fairings 6-7, gathering the shafts into a packet, on which are plotted centimeter graduations, washers 8, stem 9, multioutput reducer 10, knob 11, level indicating hand 12 [1]. The measuring converters are rigidly attached on the shafts. There are special grooves in the shafts which hold the wires running from the measuring converters to the pulse-counting unit. The placement of the wires in the grooves precludes their damage during movement of the shafts. The fairing "jaws" 6-7 are longer than the fixed shaft 1, to which, at the bottom, is attached the washer 8 and the stem 9. The lower measuring converter is attached between the fairing jaws; this makes it possible to set its axis at a distance from 2 to 20 cm from the bottom of the channel (depending on the type of bottom material). The upper measuring converter is mounted in such a way that its axis is at a distance of 2 cm from the surface of the flow. All the shafts in their upper part have plugs for joining the cable from the pulse-counting unit. The rod is fabricated from alloys of aluminum and stainless steel.

Pulse-counting unit (Fig. 3). This unit is intended for amplification of the pulses arriving from the measuring converters and their registry. It consists of five amplifiers, mounted in a common housing, five frequency dividers (division by 2), five MES-54 counters, timer, synchronizer for switching the counters and timer on and off, current source -- 373 elements and a lever for the total feedout of counter readings.

The measurement is made in the following sequence.

The rod is connected by a cable to the pulse-counting unit and the "Current" switch is turned on. At the vertical to be measured the rod is inserted into the flow; then, turning the knob, the level indicator hand is moved until its needle comes into contact with the surface of the flow. At the same time the measuring converters are set, respectively, at the depths: "at the surface"; "0.2H"; "0.6H"; "0.8H" and one is set "at the bottom." Then pressure is applied to the synchronizer lever, starting up the counters and the timer, then after a selected time interval pressure is again applied to the synchronizer lever, switching the counters and timer off. The readings of the counters and timer are registered. With a third pressing on the synchronizer lever the readings of the timer are returned to zero, and with pressing on the general release lever there is simultaneous return of the readings of the five counters to zero. Then one moves on to the next measuring vertical.

Technical Specifications

Range of measured velocities, m/sec	0.03-3.0
Diameter of screw blades, mm	30
Geometric pitch of screw, mm	46
Number of measuring converters	5
Measured depths, mm	3000
Number of pulses during 2 revolutions of screw	1
Current source, V	15-18
Required current, mA	4-6
Measurements of pulse-counting unit, mm	400 x 200 x 120
Mass of pulse-counting unit, kg	6
Mass of rod with measuring converters, kg	7

The effectiveness of the method and apparatus is confirmed by the marked reduction of time expenditures on measurements. For example, when working from a small boat with a width of 27 m with eight measuring verticals the time expenditures are 25 minutes, including the time necessary for attachment of the cable. Two or three measurements are made at each measuring vertical.

The instrument can be used in scientific investigations, measurements of water discharge in a melioration network, and also for calibration of water-gaging hydraulic structures.

BIBLIOGRAPHY

1. Biritskiy, M. I., Author's Certificate 340 897 (USSR), BYULL. OIPOTZ (expansion unknown), No 18, 1972.

2. Biritskiy, M. I., Neronenya, L. S., "New Instruments for Measuring Water Velocity," VOPROSY GIDROLOGICHESKOGO PRIBOROSTROYENIYA (Problems in Hydrological Instrument Making), Leningrad, Gidrometeoizdat, 1977.

3. Burtsev, P. N., "Ways to Improve a Hydrometric Current Meter," TRUDY III VSESOYUZNOGO GIDROLOGICHESKOGO S"YEZDA (Transactions of the Third All-Union Hydrological Congress), Vol VIII, Leningrad, Gidrometeoizdat, 1959.

4. Zheleznyakov, G. V., ISSLEDOVANIYE RABOTY GIDROMETRICHESKIKH PRIBOROV (Investigations of the Operation of Hydrometric Instruments), Moscow, Izd-vo AN SSSR, 1952.

5. Prokhazka, Y., TOCHNOST' IZMERENIYA SKOROSTEY I RASKHODOV VODY GIDROMETRICHESKOY VERTUSHKOY, VUV (Accuracy in Measuring Water Velocities and Discharges With the VUV Hydrometric Current Meter), Vol 1, Bratislava, Pratse a shtudiye, 1958.

UDC 551.(510.4:588)

DISCUSSION OF THE CARBON DIOXIDE PROBLEM

Moscow METEOROLOGIYA I GIDROLOGIYA in Russian No 8, Aug 79 pp 117-120

[Article by Candidate of Physical and Mathematical Sciences K. Ya. Vinnikov, State Hydrological Institute, submitted for publication 11 December 1978]

Abstract: The article examines the results of a bilateral Soviet-American symposium on the carbon dioxide problem held in October 1978 at Dushanbe. The content of the reports is discussed.

[Text] During recent years the scientists of many countries have been very carefully watching the results of investigations of the cycling of carbon in nature. The reason for this interest lies in the experimentally discovered appreciable increase in the content of carbon dioxide in the atmosphere and theoretical conclusions indicating that this growth is related to the development of fuel energy. At the same time, fears have been expressed that some biotic reservoirs of carbon are subject to intensive anthropogenic influence, which leads to an additional disruption of the cycling of carbon and a further acceleration of increase in the atmospheric content of CO_2.

On the other hand, one of the results of the modern physical theory of climate is the conclusion that an increase in the concentration of carbon dioxide in the atmosphere will be accompanied by a process of global warming and a substantial change in local climatic conditions over the greater part of the earth. This process can exert a substantial influence also on man's economic activity.

Precisely for this reason a major event in the scientific life of our country was a meeting held in Dushanbe in October 1978, an interdisciplinary symposium on the carbon dioxide problem, organized within the framework of bilateral Soviet-American cooperation in the field of preservation of the environment.

A group of well-known American scientists, headed by E. Epstein, arrived for participation in the symposium in the Soviet Union. Epstein was recently named director of the institute responsible for direction of the US national program on climatic research.

The Soviet delegation, headed by Corresponding Member USSR Academy of Sciences M. I. Budyko, consisted of representatives of about 20 scientific research institutes of the State Committee on Hydrometeorology, USSR Academy of Sciences and others.

The work of the symposium and its scientific program, including 10 reports of American scientists and 15 reports of Soviet specialists, was prepared by an organizing committee which was headed by the first deputy chairman of the State Committee on Hydrometeorology Professor Yu. S. Sedunov.

Five reports were devoted to the problem of study of the global cycling of carbon.

Much interest was shown in a report by Corresponding Member USSR Academy of Sciences A. B. Ronov, in which, on the basis of a generalization of global geochemical data, a study was made of the problem of determination of the resources of organic and inorganic carbon incorporated in sedimentary rocks. An approximate solution of the problem became possible due to quantitative methods, by means of which it was possible to obtain estimates of the masses of carbon in the sedimentary complex, differentiated for different periods of the Phanerozoic. These estimates were compared with the masses of rocks of volcanic origin, being a measure of the intensity of volcanic processes replenishing the reserves of atmospheric carbon dioxide from deep sources. On the basis of an analysis of these materials A. B. Ronov formulated the geochemical principle of preservation of life on earth.

A report by V. S. Broeker dealt with the paths followed by carbon dioxide entering the atmosphere during the combustion of fossil fuel and the annihilation of forests. It was demonstrated that the atmospheric content of CO_2 during the period 1958-1974 increased from 48 to 56% of the total quantity of entering gas. According to model estimates, during this same time the ocean absorbed 37±4% of the CO_2 entering the atmosphere. On the basis of an investigation of the ratio for the isotopes $^{13}C/^{12}C$ in tree rings, the author concluded that the biomass of the land during the last two decades has not experienced appreciable changes.

A report by R. S. Loomis examined the influence exerted on the present-day balance of organic carbon by biotic components, including the cutting of forests and a decrease in the quantity of humus in the worked soils. The speaker noted the great difficulty in a quantitative evaluation of the mentioned factors and expressed the opinion that these factors play a lesser role in the carbon balance than followed from some estimates made earlier.

E. K. Byutner and N. Z. Ariyel', in their report, discussed the results of computations of the flux of carbon dioxide through the ocean surface. The speakers established that a petroleum film poured on the surface decreases exchange fluxes by a factor of 2-3 and can constitute a danger for the vital functioning of organisms in the upper layers of ocean waters.

The speaker noted the particular importance of the possibility of determining the influence of carbon dioxide on climate on the basis of paleoclimatic data for epochs when the carbon dioxide concentration was considerably greater than today. For example, in particular, in the Neogene (Miocene-Pliocene) the quantity of atmospheric carbon dioxide was approximately twice as great as in our times. In this connection, using data on climatic conditions of the Neogene, it is possible to construct maps characterizing the meteorological regime when there is a high content of carbon dioxide. The report presented maps of air temperature, precipitation and other climatic elements obtained in this way for conditions of a doubled CO_2 concentration.

A report by W. L. Gates examined models in the theory of climate used in the United States for evaluating climatic conditions corresponding to an increased CO_2 content in the atmosphere. Gates pointed out that at the present time there are no contradictions between the results obtained using both a model of general circulation of the atmosphere and energy balance models (with parameterized dynamics). The speaker noted that in the near future new computations will be completed in the United States which will be carried out using models of general circulation.

In a discussion of the Gates report S. B. Fels, a specialist in the Princeton Laboratory of Geophysical Hydrodynamics, reported that S. Manabe is completing an analysis of computations of the influence of an increase in the CO_2 concentration on climate. The model of the theory of climate used by Manabe contains an allowance for the annual variation of meteorological elements and predicted cloud cover; the computation region reaches to the poles (in contrast to the preceding model, where it was limited to 80° latitude). Fels noted that the estimates of climate sensitivity obtained earlier by Manabe in his new investigation are being refined insignificantly and the inclusion of a feedback mechanism with cloud cover exerts little influence on the results.

The report by Fels discussed the algorithm which he formulated for computing radiation changes in temperature caused by the CO_2 absorption band 15 μm and some results of use of this algorithm in numerical experiments with a general circulation model.

Using a 40-level model of general circulation of the atmosphere to an altitude of 80 km, Fels computed the changes in mean annual distributions of temperature and components of circulation in the stratosphere and mesosphere with a doubling of the present-day atmospheric CO_2 content. These changes differ little from those obtained earlier by Manabe and Wetherald with the use of a one-dimensional model of radiation-convectional adaptation and a three-dimensional model of general circulation of the atmosphere to the level 36 km. It was shown, in particular, that there is a great horizontal uniformity of changes in the stratosphere and the dynamic contribution to change in temperature is small in comparison with the contribution from radiation.

The report of Yu. M. Svirazhev and A. M. Tarko was devoted to an analysis of the role of the "atmosphere-plant-soil and ocean" system in the absorption of anthropogenic discharge of CO_2 into the atmosphere.

Using the systems analysis method for study of this problem, the speakers concluded that there will inevitably be an increase in the CO_2 concentration in the near future, which will lead to a substantial change in the global climate.

The problem of monitoring the CO_2 concentration was dealt with in four reports, including the report of L. Machta, in which the authors cite considerations on the importance of the CO_2 problem, give plans for expanding the global network of stations on the basis of CO_2 measurements in the atmosphere, and present estimates of the contribution of different countries to discharge of CO_2 into the atmosphere.

A report by V. B. Alekseyev and V. A. Dergachev dealt with the organization in the USSR of a network for registering the ^{14}C concentration in atmospheric carbon dioxide at different latitudes and altitudes and discussed the first results of these measurements. The problem of radiocarbon exchange was also considered.

A report by A. M. Brounshteyn dealt with the principles for determining the total CO_2 content in a vertical column of the atmosphere and presented data from measurements carried out in 1974-1976 near Leningrad.

Some methodological problems in applying this method were discussed in a report by V. N. Aref'yev.

The most important task of the symposium was a discussion of the influence of change in the concentration of CO_2 in the atmosphere on climate.

Eight reports were devoted to this question.

A report by Corresponding Member USSR Academy of Sciences M. I. Budyko, entitled "Carbon Dioxide and Climate," stated that in the absence of a precise theory of climate the only way to obtain reliable estimates of the influence of carbon dioxide on climatic conditions is the use for this purpose of several independent computation methods, the results of which can be considered reliable if they agree satisfactorily. The report also cited data on the sensitivity of the thermal regime of the atmosphere to changes in the influx of solar energy and the carbon dioxide concentration. These data were obtained both from different models in the theory of climate and as a result of an analysis of empirical data on the annual variation of meteorological elements, on the present-day change in climate and on climatic changes in the geological past. The agreement of sensitivity estimates obtained by independent methods indicated their adequate accuracy.

APPROVED FOR RELEASE: 2007/02/08: CIA-RDP82-00850R000100100036-0

A report by G. L. Potter gave the preliminary results of computations of changes in the radiation and dynamic characteristics of the troposphere and stratosphere with an increase in the content of carbon dioxide by 50, 100 and 300% using a two-dimensional zonally averaged model of atmospheric circulation with mean annual characteristics. It is shown that appreciable changes in temperature distribution are proportional to the CO_2 increment and the changes in the radiation characteristics (albedo), precipitation and energy balance components are small, which contradicts existing estimates and is probably attributable to the shortcomings of the model used.

The report by R. D. Sess contained an estimate of response of the thermal regime of the atmosphere to changes in the heat influx and concentration of carbon dioxide obtained on the basis of processing of data from satellite observations of radiation fluxes. The results agree well with the conclusions drawn from similar computations carried out by other independent methods both in the United States and in our country.

It is worth noting the confirmation of the conclusion that the feedback with cloud cover has an insignificant influence on estimates of response of the global thermal regime to changes in the heat influx.

A report by I. L. Karol' presented a scheme for investigating photochemical interactions and the vertical transport of ozone and small gas admixtures associated with them as a result of an increase in the content of atmospheric carbon dioxide. The use of systems analysis made it possible to investigate the influence of different factors on change in ozone content in the stratosphere and demonstrated that the change is insignificant considering the available estimates of the dependence of the intensity of transport through the tropopause on the vertical temperature gradient. An increase in the transfer of gases destroying ozone in the stratosphere is compensated by an increase in the rate of their photochemical destruction during cooling of the stratosphere.

The report of H. Van Loon was devoted to an empirical study of the mechanisms and structure of modern climatic changes. Van Loon noted the complex correlation between the mean meridional air temperature gradients and meridional transfer of heat by stationary and moving eddies.

We can assign to this same group a report by Corresponding Member USSR Academy of Sciences K. Ya. Kondrat'yev. He presented the results of computations of transmission functions and other radiation characteristics in the IR region, taking into account absorption by carbon dioxide, methane, nitrous oxide, water vapor and other gas admixtures at different levels in the atmosphere. The report also discussed the "greenhouse effect" and the speaker examined its peculiarities for different levels of atmospheric carbon dioxide content.

Six reports of Soviet authors were devoted to the problem of the influence of changes in the concentration of carbon dioxide and climate on the productivity of vegetation.

A report by G. V. Menzhulin and S. P. Savvateyev presented the results of computations of changes in the productivity of agricultural crops in connection with the changes in climate and the CO_2 concentration which are transpiring, carried out using a parameterized model of the production process. The authors gave a prediction of the productivity for the grain-producing regions of the USSR and the United States.

Corresponding Member Academy of Sciences Tadzhik SSR Yu. S. Nasyrov devoted his communication to the problems involved in the photosynthetic fixation of carbon dioxide. He cited current data on the biochemical mechanisms of CO_2 absorption by plants of different types. The report discussed the possibilities of developing new, highly productive varieties of such agricultural crops as wheat, cotton and others.

A report by K. I. Kobak presented the results of long-term experimental investigations of the carbon dioxide regime of natural plant covers and considered the peculiarities of the CO_2 regime both in natural associations of different types and in agroecosystems.

The report of N. A. Yefimova, devoted to the influence of photosynthesis on the cycling of carbon dioxide, contained data on productivity of the plant cover relating to the current epoch and the Pliocene. It was demonstrated that the biological component of the global cycling of CO_2 in the Pliocene exceeded by 50% its present-day value.

A report by O. D. Sirotenko and A. P. Boyko discussed the properties of a simulation model of the "soil-plant-atmosphere" system intended for evaluation of the influence of changes in CO_2 concentration on the productivity of agrocoenoses. The speakers presented the results of computations of changes in productivity with a doubling of the concentration of carbon dioxide in atmospheric air.

The structure of dynamic models of the cycling of carbon in the "soil-plant-surface layer of the atmosphere" system was discussed in a report presented by R. A. Poduektov. He examined the problems involved in the designing of such models and gave computed data on individual elements of an integral model which can be developed.

Reports by E. W. Byerly and E. Epstein, devoted to more general problems, were presented at the end of the symposium.

The first of these communications enumerated the different forms of influence of the increase in carbon dioxide concentration and the related climatic changes on different branches of economic activity. The speaker noted the lack of any reliable estimates of the economic importance of the mentioned influence. Pointing out that in order to prevent an increase in the concentration of carbon dioxide in the atmosphere in the future it will possibly be necessary to limit the consumption of coal and petroleum, the speaker mentioned the need for long-term preparations for introducing such a restriction.

The Epstein report was devoted to an exposition of the principles and organizational bases of development of work on investigation of climatic changes in the United States.

After analyzing the results of the symposium's work, the following conclusions can be drawn.

The Soviet-American symposium was the first scientific conference in our country devoted to the influence of an increase in the concentration of atmospheric carbon dioxide on climate and other components of the environment. The participation of outstanding Soviet and American scientists of different fields of specialization in this symposium made possible a broad interdisciplinary examination of the carbon dioxide problem, including an analysis of meteorological, bioclimatic and geochemical aspects of the problem.

The principal result of work of the symposium, reflected in the final document, was the recognition of the real possibility of a change in global climate as a result of an increase in the concentration of carbon dioxide in the atmosphere. This conclusion makes it very timely to study the carbon dioxide problem and makes necessary the maximum acceleration of investigations of this problem.

In the declarative part of the final document from the symposium it is written: "The participants in the symposium note that on the basis of empirical and theoretical investigations it is possible to expect an appreciable increase in the future concentration of atmospheric carbon dioxide. Numerous data were presented showing that this will lead to a change in global climate and concern was expressed that this will exert an influence on different components of the environment and man's activity, including agriculture."

The materials presented at the symposium gave definite information on the climate of the future under conditions of an increase in atmospheric carbon dioxide. In the immediate future these materials will evidently be substantially supplemented by the results of computations using models of general circulation of the atmosphere, which now are being finalized in the United States. After completion of these computations and comparison of their results with available materials from similar Soviet investigations, carried out with the use of paleoclimatic data and semiempirical models of the theory of climate, the problem of climatic conditions of the future can be clarified to a considerable degree.

The symposium demonstrated the existence of the lead of Soviet scientists in study of evolution of the chemical composition of the atmosphere in the geological past, in the use of paleogeographic data for study of the climate of the future, in the development of semiempirical models of the theory of climate, and in study of the influence of carbon dioxide on productivity of the plant cover.

At the same time, it is clear that there is a lead of American research in study of the present-day cycling of carbon and development of models of general circulation of the atmosphere.

The symposium was held at a high scientific level and made it possible to obtain very valuable scientific information. It will undoubtedly exert a considerable influence on the development of research on the carbon dioxide problem.

The successful holding of this symposium, the same as the preceding Soviet-American symposia on problems relating to anthropogenic climatic change, is indicative of the high effectiveness of technical cooperation between the USSR and the United States in this field, as was noted by many Soviet and American participants in the symposium.

REVIEW OF MONOGRAPH BY A. V. KARAUSHEV: TEORIYA I METODY RASCHETA RECHNYKH NANOSOV (THEORY AND METHODS FOR COMPUTING RIVER SEDIMENTS) AND BOOK EDITED BY A. V. KARAUSHEV: STOK NANOSOV, YEGO IZUCHENIYE I GEOGRAFICHESKOYE RASPREDELENIYE (RUNOFF OF SEDIMENTS, ITS STUDY AND GEOGRAPHIC DISTRIBUTION), LENINGRAD, GIDROMETEOIZDAT, 1977

Moscow METEOROLOGIYA I GIDROLOGIYA in Russian No 8, Aug 79 pp 121-122

[Article by Candidate of Physical and Mathematical Sciences N. A. Mikhaylova]

[Text] For specialists engaged in the study of the movement of sediments and channel processes it is of great interest to examine the monographs indicated in the title, published by the Gidrometeoizdat in 1977. They constitute an integrated whole. In these monographs the science of sediments is interpreted as a complex problem, including the theory of the movement of sediments, the methods for their in situ investigation and the processes of formation of the geographic distribution of the runoff of sediments.

The first book examines different models of the movement of sediments and methods for computing the transporting capacity and discharge of sediments. In addition to the exposition of the theoretical models, formulated by the author himself, the book gives quite complete and objective information on the models and computation methods developed by other schools.

The exposition begins with a description of the practical significance of the problem (Chapter 1). The author gives a definition of the channel process, involving "channel formation, its vertical and horizontal movements, changes in its configuration and dimensions." It is emphasized that "at the basis of these processes lies the interaction between the flow and the channel." The book clearly demonstrates the role of the Russian and Soviet scientists in investigation of sediments and channel processes.

In the theoretical examination of the movement of suspended sediments (Chapter 2) the author gives preference to the diffusion theory, on which the computation schemes which are practical to use are now based. Other theories are not passed over, and in particular, the M. A. Velikanov gravitational theory and those of G. I. Barenblatt and F. I. Frankel'. There is a thorough analysis of the conditions for initial and further movement of

bottom sediments. The reader will obtain a full idea concerning the dependences for determining the initial velocity of movement of particles and discharge of entrained sediments. There is a brief exposition of the principle of the stochastic approach to description of the motion of solid particles in the turbulent flow. For practical workers it is of unquestionable interest to examine the cited analysis of the formulas derived by different authors for characterizing ridges. Worthy of note is the semiempirical solution of the problem of the length of ridges.

The monograph successfully generalizes (Chapter 3) different formulas for transporting capacity. The author's method for computing the transport of sediments is described. It is emphasized that one of the most important forms of interaction between the flow and channel is their interexchange of sediments. Chapter 4 is devoted to the total transport of sediments. This chapter examines practical problems related to the planning of hydraulic structures and operation of bottom-deepening channels; also described are methods for computing the elements of bottom ridges, playing a substantial role in the channel process.

In examining the balance of sediments (Chapter 5), the author relates channel deformations to the distribution of turbidity along the length of the flow. Also of practical importance is the analysis of channel deformations in the lower reaches with a change in the erosion base. The author correctly emphasizes (Chapter 6) that the transport and settling of sediments in reservoirs is determined by the structure of the currents, wind-wave phenomena and the turbulence characteristics. Turbidity arising from wind and waves and along-shore transport of sediments are covered in Chapter 7, which examines the process of formation of the shores of reservoirs. There is a diagram of the formation of wave and tide currents and the author gives approximate computations of the silting and clogging of ship canals and reservoirs.

The book RUNOFF OF SEDIMENTS, ITS STUDY AND GEOGRAPHIC DISTRIBUTION, written by a group of specialists at the sediments laboratory State Hydrological Institute, N. N. Bobrovitskaya, I. V. Bogolyubova, K. M. Zubkova, A. V. Karaushev, K. N. Lisitsyna, G. A. Petukhova, K. V. Razumikhina, L. G. Tkacheva, A. Ya. Shvartsman, systematizes the results of the many years of work at this laboratory. To the traditional examination of the movement of sediments in rivers and reservoirs the authors add a very important section on a matter rarely discussed in the literature, devoted to the movement of sediments on slopes. Thus, the present-day river system is considered as a whole from the slopes of the basin to the river mouth. Together with an exposition of the results obtained in the sediments laboratory, where there is need of it the section gives detailed and objective references to the results of investigations of other authors and groups of authors. The direction of the science of movement of sediments headed by A. V. Karaushev is characterized by a comprehensive approach, involving the use and clever combining of both physico-mathematical and geographic research methods.

Water erosion on slopes, runoff of sediment in streams and rivers and the formation of their channels and floodplains are examined (Chapter 1) as a uniform erosional-accumulative complex. The status of in situ observations of sediments is discussed in Chapter 2, which describes the organization of network observations in the USSR and as a comparison gives an evaluation of the state of in situ study of sediments abroad. There is a thorough exposition of methods for measuring turbidity and the discharge of suspended sediments (Chapter 3). Bearing in mind the practical needs for cases of a total absence or inadequacy of data on solid discharge, the authors (Chapter 4) give a description of such adequately reliable methods for the indirect determination of solid discharge as its computation on the basis of the deposition of sediments in reservoirs and computations using the elements of bottom ridges. A matter of practical interest is the description (Chapter 5) of different bottom sediment samplers and laboratory methods for determining the granulometric composition and density of sediments. Specific cases of the movement of sediments in reservoirs, lower reaches and ponds are described in Chapter 6. The authors note the need for a stationary study of the movement of sediments in the lower pools at hydroelectric power stations and describe the method developed for this purpose at the State Hydrological Institute.

Chapter 7 gives methods for a quantitative estimate of water erosion and give recommendations for the study of the runoff of sediments in runoff areas and at hydrometric structures. It gives a description of methods for studying surface erosion on slopes and on irrigated lands. The parameters of the runoff of sediments and methods for their computation are described in Chapter 8. Here the authors give the dependence between the mean annual discharges of sediments and water. Also examined are curves of the probability of the annual runoff of sediments and the intraannual and intradiurnal variability of the runoff of sediments is analyzed. In examining the geographical distribution of the parameters of runoff of sediments over the territory of the USSR (Chapter 9), the authors focus their attention on methods for computing the runoff of sediments in the absence of observational data. The cited maps of mean turbidity and the runoff modulus for suspended sediments in USSR rivers are of great practical interest. In the monograph much attention is devoted to the erosional regionalization of a territory.

In the exposition (Chapter 10) of the problem of the transport of sediments by the earth's rivers into the seas and oceans the authors devote attention to methods for estimating the runoff of sediments from extensive territories and give the physiographic characteristics of the continental slopes. The monograph also examines the territorial distribution of the characteristics of the granulometric composition of sediments. Also given is a regionalization of the European USSR with respect to the composition of bottom sediments.

The analysis of the hydrological factors of water erosion given in the monograph (Chapter 12) is of considerable interest not only for hydrologists, but also for soil scientists, who can make use of the classification of the stream network and the method for computing slope erosion. The monograph

gives graphs characterizing sheet erosion of different soils from slopes in dependence on water runoff. Also considered is the redeposition of sediments and sheet erosion on irrigated lands. Chapter 13 devotes attention to the peculiarities of water erosion in mountainous countries. There is an analysis of the formation and territorial distribution of mudflows; measures for contending with them are recommended.

Both the reviewed monographs are characterized by the fact that on each of the considered problems there is the greatest possible, for the present time, level of theoretical solution of the problem. However, if there is no theory at all with respect to some problem, or if the theory has not been finalized, on the basis of an analysis of the mechanism of the phenomenon and a consideration of the existing empirical formulas recommendations are given on the soundest of them. If this is not done, the authors give a possible method for an approximate evaluation of the necessary characteristics. The considered monographs are characterized by coverage of a broad complex of problems related to the movement of sediments, beginning with their formation on slopes under the influence of water erosion and ranging through their entry into the seas and oceans. At the same time, no consideration is given to cases which would not be encountered in actual practice and which frequently are not covered in the hydrological literature.

The reviewed monographs, which incorporate and generalize numerous publications of the authors in periodic publications, should become standard references both for specialists working at scientific research institutes and for engineers engaged in the designing and operation of different hydraulic structures or who are engaged in hydrological computations.

REVIEW OF MONOGRAPH BY GEORGI MARKOV: PROGNOZIRANE NA NUZHDITE OT VODA ZA NAPOYAVANE V MELIORATIVNITE RAYONI (PREDICTION OF THE NEEDS FOR WATER FOR IRRIGATION IN MELIORATED REGIONS), SOFIA, INSTITUTE OF WATER PROBLEMS, PUBLISHING HOUSE OF THE BULGARIAN ACADEMY OF SCIENCES, 1978, 128 PAGES

Moscow METEOROLOGIYA I GIDROLOGIYA in Russian No 8, Aug 79 p 123

[Review by Professor A. M. Alpat'yev]

[Text] The reviewed monograph is the result of more than 20 years of investigations by the well-known Bulgarian scientist Professor G. Markov in the field of water problems in agriculture. It consists of four sections and a summary, a concise bibliography, and abstracts in the Russian and English languages.

The first short section gives a brief exposition of the status of the problem of predicting the meteorological elements determining the total evaporation of plants.

The second, lengthier section is devoted to a description of the method for predicting meteorological elements and application of the results for irrigation purposes. In the subsections of this part of the investigation the author examines long- and short-range forecasting of meteorological elements and gives systematic instructions on their use in irrigated lands for computations of the current and long-term needs for water by cultivated phytocoenoses.

A matter of special interest in this section is the prognostic equations (regression equations) for the sums of temperatures above 10°C and the sums of the dew point spreads during the growing season, computed for 25 ameliorated regions in northern and southern Bulgaria and later employed by the author for computing the need of irrigated crops for water on the basis of the evaporability index. The deviations of the predicted values from the actually observed values in most cases did not exceed ±10%.

In the third section, constituting about 50% of the entire volume of the monograph, the author gives the results of experimental checking of the method for predicting the water needs of phytocoenoses in five state irrigation

systems in the Ruse, Petrich, Pleven, Stara Zagora and Khaskovo regions; annual meteorological indices are cited for 40 years for the precipitation sums, air temperature and dew-point spread for 10-day periods and the months April-September; on the basis of these indices for grains, lucerne, sunflowers, corn, sugar beets, vegetable crops and grapes it was possible to make forecasting computations of their need for water for each month for the April-September period, taking into account the area occupied by the crops; the deviations of the computed data from the actually observed values were computed. The difference in the retrospective review between the forecasts and the actual values of the meteorological parameters, on the basis of which the need for water was computed, did not exceed ±10% in 100% of the cases with respect to the temperature sums and in 65% of the cases with respect to dew-point spread sums.

The basis for the investigation was the bioclimatic (biophysical) method for computing the water need of phytocoenoses and the method for predicting temperature and evaporability sums, used for these same purposes, developed by Soviet scientists.

G. Markov has creatively used these methods under the conditions prevailing in Bulgaria and has successfully formulated and solved the problem of long-range prediction of the need for water resources for irrigated lands, making extensive use of electronic computers in this work.

The author has also examined the possibilities of using a similar forecast in the long-range planning of water resources for irrigation purposes.

This reviewed monograph by G. Markov, with its detailed methodological instructions on the sequence of individual types of work in the process of predicting water needs for irrigated lands is, in our opinion, of unquestionable interest for scientific and water management agencies and can be used in the current and long-range planning of water resources in agriculture.

SIXTIETH BIRTHDAY OF VERA ALEKSANDROVNA MOISEYCHIK

Moscow METEOROLOGIYA I GIDROLOGIYA in Russian No 8, Aug 79 p 124

[Article by specialists of the USSR Hydrometeorological Scientific Research Center]

[Text] Doctor of Geographical Sciences Vera Aleksandrovna Moiseychik, a senior scientific specialist at the USSR Hydrometeorological Center, marked her 60th birthday on 4 August 1979.

Vera Aleksandrovna for more than 35 years has been carrying out active and productive work in the agrometeorological servicing of agriculture and much scientific work on the development of methods for agrometeorological prediction of wintering conditions for winter crops. She is one of the leading scientists of our country in the field of agricultural meteorology.

Working from 1941 through 1948 at the Main Administration of the Agrometeorological Service of the USSR Agriculure Ministry, and during 1948-1956 as senior scientific specialist of the Central Institute of Forecasts, V. A. Moiseychik acquired great experience in practical work and from 1956 through 1962 headed the section of the agrometeorological forecasts service

of the Main Administration of the Hydrometeorological Service USSR, where she carried out much work for organizing and improving the agrometeorological servicing of agriculture in our country. Beginning in 1962, and through the present time, she has been productively working as a senior scientific specialist at the USSR Hydrometeorological Center.

In 1955 Vera Aleksandrovna successfully defended her Candidate's dissertation, and in 1973 her Doctor's dissertation on the problems involved in evaluating and predicting the conditions for the wintering of winter crops.

Over the course of many years Vera Aleksandrovna Moiseychik has been studying the laws of formation of the hydrometeorological regime in fields of winter crops during the autumn-winter-spring period. She has studied the agrometeorological conditions under which winter crops freeze, are ruined by wetting and are withered. For the first time she formulated a physical-statistical model for evaluating and predicting the conditions for the wintering of winter crops and has developed a method for long-range forecasting of the state of winter crops in spring, which makes it possible to predict, for two or three months in advance, the area of healthy and dying winter crops after wintering over the territory of oblasts, krays, republics and for the USSR as a whole.

The predictions of the wintering of winter crops prepared by the Administrations of the Hydrometeorological Service and the USSR Hydrometeorological Center by the V. A. Moiseychik method with her direct participation have a high probable success and are used by directing and planning agencies in preparations for the resowing of spring crops in spring to replace winter grain crops which have perished.

The results of the investigations of Vera Aleksandrovna have been published in two major monographs, eight methodological instructions and in aids. She has published a total of about 70 scientific works.

In addition to much scientific-production work, V. A. Moiseychik actively participates in the public life of the USSR Hydrometeorological Center and the Krasnopresnenskiy Rayon of Moscow. A member of the CPSU since 1948, she has twice been elected a deputy of the Krasnopresnenskiy Rayon Soviet and for many years was a propagandist and a member of the Party bureau. Since 1975 she has been chairman of the primary organization bureau of the "Znaniye" Society at the USSR Hydrometeorological Center.

Vera Aleksandrovna has been awarded three silver medals by the All-Union Exhibition of Achievements in the National Economy of the USSR, has been enrolled in the "Book of Honor" at the USSR Hydrometeorological Center and was awarded the medal "For Illustrious Work During the Great Fatherland War 1941-1945" for her great work in the agrometeorological servicing of agriculture and the practical introduction of scientific methods for making agrometeorological forecasts of the wintering of crops.

We congratulate Vera Aleksandrovna on her birthday and wish her further productive scientific-production activity and excellent health.

SIXTIETH BIRTHDAY OF ARKADIY IVANOVICH KOROVIN

Moscow METEOROLOGIYA I GIDROLOGIYA in Russian No 8, Aug 79 p 125

[Article by a group of comrades]

[Text] Doctor of Biological Sciences Professor Arkadiy Ivanovich Korovin, a well-known scientist in the field of experimental agrometeorology in our country, marked his 60th birthday on 8 March 1979.

A. I. Korovin began his work activity in 1936 as a teacher. In 1945 he graduated from Perm' University, in 1949 he completed his work as a graduate student, in 1950 successfully defended his Candidate's dissertation, and then his Doctor's dissertation. In 1968 he was awarded the title professor.

Heading the Laboratory of Physiology and Ecology in the system of the USSR Academy of Sciences, the section on agricultural meteorology of the Institute of Experimental Meteorology, and since 1973, the agrometeorology division

at the All-Union Institute of Plant Cultivation, Arkadiy Ivanovich is progressively improving means and methods for determining plant reactions to different meteorological conditions. He has carried out interesting investigations in the field of the influence of soil and air temperature on the plant nutrition process, the results of which he generalized in the book ROL' TEMPERATURY V MINERAL'NOM PITANII RASTENIY (Role of Temperature in the Mineral Nutrition of Plants). He established that during severe frosts, grain crops, for example, require more calcium and sulfur and virtually dispense with calcium, phosphorus and nitrogen; during a cooling tomatoes require more phosphorus, legumes require molybdenum, etc. In other words, meteorological conditions, the crop and variety dictate the mineral nutrition of plants.

A. I. Korovin has devoted much attention to study of the influence of autumn and spring conditions on the yield of winter crops. The purpose of his studies in this field of agrometeorological sciences is seeking methods for the relatively rapid evaluation of resistance to the cold, tolerance to both frosts and drought, and other criteria of resistance of crop plants. He proposed that these problems be solved by the methods of modeling of the necessary meteorological factors by means of technical apparatus against a background of natural seasons of the year in light-transparent chambers.

Placing such a difficult problem before himself, Arkadiy Ivanovich has expended much effort on creating an agrometeorological complex in which a number of methods for evaluating the reaction of varieties to different meteorological factors are being developed. In this work direction he, in collaboration with his students, has published the book OSENNE-VESENNIYE USLOVIYA POGODY I UROZHAY OZIMYKH (Autumn-Spring Weather Conditions and the Yield of Winter Crops).

The principal task that Arkadiy Ivanovich wishes to solve is an evaluation of varieties and samples of agricultural crops with respect to agrometeorological indices applicable to the problems of selection and agrometeorological regionalization. For this purpose Arkadiy Ivanovich has developed a "Blank for Agrometeorological Certification of a Variety of Agricultural Crops."

A. I. Korovin has published a total of 160 scientific studies.

We congratulate Arkadiy Ivanovich on this splendid anniversary and wish him health and further creative successes in the development of experimental agrometeorology.

CONFERENCES, MEETINGS AND SEMINARS

Moscow METEOROLOGIYA I GIDROLOGIYA in Russian No 8, Aug 79 pp 126-127

[Article by Yu. G. Slatinskiy and K. P. Vasil'yev]

[Text] A conference devoted to the work of the marine shipboard network of the Administration of the Hydrometeorological Service Ukrainian SSR was held during the period 20-21 February 1979 in Sevastopol'. The conference was attended by representatives of the State Committee on Hydrometeorology and Environmental Monitoring, the organization and planning section of the Administration of the Hydrometeorological Service Ukrainian SSR, the marine section of the Crimean Hydrometeorological Observatory, the Sevastopol' Division of the State Oceanographic Institute, the weather bureaus of the Black Sea and the Sea of Azov, shipboard inspectors of the marine inspectorates at Odessa and Opasnoye, specialists of the navigation sections of Yugrybpromrazvedka, Yugrybkholodflot, SEKB of the Fishing Ministry and other organizations.

A study was made of the problems involved in operation of shipboard stations and on measures for increasing the scope and improving the quality of hydrometeorological information received at operational-prognostic agencies of the State Committee on Hydrometeorology.

In the reports and communications of the conferees it was noted that the hydrometeorological observations carried out by navigators on many vessels of the Merchant Marine Ministry, Fishing Ministry, Ukrainian Academy of Sciences and other departments, play an important role in ensuring that the operational-prognostic agencies of the State Committee on Hydrometeorology receive information on the weather and sea conditions in the most different corners of the world ocean. In this connection, during the past three years of the Tenth Five-Year Plan much has been done for improving the activity of the shipboard network and increasing the quality of the information received from it. At the present time the Administration of the Hydrometeorological Service Ukrainian SSR has 318 shipboard stations, of which more than 60% are on ships of the Merchant Marine Ministry. Data from 75-80 thousand observations are annually received from all shipboard stations at the USSR Hydrometeorological Center, the weather bureaus of the Black Sea and the Sea of Azov and other prognostic agencies. Through the efforts of the shipboard inspectors of the Odessa, Opasnoye marine inspectorates and the Crimean Hydrometeorological Observatory it has been possible to achieve

an appreciable reduction in the number of errors, in particular, in determining the form of the cloud cover, the type of falling precipitation, etc. There has been a decrease in the number of errors introduced in the coding of individual types of meteorological observations. Each year shipboard inspectors carry out inspections and visits to virtually all shipboard stations when the ships call at their home ports. During 1977-1978 alone the inspector groups of the Administration of the Hydrometeorological Service Ukrainian SSR carried out 559 inspections and visited ships on 478 occasions.

Noting definite attainments in the operation of the shipboard network, the conferees also noted a number of unsolved problems in the activity of shipboard stations. The checking of the ship's logs with data on the receipt of summaries at the USSR Hydrometeorological Center, the weather bureaus of the Black Sea and Sea of Azov and other forecasting agencies has indicated that some of the information is not taken into account.

It was also noted that the normal operation of shipboard stations is greatly hindered by the absence of laboratories for checking instruments at the base ports.

An analysis of the records of inspections at shipboard stations indicates that most of the observers have long been working without the "Abbreviated Cloud Atlas." The operation of the shipboard stations is also hindered by the inconvenient form of the KGM-15V journal book. The KN-09-S code is also in need of considerable improvement.

In their addresses the conferees particularly noted the need for improving the quality of the training of navigators in the field of hydrometeorology and improving the procedures for the recertification of specialists making shipboard observations.

A conference resolution formulated a number of primary problems in improving the operation of the shipboard network of the Administration of the Hydrometeorological Service Ukrainian SSR. In particular, it was resolved to ask the State Committee on Hydrometeorology to accelerate solution of the problem of development and standard production of new apparatus for outfitting the shipboard stations, to examine, in collaboration with the Navy Ministry and Fishing Ministry, the problem of creating a permanently continuing series of courses for enhancing the skills of navigation personnel in the field of hydrometeorology and in the shortest possible time to reissue all the necessary aids and blank materials.

*****

An international seminar and conference on oceanographic production, the system for processing data and servicing the Combined Global System of Oceanic Stations was held in Moscow during the period 2-11 April 1979. The seminar and conference were organized by the WMO and the Intergovernmental Oceanographic Commission of UNESCO jointly with the USSR State Committee on Hydrometeorology and Environmental Monitoring.

The purpose of the seminar and conference was:
a) to determine the sphere and effectiveness of use of presently existing and future oceanographic production by different marine users;
b) to bring present and future production to potential groups of users and to determine the possible economic, scientific and social advantages which can can be obtained as a result of the effective use of this production in oceanic activity;
c) to examine the oceanographic production turned out and the methods which are used in preparing such production;
d) to determine new types of required production and also the basic data and processing methods required in producing these products;
e) to convey to member-countries which are still not actively participating in the Combined Global System of Oceanic Stations program information on the economic and social advantages which can be obtained by participation in this program;
f) to develop a plan for a "Manual on Oceanographic Production, a System for the Collection and Processing of Data and Servicing of the Combined Global System of Oceanic Stations";
g) to examine critically the draft of a "Glossary" of terms used in the Combined Global System of Oceanic Stations program.

Thirty-two reports on six subjects were presented at the seminar and conference:
1) Use of existing and future production by different groups of users and the advantage obtained from this;
2) Review and evaluation of existing oceanographic production;
3) Review of methods for preparation of oceanographic production;
4) Processing of data, including quality control, standardization of methods and processing technology;
5) Determination of the data base necessary for the preparation of oceanographic products and also means for ensuring the data base;
6) Use of satellites in monitoring the ocean and use of these data in preparing oceanographic production.

In the course of discussion of the reports it was noted that during a relatively short period (1972-1978) considerable successes had been attained in carrying out the Combined Global System of Oceanic Stations program not only in formulating observations, collection and exchange of observational data, but also in the processing of data and on their basis preparation of analyses and forecasts for satisfying the rapidly growing needs of practice and science.

This seminar not only favored the establishing of contacts and exchange of opinions among scientists of different countries on the problems relating to the methods employed in the processing of data, the preparation of analyses and forecasts for the Combined Global System of Oceanic Stations, but most importantly, it demonstrated what economic advantages can be obtained by the countries from the Combined Global System of Oceanic Stations program.

In the reports devoted to the use of satellites for obtaining oceanographic information it was convincingly demonstrated what great possibilities exist for successful development of the Combined Global System of Oceanic Stations Program and thereby for a more complete satisfaction of scientific and practical needs for obtaining oceanographic data and production.

In the course of discussion of the reports, and then at a conference of the group of experts it was decided to prepare a manual which should cover the following matters:
-- requirements on production and servicing;
-- organization of the system for data processing and servicing;
-- existing production and servicing;
-- methods and technology used in preparing oceanographic production;
-- form and finalization of production;
-- organization and procedure for collection and dissemination of Combined Global System of Oceanic Stations data;
-- storage and exchange of Combined Global System of Oceanic Stations data.

The issuance of the manual will exert a substantial influence on improvement in the quality of production from the Combined Global System of Oceanic Stations and implementation of the program as a whole.

In conclusion there was a discussion of the "Glossary of Oceanographic Terms Used in the Combined Global System of Oceanic Stations" prepared by IOC/WMO experts.

NOTES FROM ABROAD

Moscow METEOROLOGIYA I GIDROLOGIYA in Russian No 8, Aug 79 pp 127-128

[Article by B. I. Silkin]

[Text] As reported in SCIENCE NEWS, Vol 115, No 4, p 56, 1979, in January 1979 the New York State Academy of Sciences held a conference on the theme: "Influence of Aerosols Ejected into the Atmosphere in the Course of Industrial Activity on the State of the Environment." This conference was addressed by a scientific specialist of the School of Oceanography at the University of Rhode Island (Kingston, Rhode Island) Kenneth Ron, who presented the results of study of changes in the air space of the Arctic arising as a result of its contamination by man.

The phenomenon of so-called "arctic haze" was for the first time discovered during flights of meteorological aircraft laboratories already in the 1950's. However, severe climatic conditions and the difficult accessibility of the North have long impeded study of this phenomenon, which can be compared with known cases of smog in the city of Cincinatti (Ohio), observed in the 1960's.

In 1975 K. Ron and his associate J. Chu began to carry out systematic measurements of atmospheric contamination in the Barrow region (extreme north of the state of Alaska). Their first hypothesis was that the haze is caused by dust particles of natural origin. However, later, when they discovered that the principal component of contamination here was aerosol sulfates, that is, long-known products of decomposition of industrial effluent, it became clear that the cause is man's industrial activity, and not natural factors.

The final confirmation of such an opinion was the detection of vanadium in the air samples, this being a result of the combustion of heavy types of petroleum products frequently used for industrial purposes. It can be postulated that these elements enter the air space of Alaska from regions of Northern Europe, since air currents from other regions of North America, from Japan, China and Korea, passing over the expanses of the world ocean, are considerably purified. A study of the air masses over Alaska thereby confirmed that the sources of contamination under definite conditions can be situated at distances attaining 13,000 km from the place of its detection.

The Antarctic, in comparison with the Arctic, for the time being still does not know such a problem because the earth's southern hemisphere is characterized by a considerably lesser industrialization than the northern hemisphere. In addition, the south polar continent is separated from populated regions by a broad band of seas, passing over which the air currents to a considerable degree lose the particles contaminating them. Finally, Antarctica, in contrast to the Arctic, has a highly dissected local relief; a considerable part of it attains elevations of about 3,000 m above sea level, which also favors a loss of contaminating elements by air masses overcoming these relief irregularities.

As reported in NEW SCIENTIST, Vol 78, No 1109, p 916, 1978, a tornado, being a narrowly local and relatively short-lived phenomenon, is difficult to study as a result of the difficulty in collecting scientific facts characterizing it. Physical modeling of a tornado in a water basin and attempts at its mathematical modeling until now have met with little success.

Now the studies of R. Smith (Melbourne, Victoria) and L. Leslie (Australian Center for Mathematical Research, Melbourne) are closer to reality. The basis for their model is the assumption that the beginning of a tornado is a powerful upward-directed air gust within a thunderstorm cloud.

Such a gust draws air into the central part of a cloud from its peripheral region; the entering mass acquires a spiral, rotational motion. With a decrease in the radius of rotation the velocity becomes greater. This leads to an increase in the centripetal force, which continues until there is an equalization of the forces responsible for the spiral motion of the air. Thus, the "nucleus" of a tornado arises, having the form of a hollow vertical column rotating about the ascending current at the center of the thunderstorm cloud. Newer and newer air masses are drawn through the lower end of this column and they also begin to experience rotational motion until the column reaches the underlying earth's surface.

It could be expected that from this moment, deprived of receipts of new air, the tornado begins to die. However, the computations made by R. Smith and L. Leslie, show differently. Friction at the earth's surface slows the velocity of rotation of the lower part of the column to such an extent that the air from the thin surface layer even under these conditions can be sucked from it. Thus, the ascending movement of the atmosphere continues and the column continues its existence.

Making use of their mathematical model, describing all these processes, the Australian scientists could precisely reproduce the parameters of the specific tornado, correctly designating the dimensions of the central part of its funnel, the wind intensity in it, the decrease in atmospheric pressure with advance toward the center and the rate of increase in wind intensity. They also established that in order for a tornado to develop the initial, upward directed gust and the primary rotational velocity should fall in definite, extremely narrow quantitative limits. In addition, the funnel-like

eddy rapidly will die out if from the very beginning there is not at least a weak rotational air movement beneath it. This also explains the fact that few thunderstorms generate tornadoes and only a few of them reach the earth's surface.

A confirmation of the correctness of the Smith-Leslie models is the observations made in the United States using radar equipment. As predicted, the formation of the funnel occurs in the middle (vertically) part of the cloud at an altitude of 4-5 km. The lower edge of the funnel reaches the earth approximately a half-hour thereafter.

[11-5303] -END-

5303
CSO: 1864